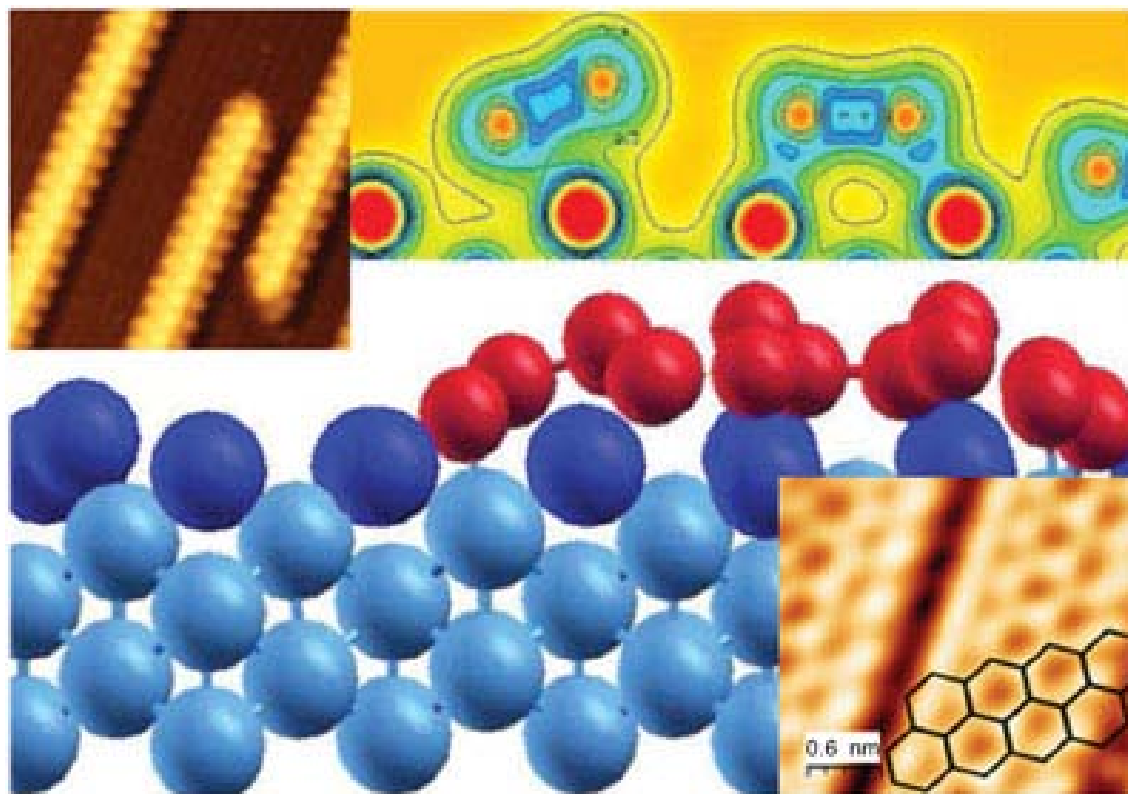


Silicene: the silicon based counterpart of graphene

Guy Le Lay

Université de Provence, Marseille, France

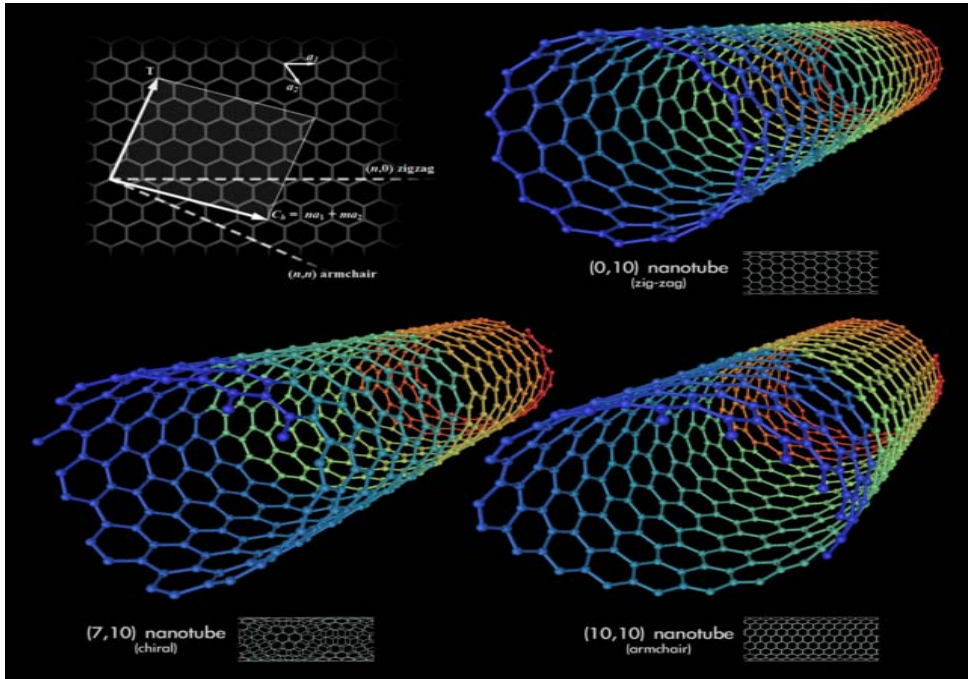


CINaM-CNRS, Marseille (France) CINaM-CNRS, Marseille (France)

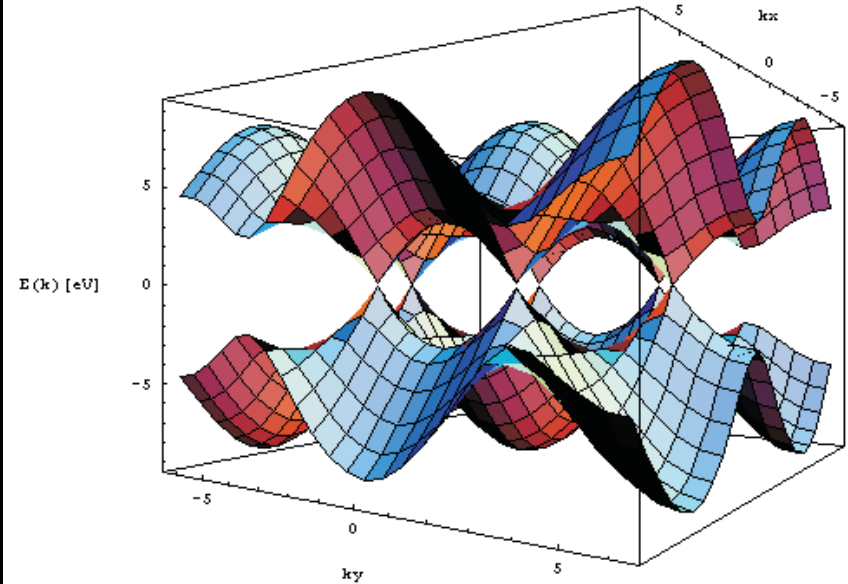
Synopsis

- An introduction to **silicene** and Si NTs
- Semiconductor-on-metal systems, an archetype: Au/Si(111)
- Si nano-ribbons on Ag(110)
- 1D physics
- STM/DFT calculations: **silicene** stripes
- Silicene **stripes** on Ag(100)
- Silicene **sheets** on Ag(111)

From graphene to **silicene**?



Graphene & carbon nanotubes



Energy dispersion relation $E(k)$ for graphene: 3D energy surface in k space.

Graphene has a very special electronic structure: linear dispersion of the π and π^* bands close to the so-called Dirac point where they touch at the Fermi energy at the corner of the Brillouin zone.

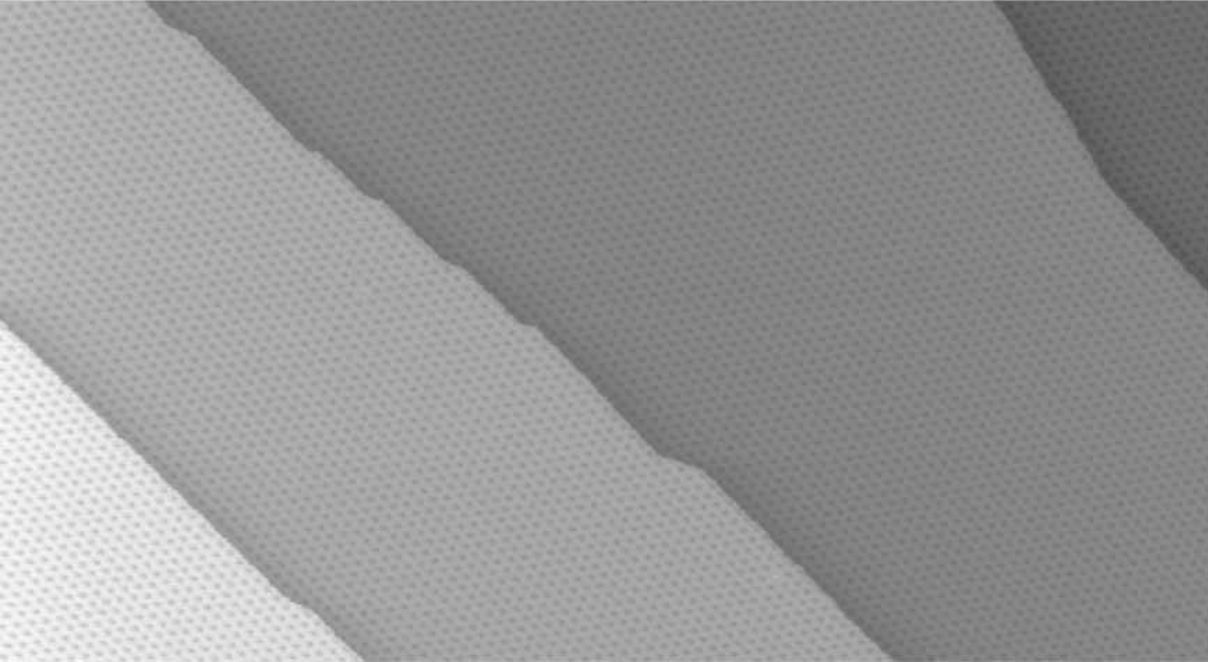
It has exotic electronic transport properties: the charge carriers behave like relativistic particles \rightarrow anomalous quantum Hall effect; ballistic charge carrier transport at RT and high carrier concentrations \rightarrow electronic devices

Silicene might from an electronic point of view be equivalent to graphene with the advantage that it is probably more easily interfaced with existing electronic devices and technologies. The obvious disadvantage is that sp^2 bonded Si is much less common than for C and **the synthesis of Si in a graphene-like structure is extremely demanding**. S. Lebègue and O. Eriksson, Phys. Rev. B 79, 115409 (2009)

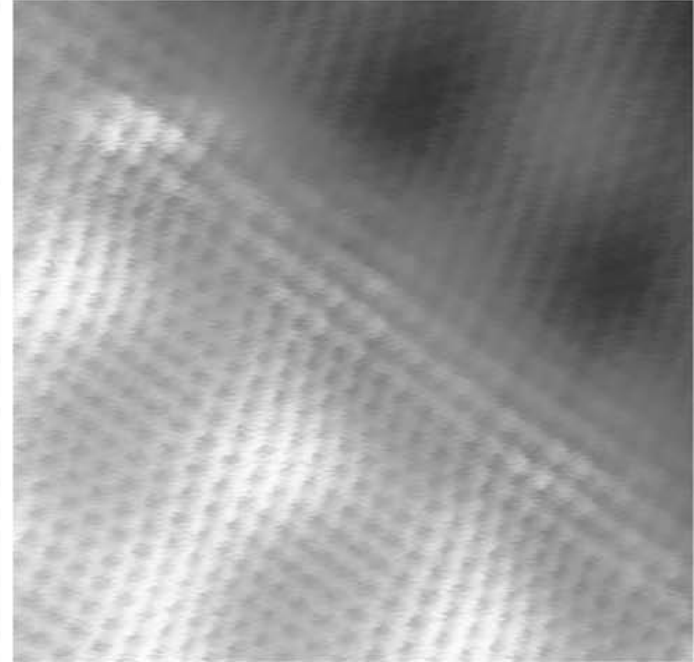
Graphene on metal surfaces

J. Winterlin, M.-L. Bocquet Surface Sci., 603 (2009) 1841

a



b



- (a) STM image of the graphene moiré structure on Ir(111), prepared by decomposition of ethylene at 1320 K. Graphene forms a coherent domain that covers several terraces. Image size 2500 Å x 1250 Å.
- (b) Detail of an area around a step, showing the atomic graphene structure at the step edge. Image size 50 Å x 50 Å

Graphene has been called the prototypical bench-top relativistic quantum system. Due to its peculiar band structure, the charge carriers in graphene behave as relativistic particles with zero effective mass.

Graphene on copper foils

Xuesong Li et al., Science 324 (2009) 1312

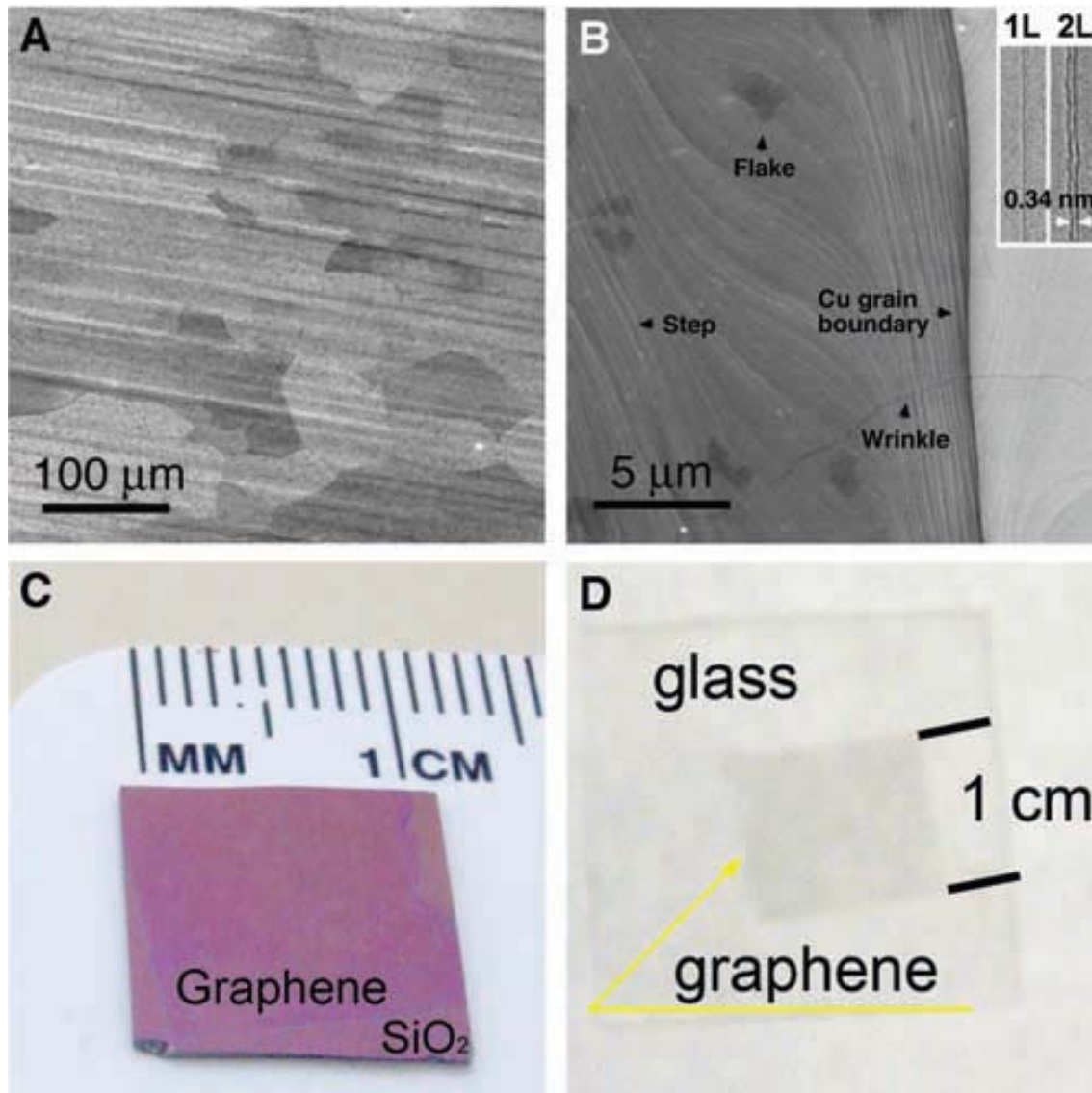
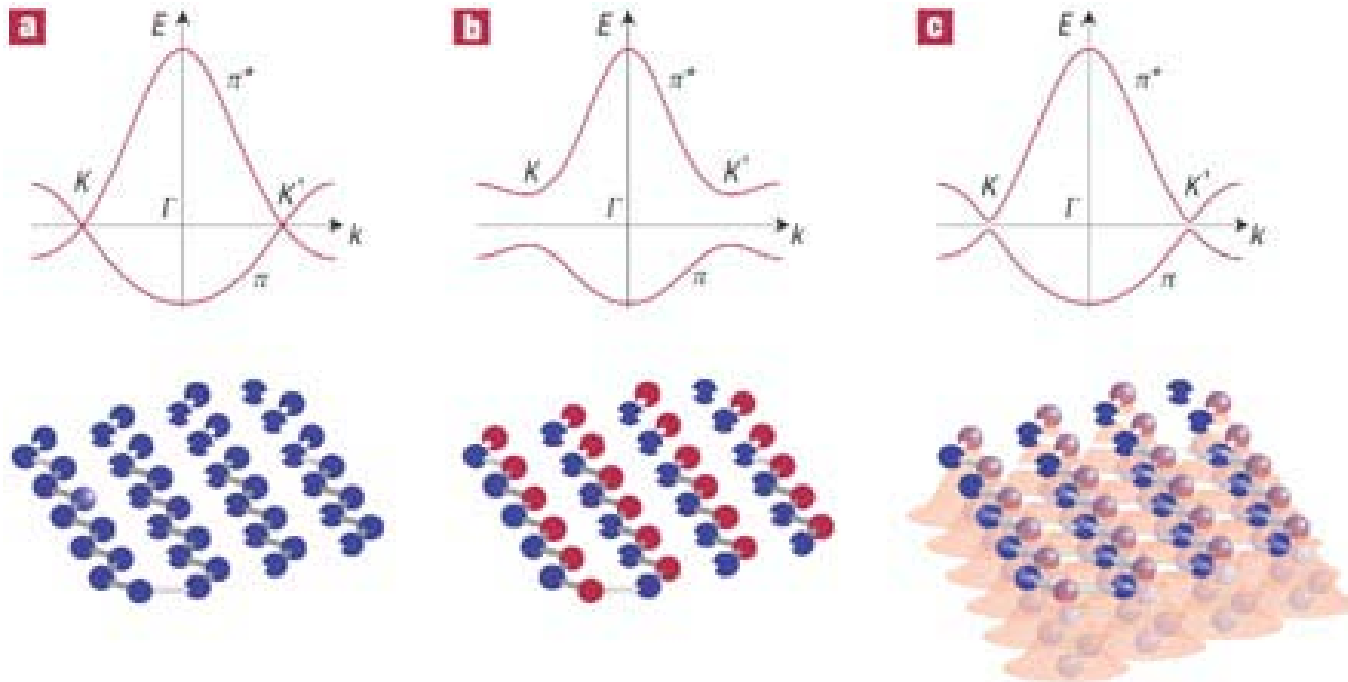


Fig. 1. (A) SEM image of graphene on a copper foil with a growth time of 30 min. (B) High-resolution SEM image showing a Cu grain boundary and steps, two- and three-layer graphene flakes, and graphene wrinkles. Inset in (B) shows TEM images of folded graphene edges. 1L, one layer; 2L, two layers. (C and D) Graphene films transferred onto a SiO₂/Si substrate and a glass plate, respectively.

Schematic representation of 2D crystals and electronic band structures (only π bands are shown)



a, Free-standing graphene. **b**, Boron-nitride. **c**, Epitaxial graphene. Symmetry between the sublattices in graphene guarantees gapless spectra around K points. This symmetry is broken in boron-nitride (one sublattice consists of boron atoms, another of nitrogen), which immediately opens a gap. In epitaxial graphene, the commensurate underlying potential gives rise to different on-site energies for the two sublattices, which opens a small gap around K points.

Kostya Novoselov, Nature Materials 6, 720 - 721 (2007)

May silicene exist?

E.F. Sheka

Abstract. The letter presents arguments, supported by quantum-chemical calculations,

against silicene to be produced

arXiv:0901.3663

Theoretical proposal of planar silicon oligomer and **silicon benzene**

M. Takahashi , Y.Kawazoe

Computational Materials Science 36 (2006) 30–35

Carbon/Silicon: difference in chemistry

⇒ difference π in bonding capability¹

→ Energetics of the valence s and p orbitals:

energy difference ~ about twice for C (for C/Si: $E_{2p} - E_{2s} = 10.60 \text{ eV}/5.66 \text{ eV}$)

As a result, Si tends to utilize all three of its p orbitals resulting in sp^3 hybridization, while, in contrast, C “activates” one valence p orbital at a time, as required by the bonding situation, giving rise, in turn, to sp , sp^2 , sp^3 hybridizations.

→ Extent of overlap of the π orbitals:

The π – π overlap decreases by roughly an order of magnitude in going from C to Si due to the significant increase in atomic distance, resulting in much weaker π bonding for Si versus C. Hence, Si=Si bonds are in general much weaker than C=C bonds.

→ Carbon / Silicon

C stable form: graphite (hexagonal, 7.37 eV/atom), metastable one diamond / Si stable form diamond-like (4.63 eV/atom), metastable one hexagonal; forming the metastable forms requires special kinetic paths (high P, high T)

⇒ comparison between Si NTs and C NTs²

→ Cohesive energy of studied Si NTs: only 82% of that of bulk Si in diamond structure, compared to 99% for C NTs versus crystalline graphite; consequence:

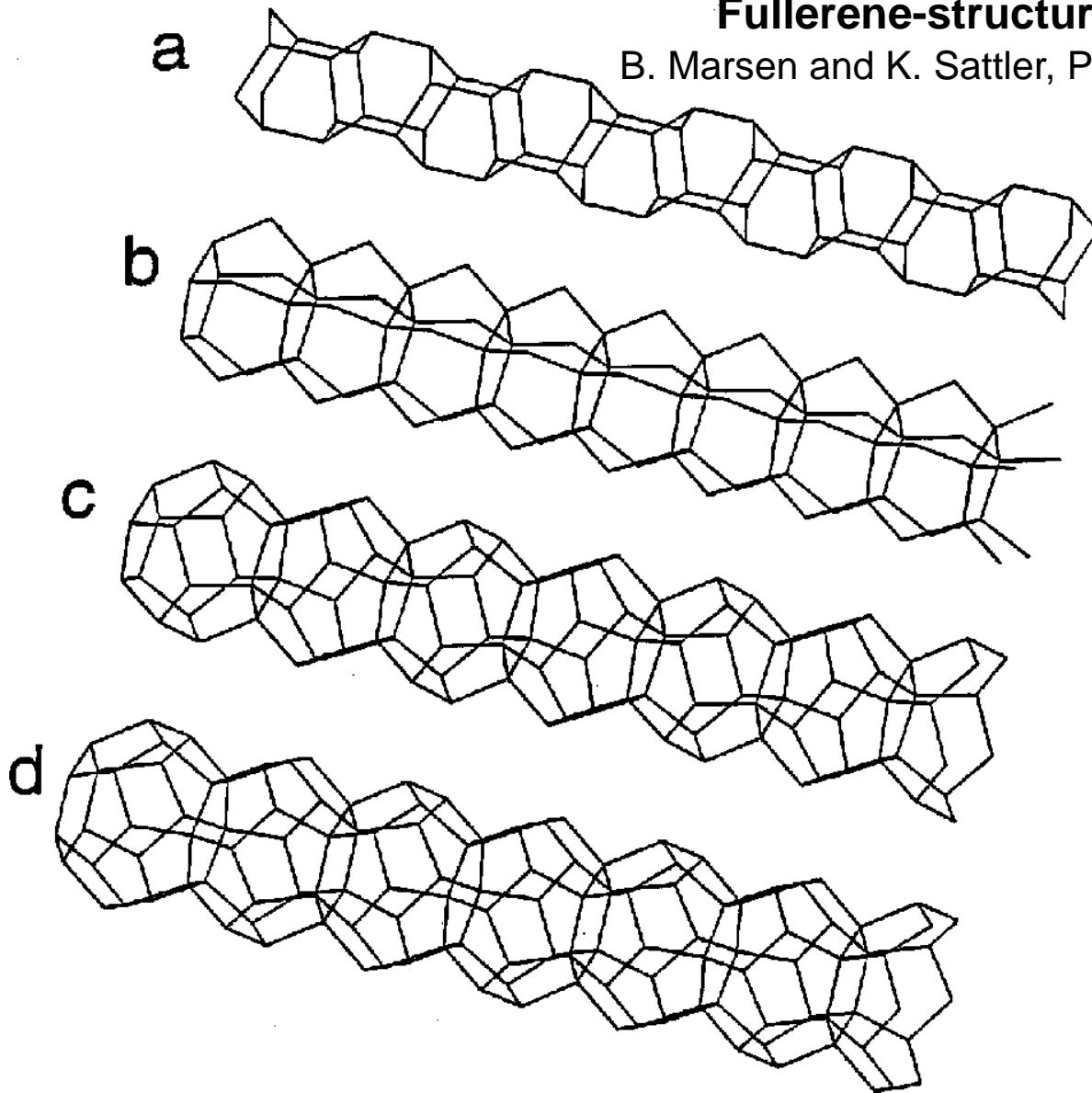
→ **difficulty in producing Si NTs, and, especially, silicene**

¹Zhang et al., Chem. Phys. Lett., 364 (2002) 251

²Fagan et al., J. Mol. Struct. (Theochem) 539 (2001) 101

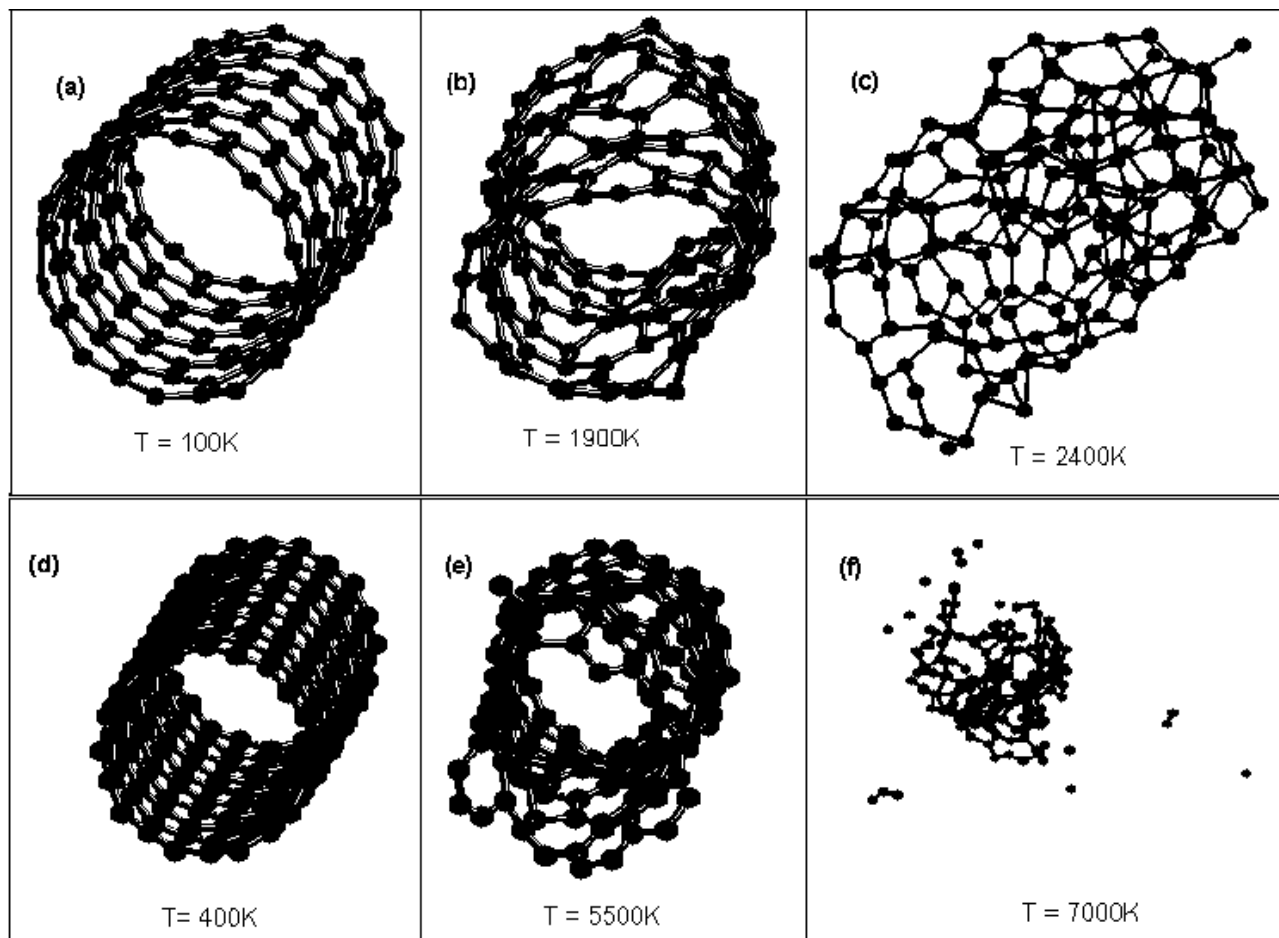
Fullerene-structured nanowires of silicon

B. Marsen and K. Sattler, Phys. Rev. B 60 (1999) 11593



Four models of possible nanowire core structures. a) Si₁₂ cage polymer. b) Si₁₅ cage polymer. c) Si₂₀ cage polymer. d) Si₂₄ cage polymer.

S.B. Fagan et al., Journal of Molecular Structure (Theochem) 539 (2001) 101;
Phys. Rev. B 61 (2000) 9994.



Disintegration processes for the (a)-(c) silicon (10,0); and (d)-(f) carbon (10,0) nanotubes at different temperatures.

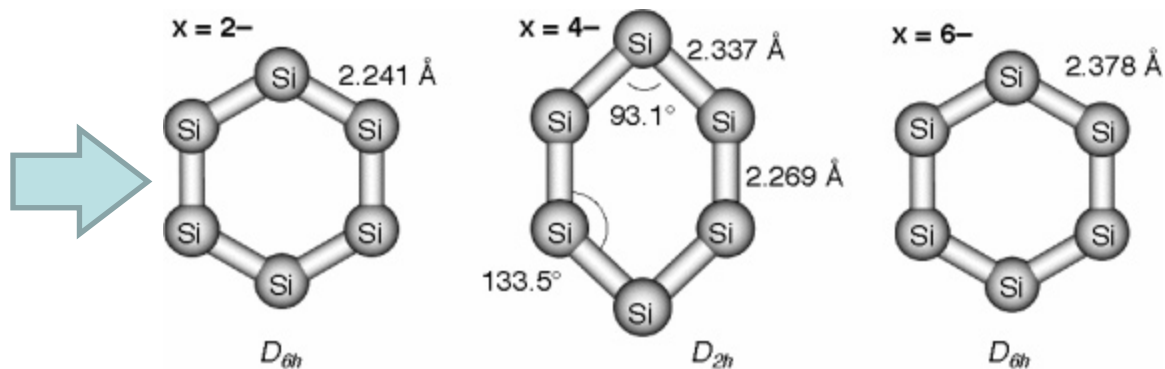
Silicon nanotubes: why not?

Zhang et al., Chem. Phys. Lett. 364 (2002) 251

SiNT can in principle be formed. The resulting energy minimized SiNT, however, adopts a severely puckered structure (with a corrugated surface) with **Si-Si distances ranging from 1.85 to 2.25 Å**.

Theoretical Study on Planar Cyclic Si₆ Anions with D_{6h} Symmetry

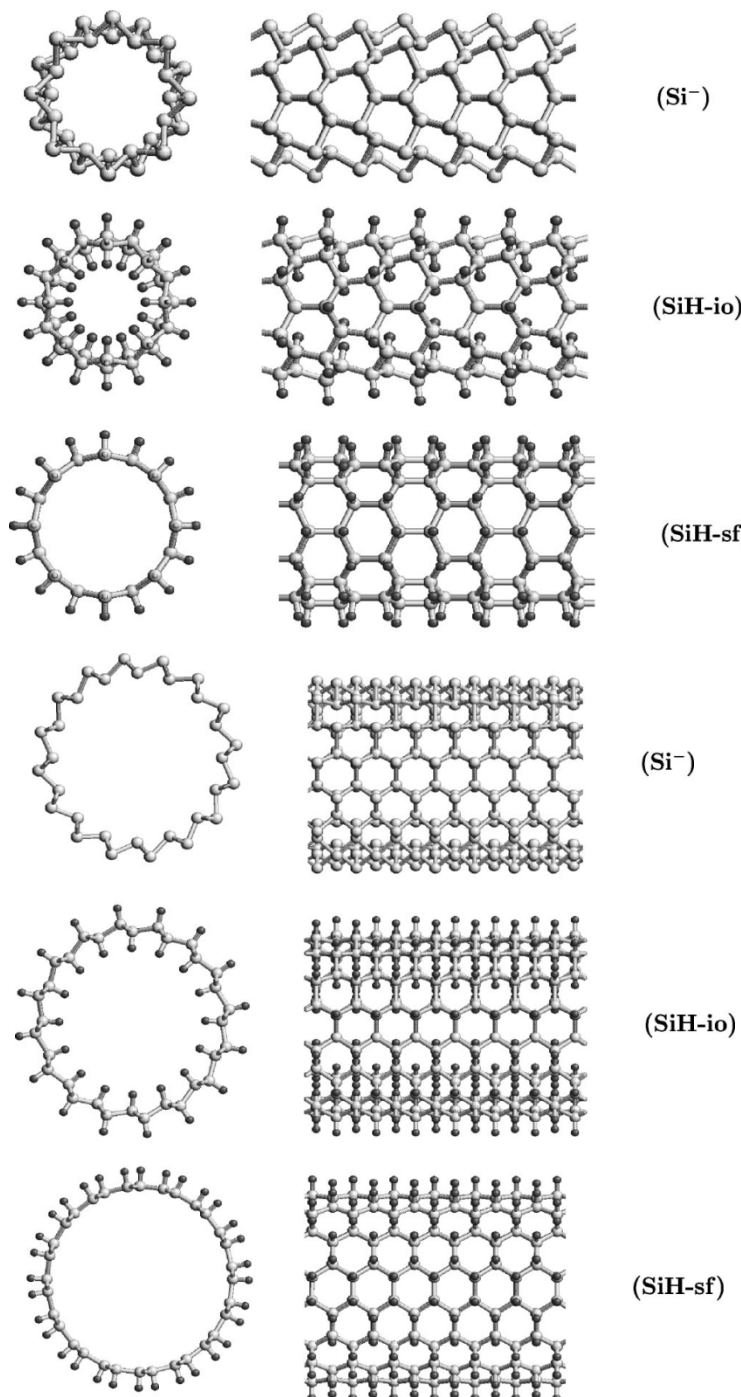
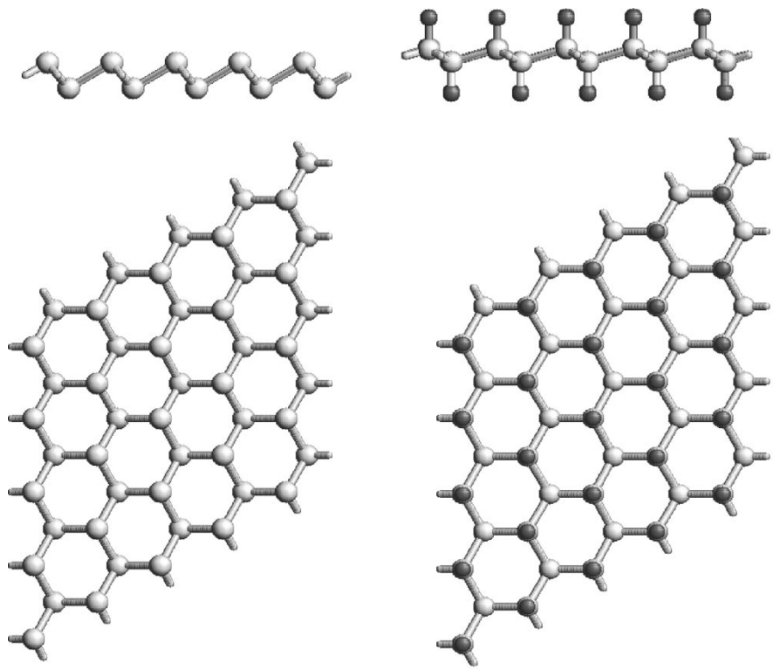
M. Takahashi and Y. Kawazoe
Organometallics 24 (2005) 2433



Silicon benzene (D_{6h}-Si₆ 2-) : **Si-Si bond lengths become short (2.24 Å)**. The lengths are between the distances of **Si-Si single** and **double bonds (2.339 Å** for Si₂H₆ and **2.163 Å** for Si₂H₄ at the MP2/6-311++G(d, p) level). This feature is the same as in benzene where C-C bond length is between the distances of C-C single and double bonds.

Tubular structures of silicon (derived from alkaline-earth-metal silicides, e.g., CaSi_2)

Structure of the (8,0) silicide, $\text{SiH-}i_o^*$, and SiH-sf^* NTs.
 Right: side views; Left, views down the axis of the NTs.
 i_o : inside & outside, sf @ the surface



The structure (side views, up; top view, below) of a silicide (left) and SiH layer (right) as predicted by DFTB calculations. From the side view **the puckered structure** of the layer is clearly visible.

Structure of the (8,8) silicide, $\text{SiH-}i_o$, and SiH-sf NTs.

Electronic structure of two-dimensional crystals from *ab initio* theory

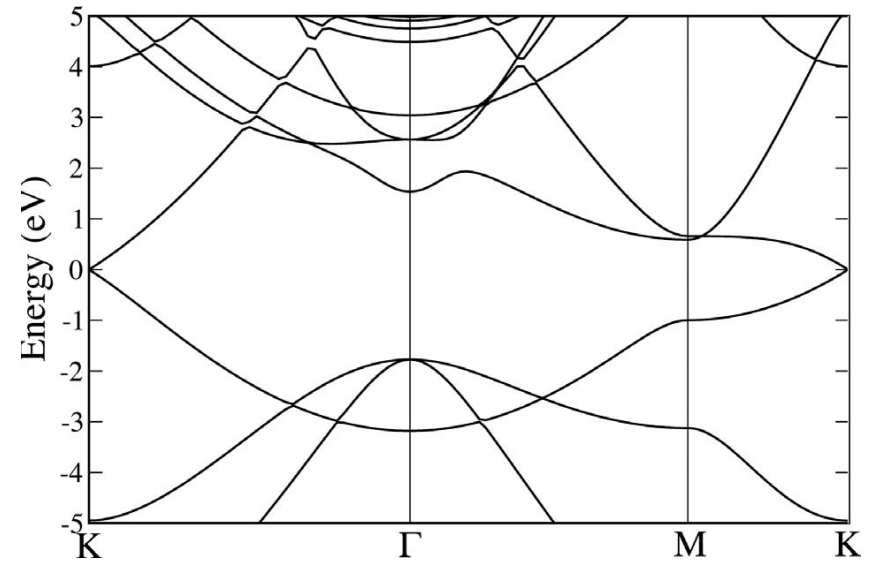
S. Lebègue and O. Eriksson Phys. Rev. B 79 (2009)115409

Lattice parameters of hexagonal Si and Ge computed with either LDA or GGA:

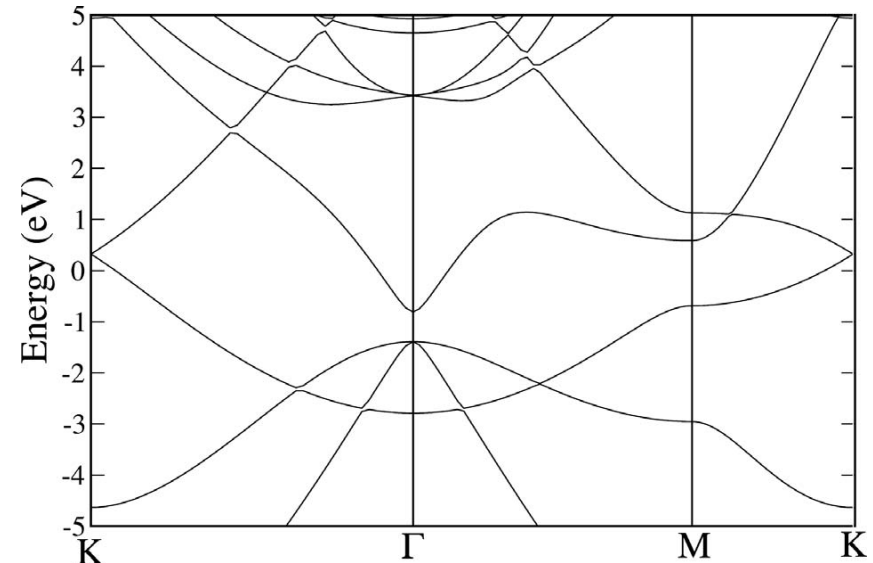
Si 3.860/3.901 Å

Ge 4.034/4.126 Å

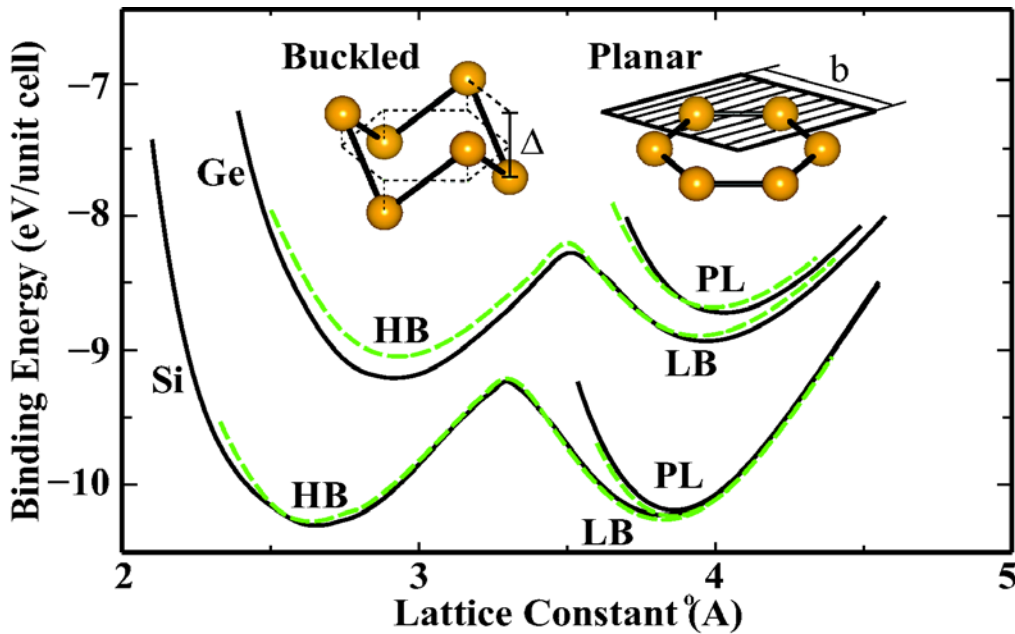
Silicene, has an electronic structure very similar to the one of graphene, making them possibly equivalent.



Band structure of silicene (E_F @ 0 eV)



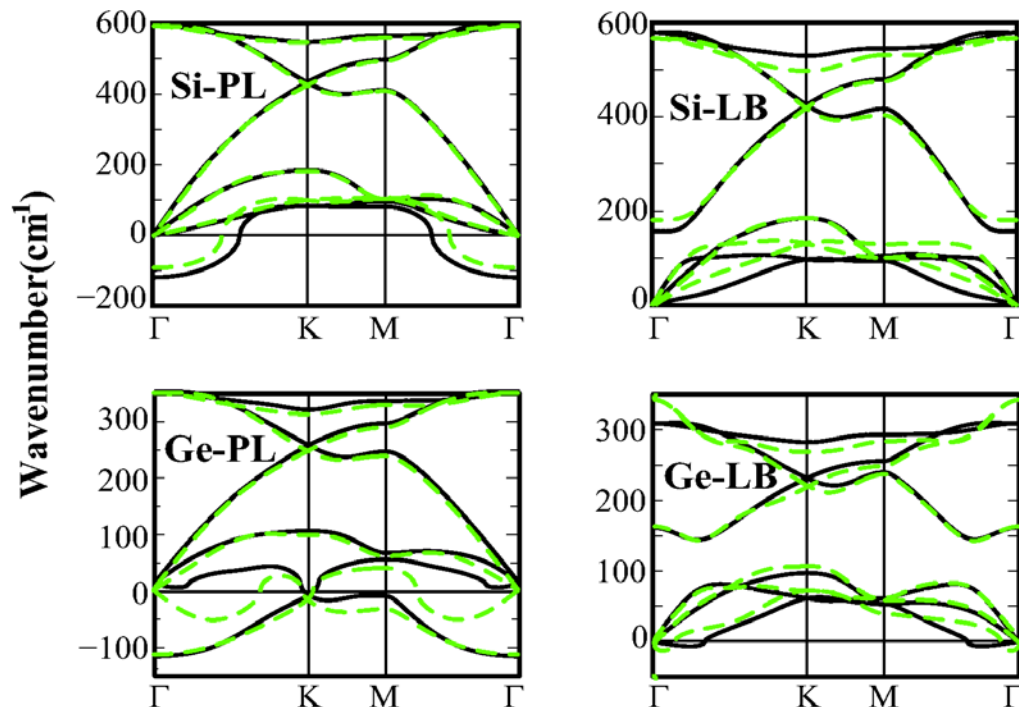
The band structure of two-dimensional Ge. (E_F @ 0 eV)



Binding energy versus lattice constant of 2D Si and Ge are calculated for various honeycomb structures.

Black and dashed green curves for binding energy are calculated by LDA using PAW potential and ultrasoft pseudopotentials, respectively.

Planar (PL) and buckled geometries (HB*: 2.13 Å, LB*: 0.44 Å) together with buckling distance and lattice constant of the hexagonal primitive unit cell, b are shown by inset (nn distance & cohesive energy for LB Si: 2.25 Å & 5.16 eV).



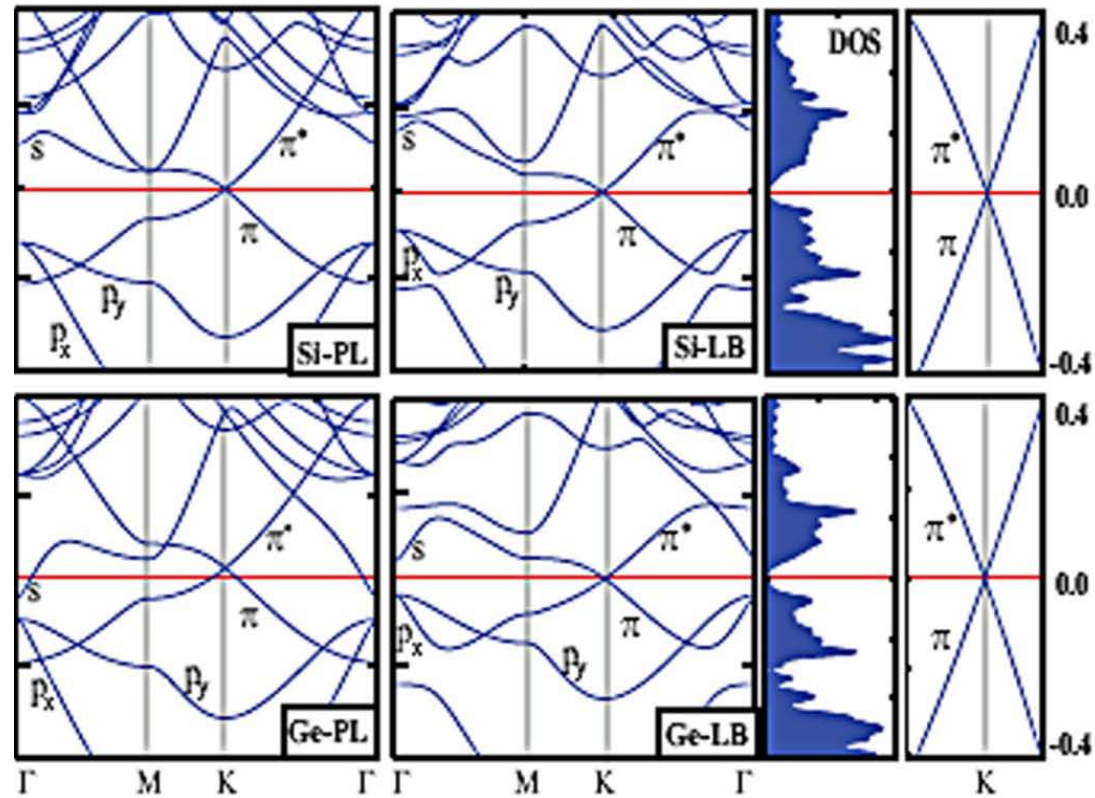
Phonon dispersion curves obtained by force constant and linear response theory are presented by black and dashed green curves, respectively. LB and HB indicate low and high buckling, respectively.

Despite the weakened π bonding, the stability of the LB structures is maintained by puckering induced dehybridization. As a result, the perpendicular p_z orbital, which forms π bonding and hence π and π^* bands, combines with the s orbital.

*LB and HB indicate low and high buckling, respectively.

S. Cahangirov,
M. Topsakal, E. Aktürk,
H. Sahin and S. Ciraci,

Phys. Rev. Lett. 102 (2009)
236804



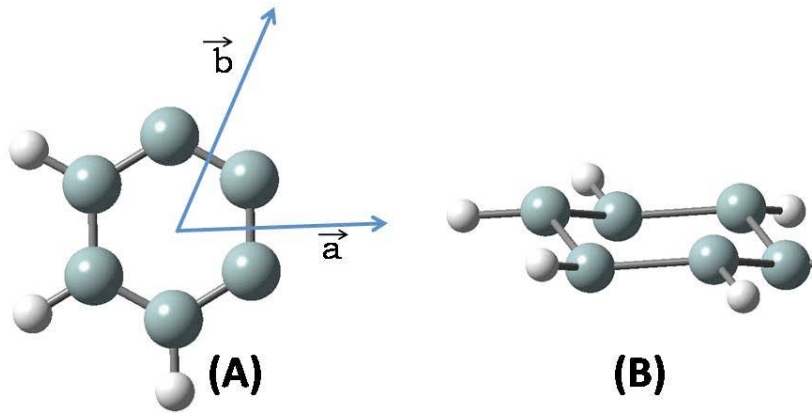
Energy band structures of **silicene** and of the germanium analogue calculated for low-buckled (LB) and planar (PL) geometries.

In the LB case the density of states is also presented.

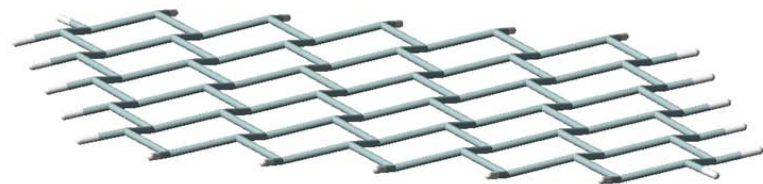
The crossing of **the π and π^* bands at the K points of the BZ** is amplified to show they **are linear near the crossing point**.

Zero of energy is set at E_F .

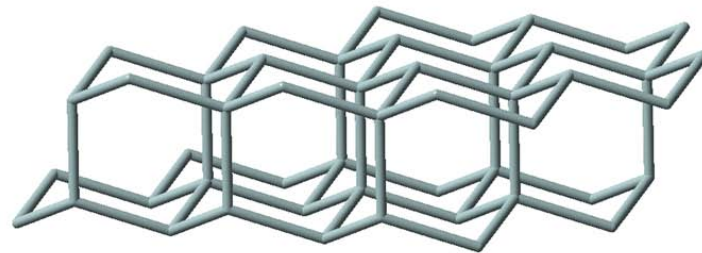
s, $p_{x,y}$ character of bands are indicated.



(A)

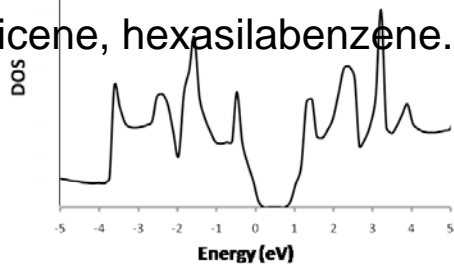


(B)



(A) Ripples in (5,5) silicene strip. (B) Structure of bulk Si viewed along the rippled layers.

(A) The translational units used to construct silicenes of various nuclearities. (B) Structure of a single aromatic unit of silicene, hexasilabenzene.



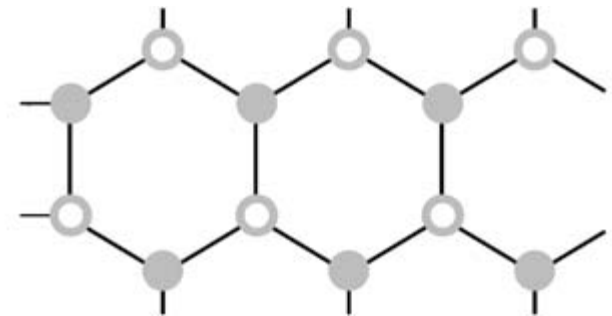
Density-of-States for silicene.

The structures for all the clusters were optimized using the hybrid B3PW91 DFT functional at the triple- ξ - valence polarized basis set level

Ayan Datta preprint «The binding energy per Si-atom is -1.026 eV for (5,5) silicene cluster and an asymptotic fitting leads to a value -1.21 eV for the infinite strip. It is important to note that such formidable binding energy suggest stability and existence of silicene even in the absence of a surface support»

Graphene Diamond Silicene Silicon

$D, \text{\AA}$	1.42	1.54	2.25	2.35
$ V_2 , \text{eV}$	12.32	10.35	4.91	4.44
$ V_1 , \text{eV}$	2.08	2.08	1.80	1.80
λ	0.66	0.85	0.66	0.85
E_{atom}, eV	13.5	15.9	7.1	9.6
C_0, eV	66.9	70.3	16.3	13.6
$k_0, \text{N/m}$	177	119	17.1	9.9
C_1, eV	14.7	19.9	3.6	3.9
$k_1, \text{N/m}$	38.9	33.7	3.8	2.8

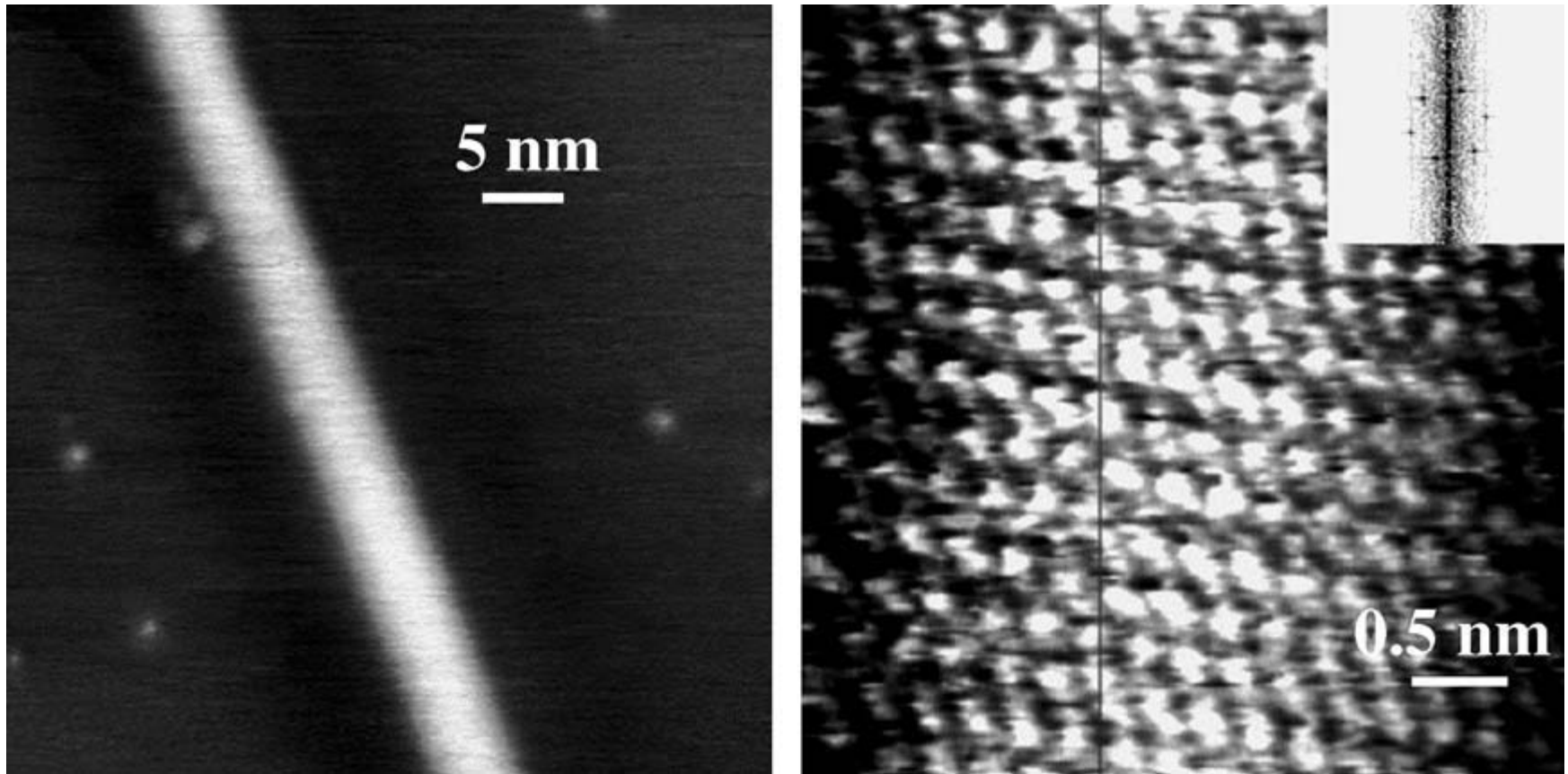


Parameters and the results of the calculations for graphene, diamond, silicene, and silicon

Calculations based on the modified Harrison bond orbital method

S. Yu. Davydov, *Physics of the Solid State*, **52** (2010) 184

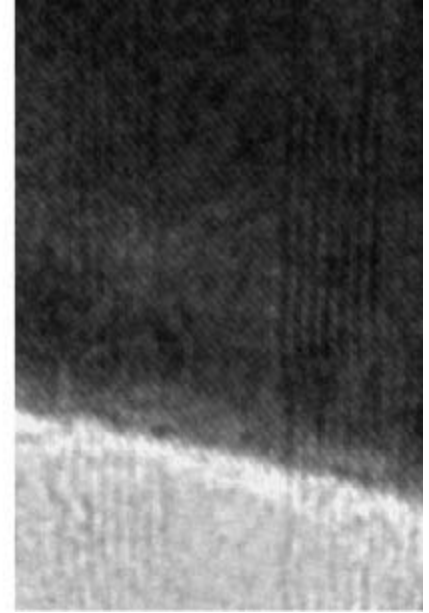
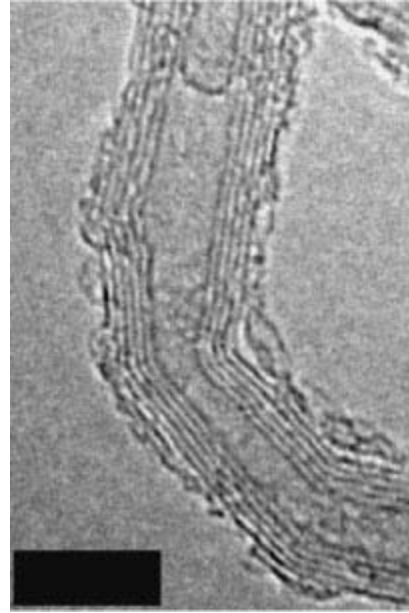
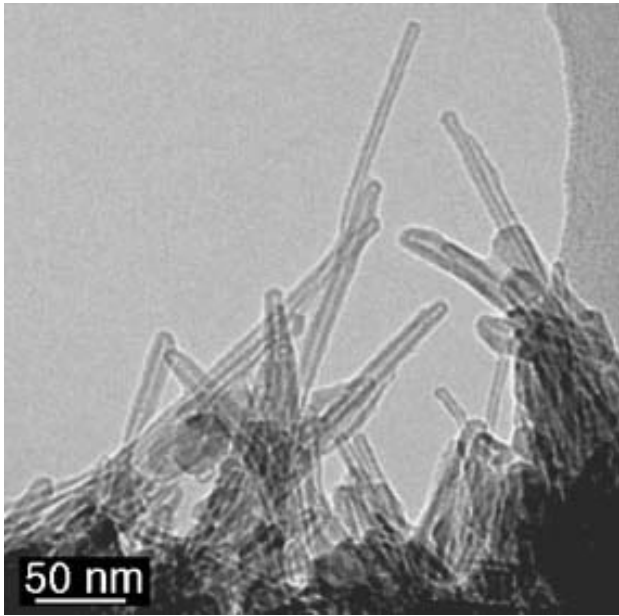
Silicon Nanotubes



(a) STM image (50 nm x 50 nm) of a straight nanotube and nanoparticles on HOPG surface. $I_{tunn}=0.15$ nA; $V_{bias}=0.4$ V; (b) STM atomically resolved image (4 nm x 4 nm) of a part of the lateral surface of the silicon nanotube. $I_{tunn}=0.8$ nA; $V_{bias}=0.7$ V.

Experimental Evidence for Nanostructural Tube Formation of Silicon Atoms

S. Yamada and H. Fujiki, Japan. J. Appl. Phys. 45 (2006) L837

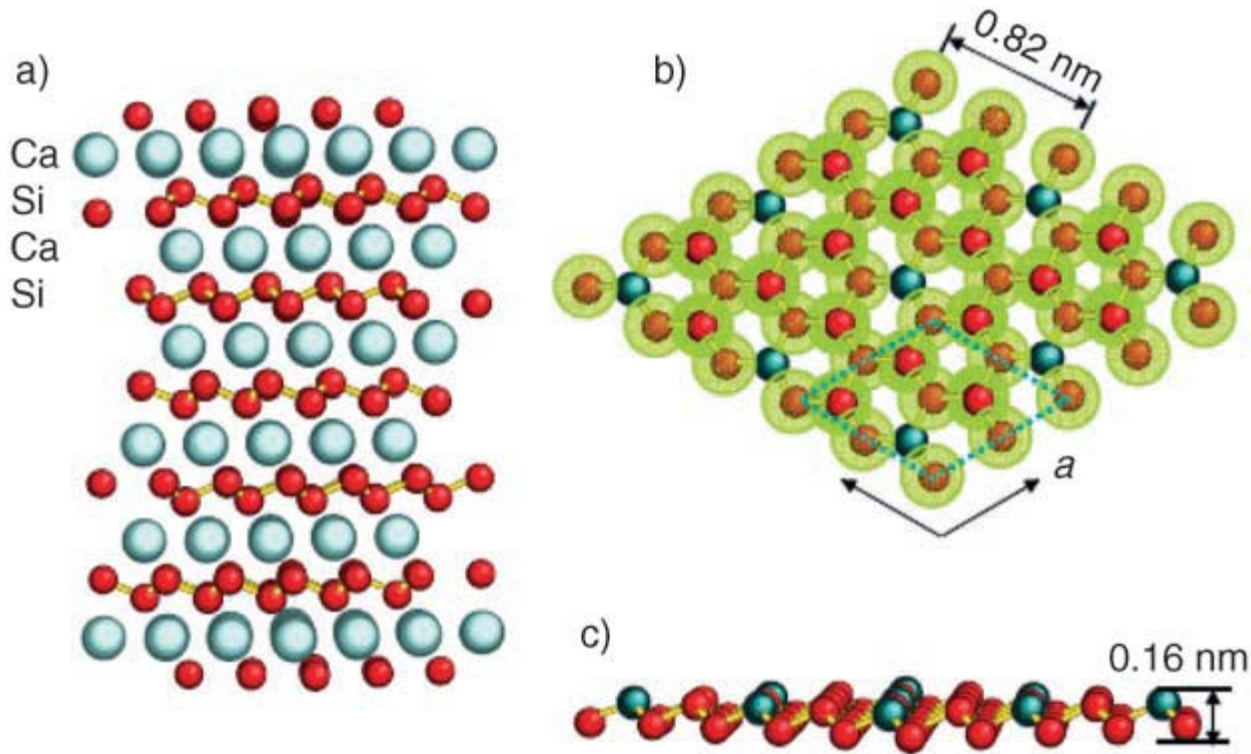


Bright-field low-magnification TEM image of straight SiNTs. The image was underfocused to enhance the phase contrast of the tubes.

HRTEM images of SiNTs. (a) Five-wall buckled tube. (b) Eightwall straight tube with Au foil. The lattice fringe of the tube overlaps that of Au in the upper part of the figure.

The presence of silicon nanotubes (SiNTs) composed of **rolled-up quasi-two-dimensional honeycomb nets** was first revealed by TEM, energy dispersive X-ray spectroscopy, and electron diffraction analysis, among products synthesized using a simple laser ablation technique. They were coaxial multiwall high-purity SiNTs with cylindrical symmetry, smallest inner and outer diameters of 1 and 4 nm, respectively, lengths up to 1 μm , and an interwall distance of 0.36 nm.

Two-dimensional atomic crystals



Structural model of CaSi₂.

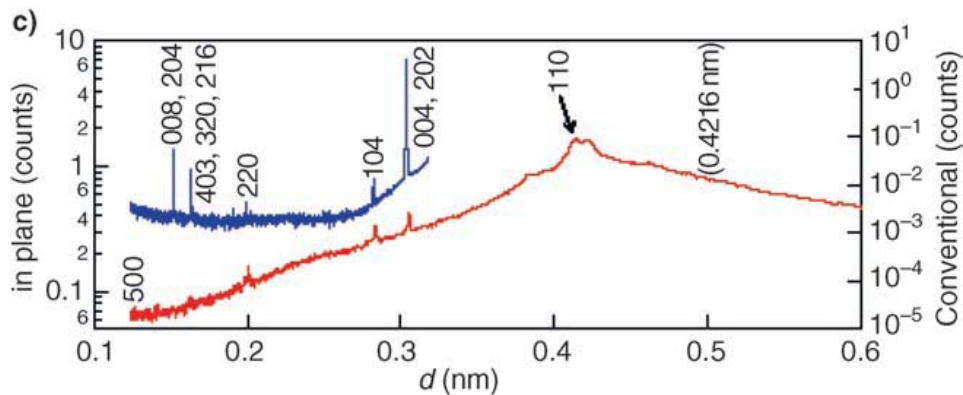
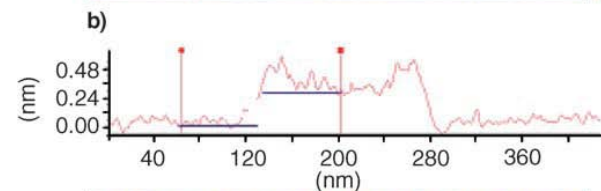
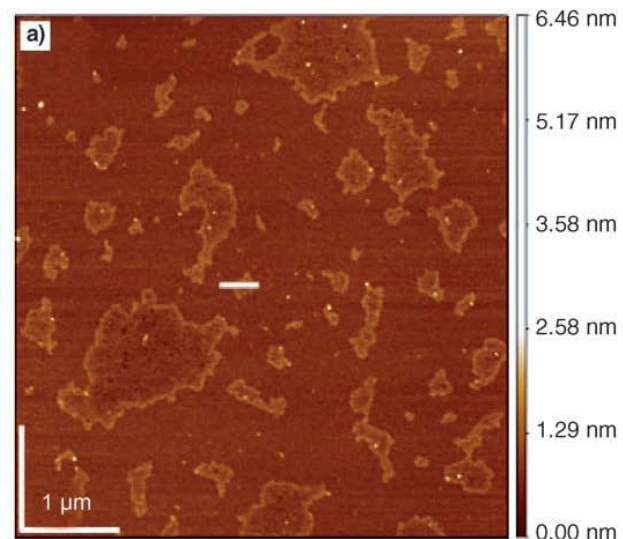
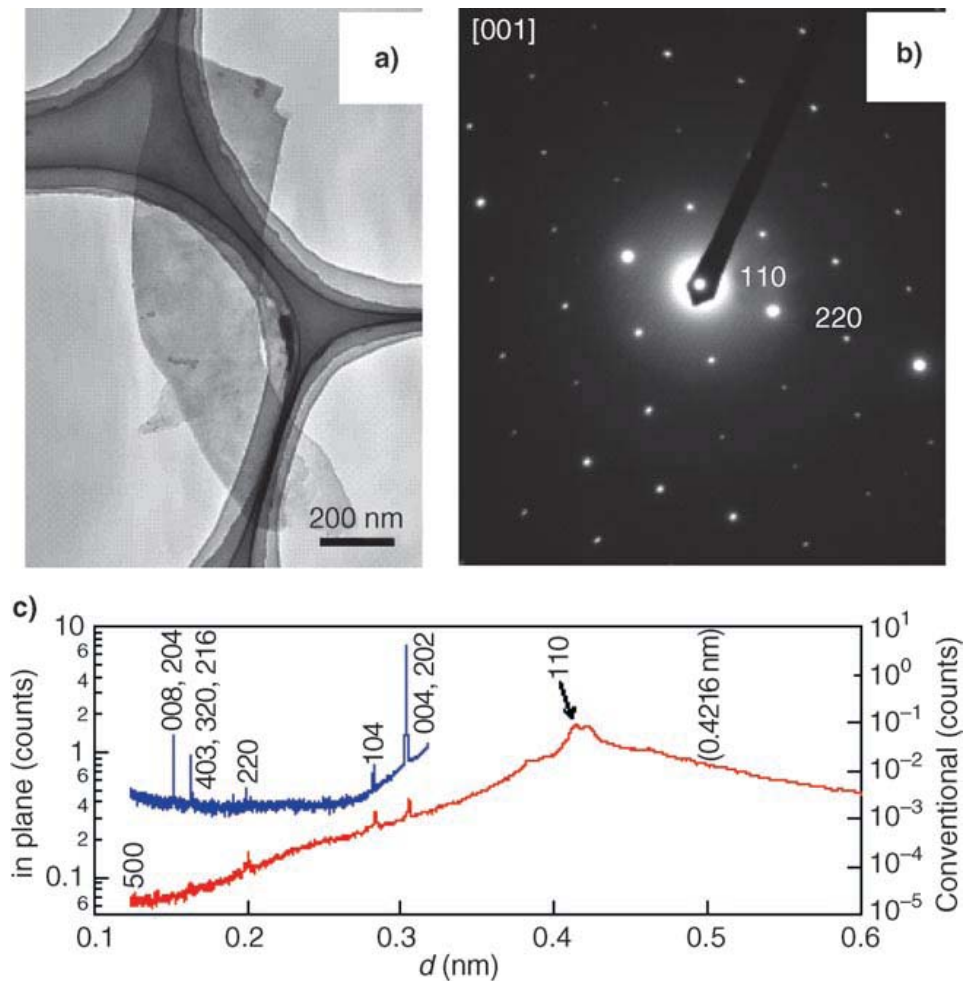
b) Top view of **Mg-doped silicon sheet capped with oxygen**;

the axis notation follows that for the hexagonal crystal structure of the parent layered silicon.

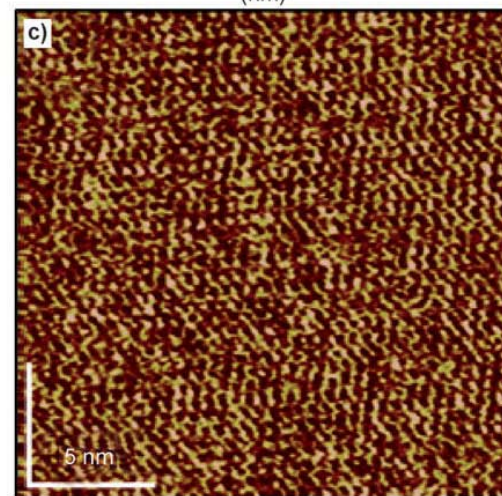
c) Side view of the core of the silicon sheet; the large yellow-green circles represent oxygen atoms, small red (Si) and green (Mg) circles represent the Si(111) plane in the layer below.

Soft Synthesis of Single-Crystal Silicon Monolayer Sheets

H. Nakano et al., Angew. Chem. Int. Ed. 45, 2006, 6303



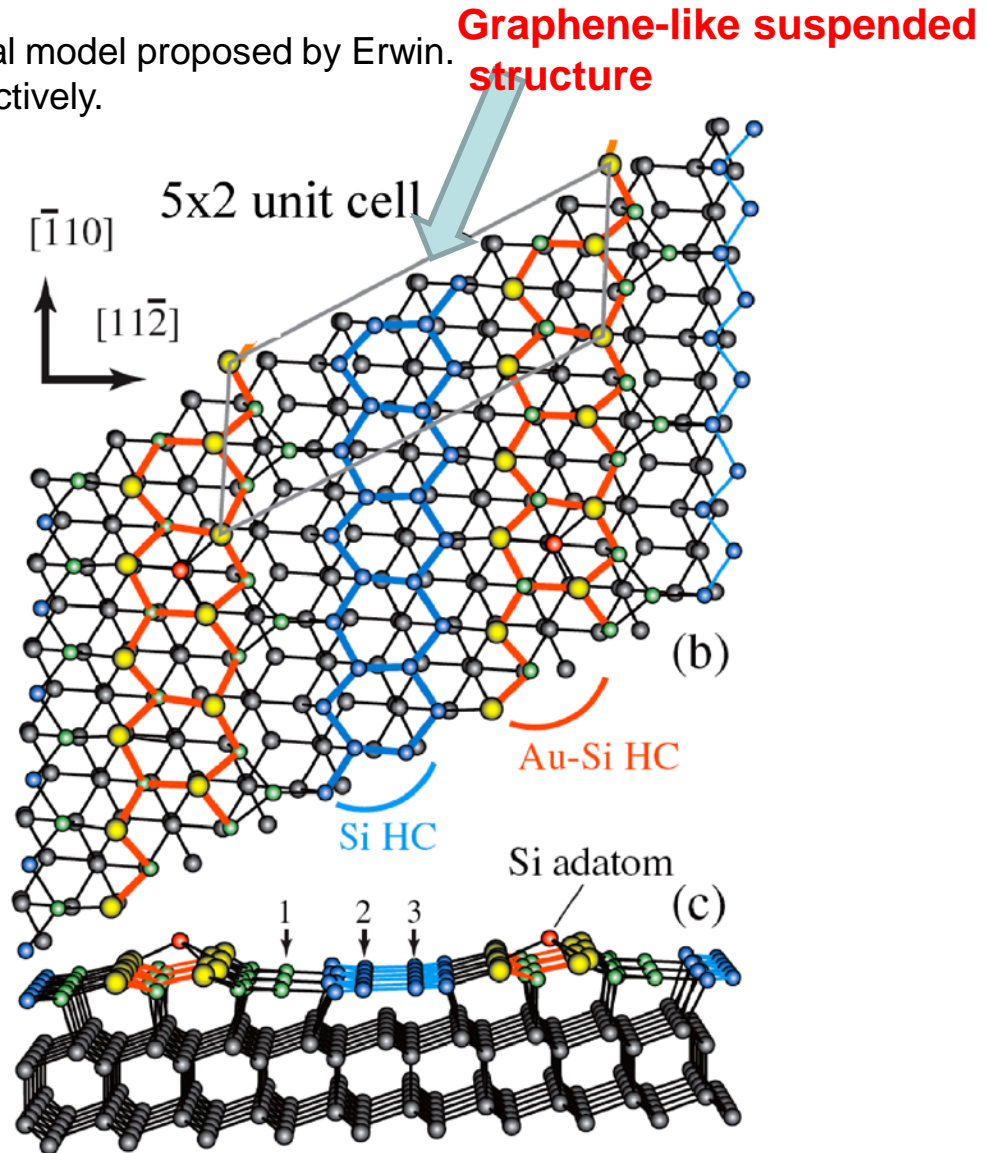
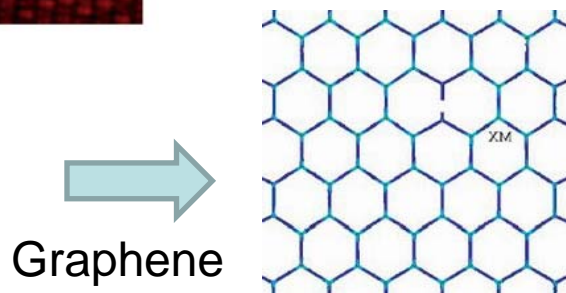
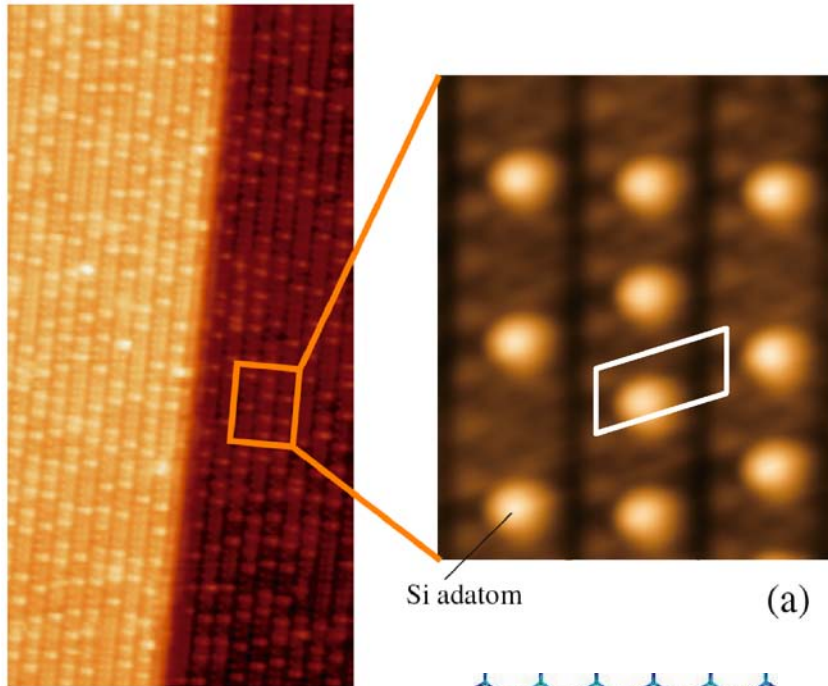
a) TEM image of the sheet. b) ED pattern recorded along the [001] zone axis perpendicular to the surface of the sheet. c) In-plane XRD scans with an incident angle of 0.28 (red line) and conventional θ - 2θ scans (blue line) of the silicon sheets.



Noncontact mode AFM image of the silicon sheets, and b) its line profile taken along the white line in (a). c) Atomically resolved AFM image of silicon sheets.

Si(111)5x2-Au surface

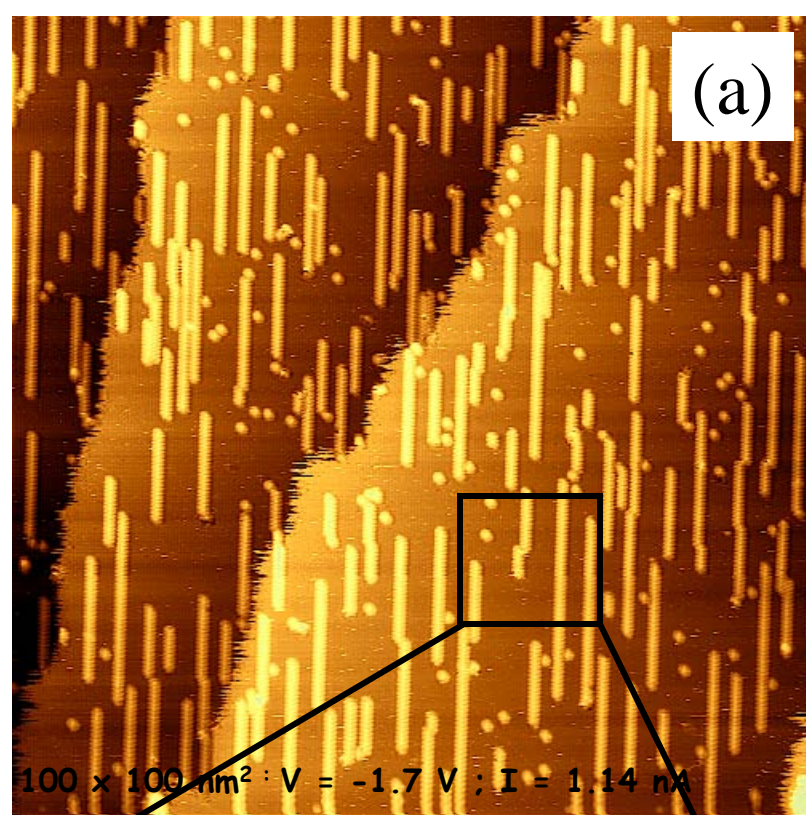
- a) 30x16.5 (nm²) STM image ($V_s = 1.5$ V) showing a step as well as the array of 1D atomic wires running along the $[-110]$ direction and a zoom-in (2.2x1.8 (nm²), $V_s = -1.0$ V) showing clearly the topographic atomic features
- b) and c) show the top and side view of the structural model proposed by Erwin. Large and small balls are Au and Si atoms, respectively.



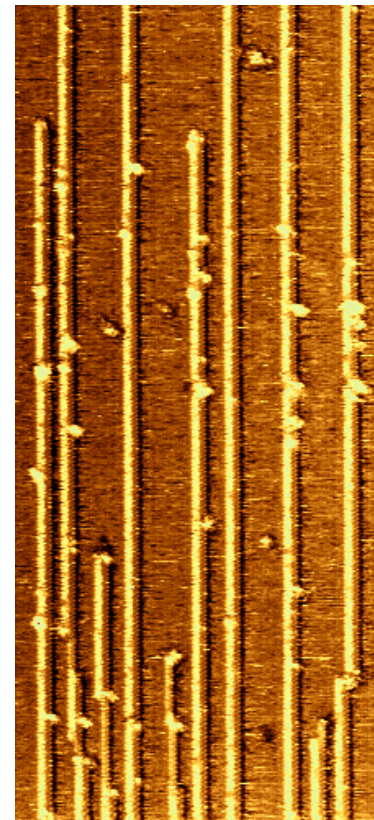
Si/Ag(110)

Annealing at 230°C

(a)



(b)

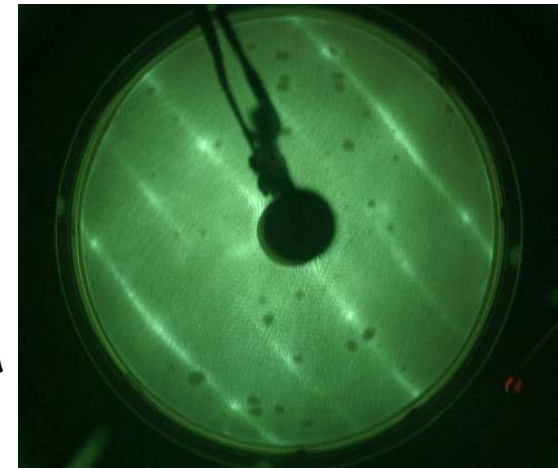


x2 periodicity along the [1-10] direction

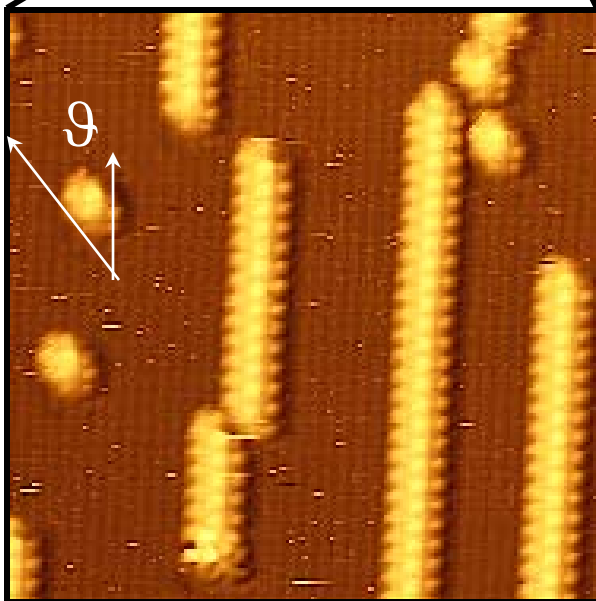
Lengths:
>100 nm



(c)



RT



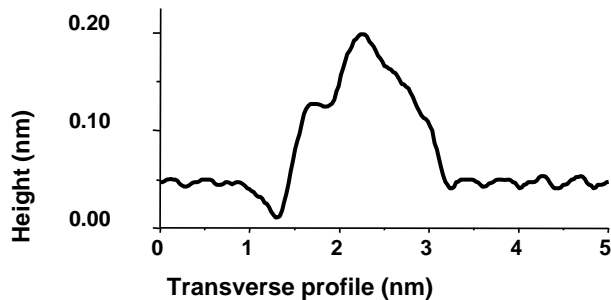
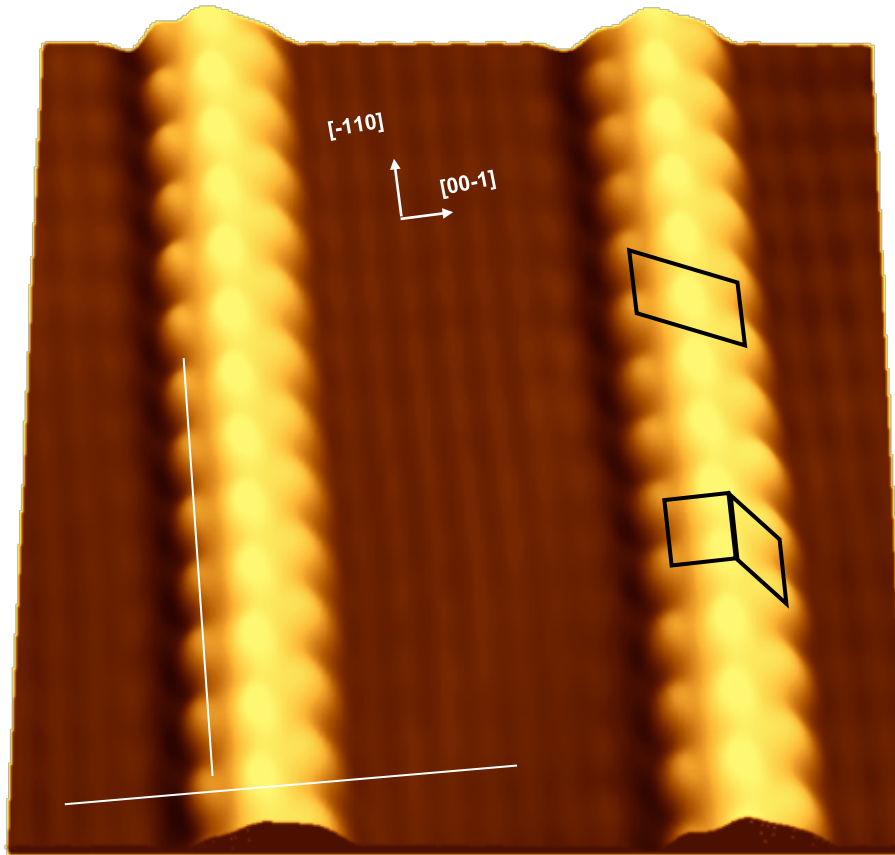
[1-10]
[001]

Ag(110)

Si stripes

~ 0.4 monolayer Si on Ag(110)

Broken symmetry!



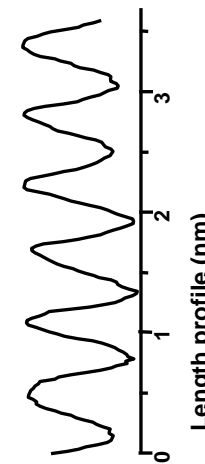
“Magic” width of
~ 1.6 nm

x2 periodicity along
the edges

Repeat unit:
parallelogram
or
square-plus-losange

Dip on the left side

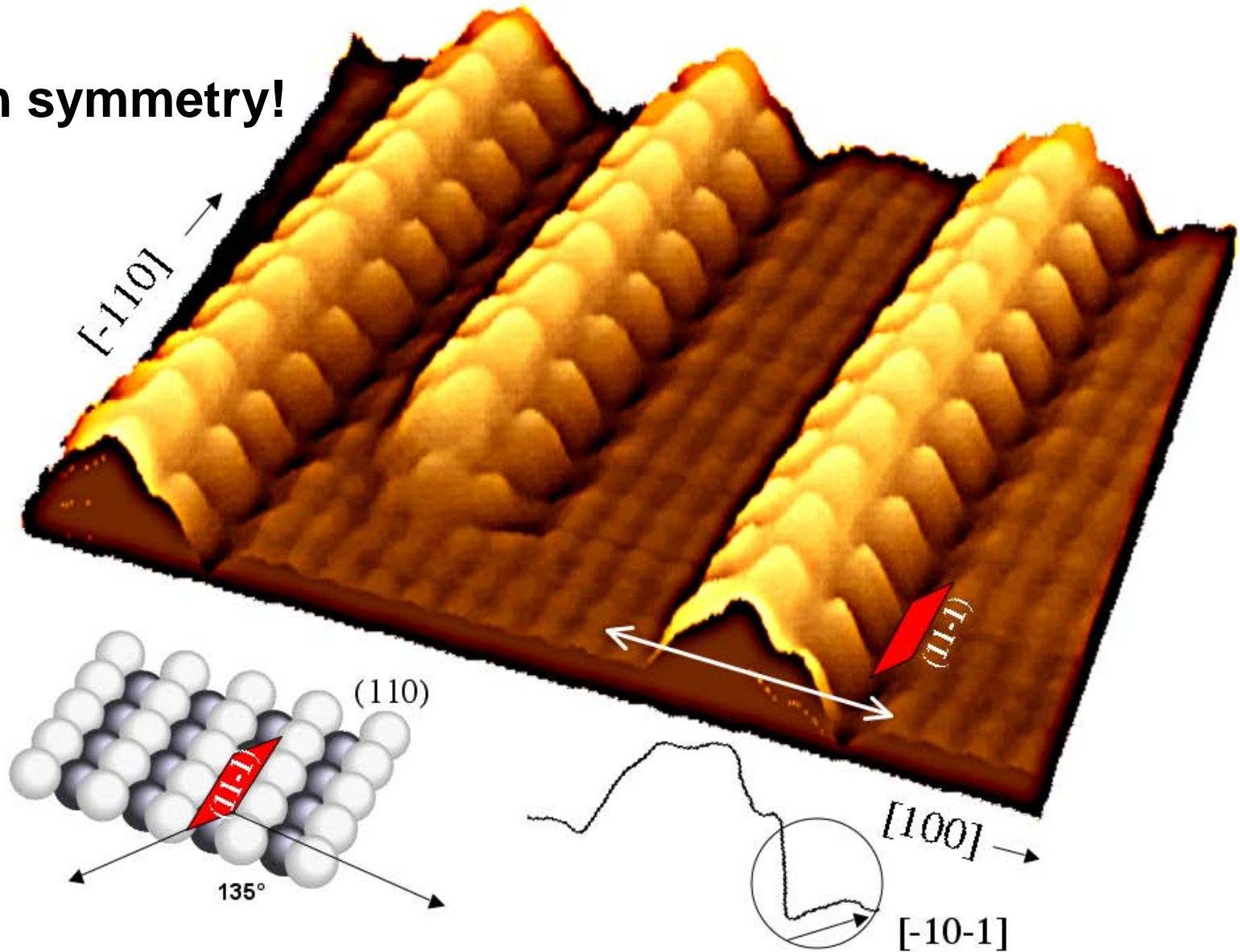
Glide of one lattice
parameter along the
[-110] direction of the
right versus left side
protusions



x2 periodicity
induced on the bare
Ag(110) surface!

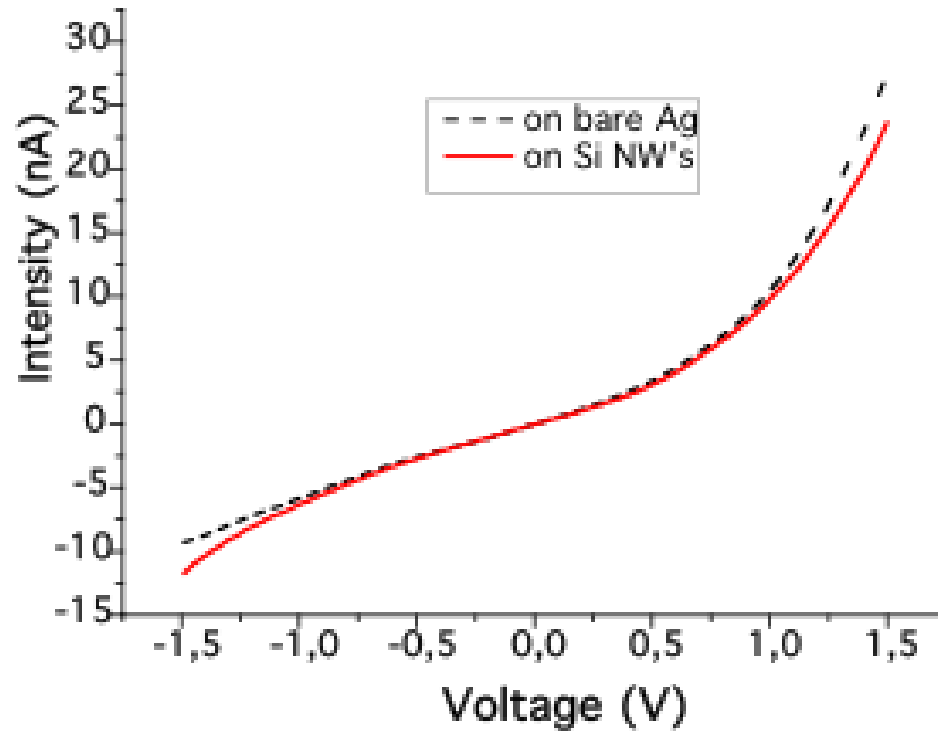
Self-organization into large “magnetic-like” domains

Broken symmetry!

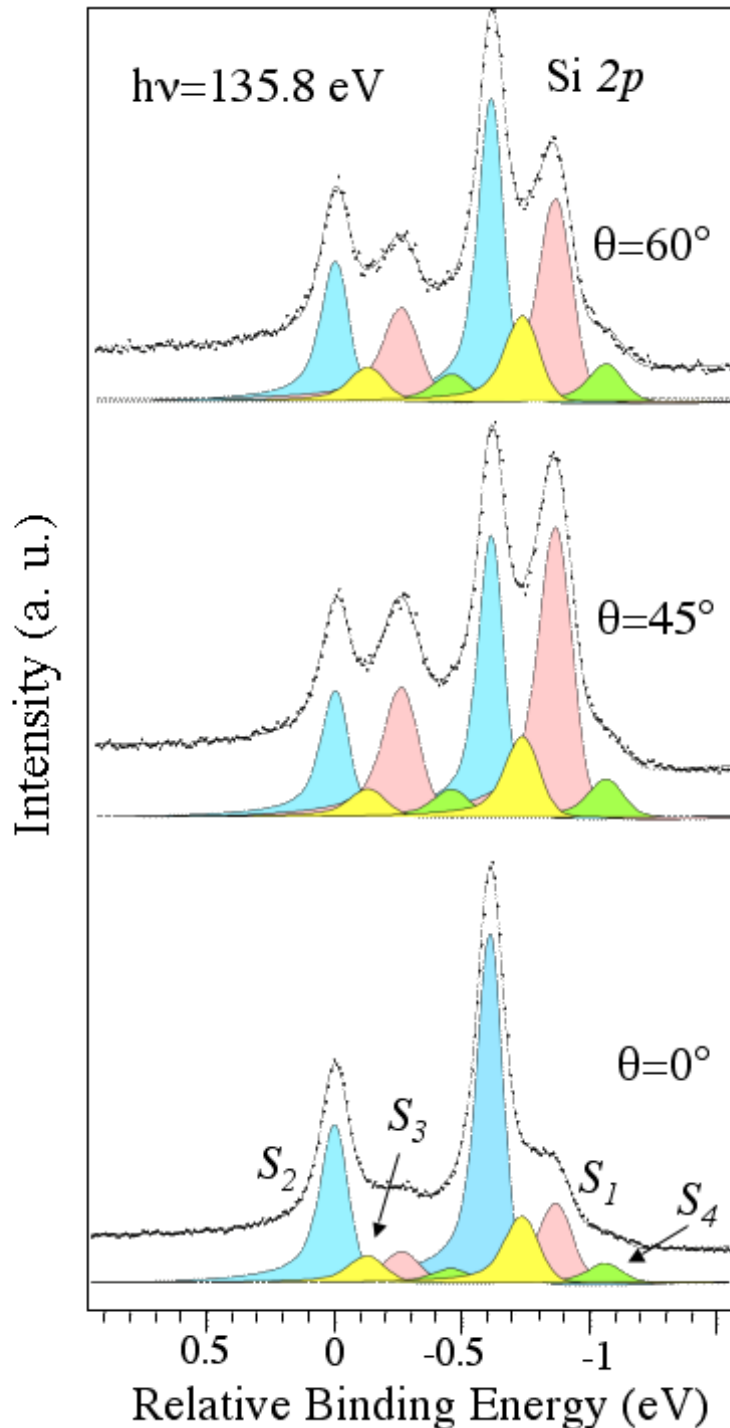


3D view of $10.2 \times 10.2 \text{ nm}^2$ filled-states STM image: dip asymmetry on the right-side

Metallic character



I-V characteristic of 0.5- ML of Si on Ag(110).



Normal ($\vartheta=0^\circ$)-, ($\vartheta=45^\circ$)- and grazing ($\vartheta=60^\circ$)- emission convoluted Si 2p core levels from SiNWs after the deposition of 0.5- ML of Si on Ag(110). PES measurements @ 150K

Synthesis with spin-orbit splitted Doniach-Sunjich functions: 4 doublets

Parameters: S.O. = 609 ± 5 meV
B.R. = 0.53

$\alpha = 0.122 \rightarrow$ strong metallic character

Gaussian FWHMs: just 95 meV for S2,
135 meV for S1,S3,S4

Lorentzian FWHMs:

Koster-Cronig transition: $\Gamma_{1/2} > \Gamma_{3/2}$ by 15 meV

$\Gamma_{3/2} = 25$ meV; $\Gamma_{1/2} = 40$ meV \rightarrow Coster-Kronig transition

Narrowest Si 2p core-levels ever seen in condensed matter physics:
atomically perfect Si stripes!

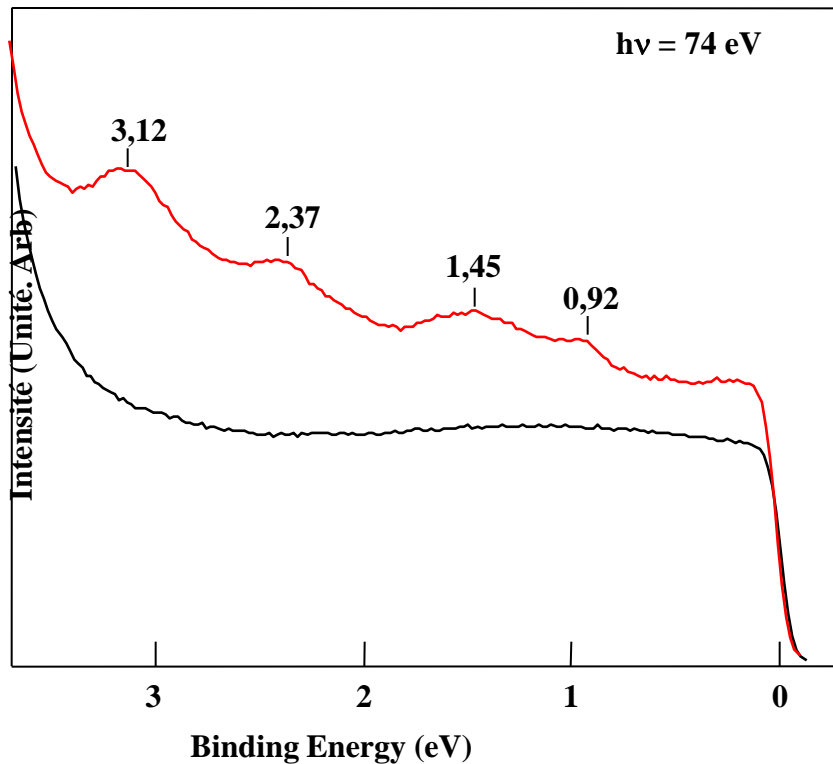
Electronic structure: Valence band PES, Ag sp region

$\theta \approx 0.5 \text{ ML}$

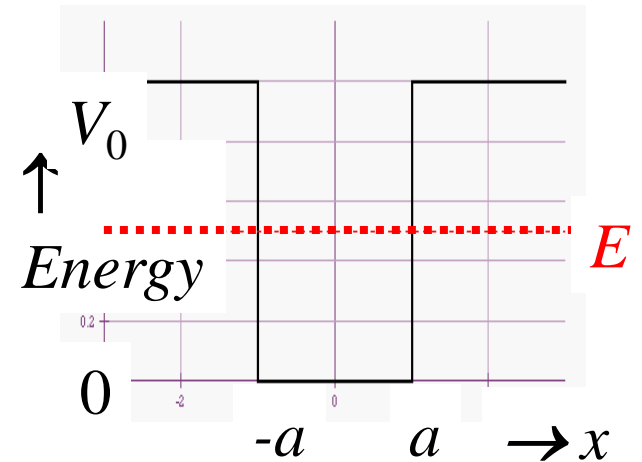
Discrete electronic states

Valence band, silver sp region

➔ Quantum Confinement

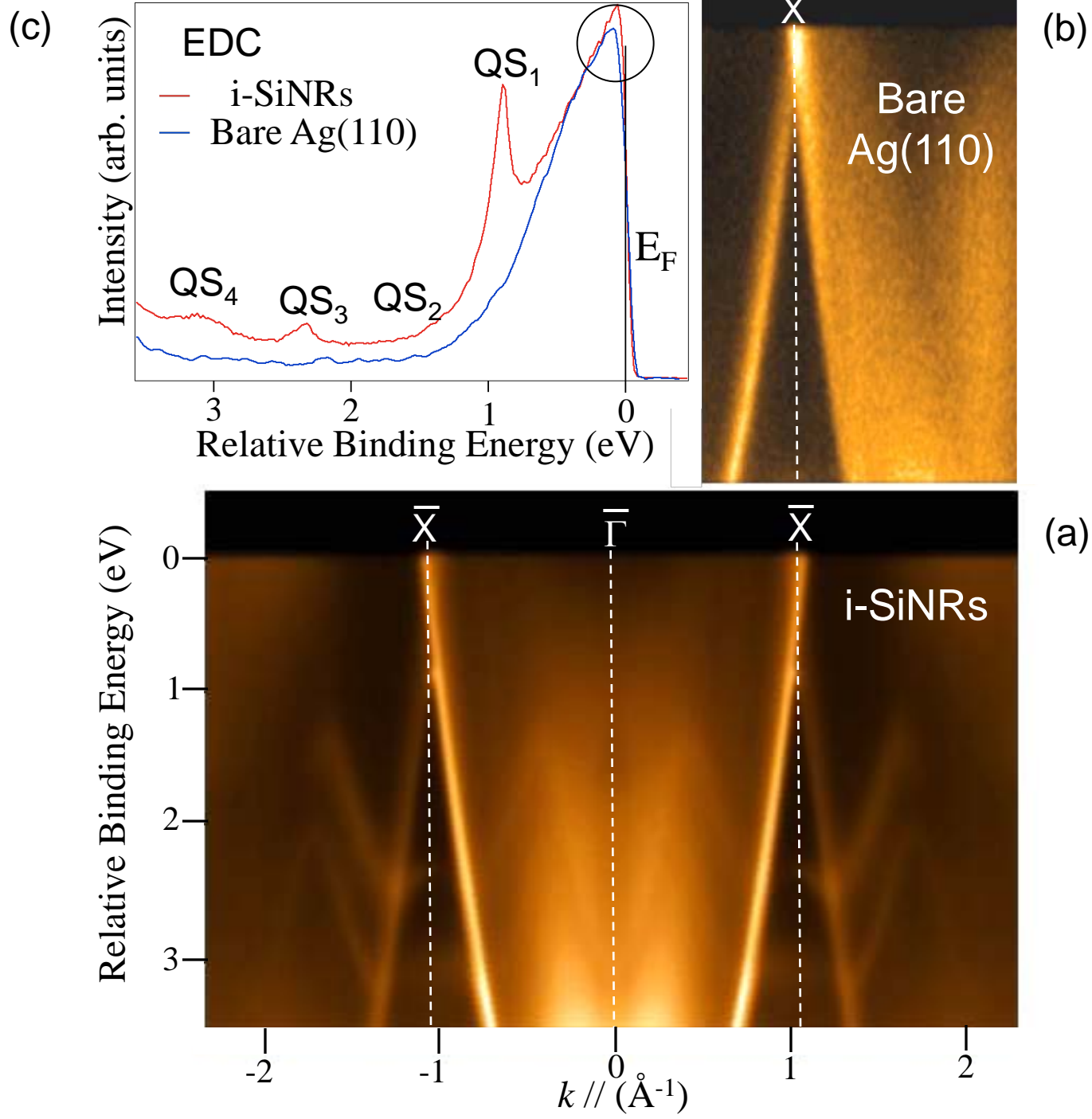


— Si/Ag
— clean Ag

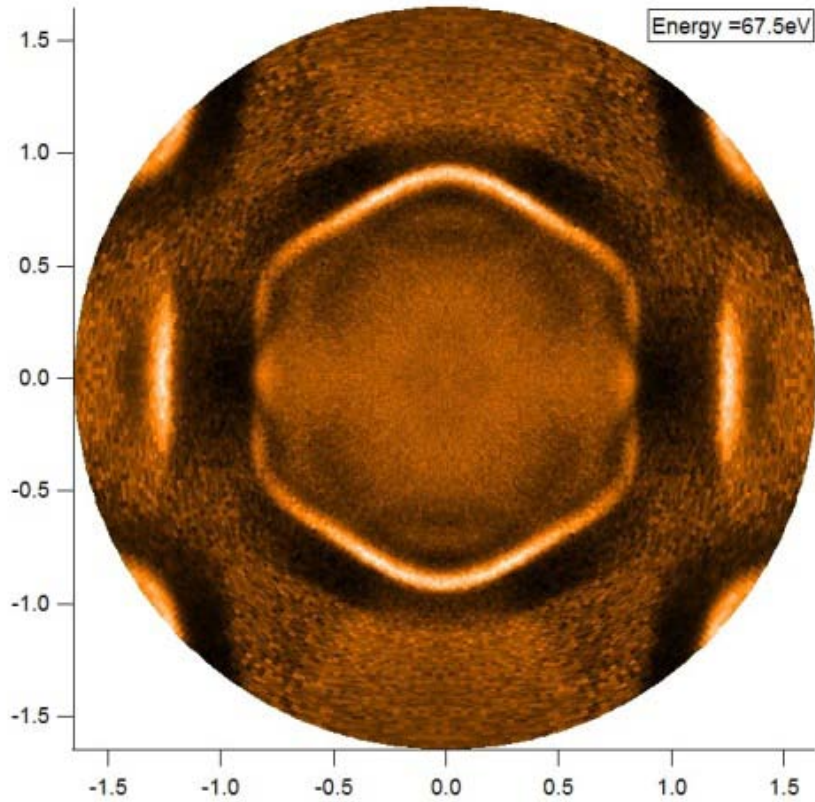


$V_0 \sim 3.7 \text{ eV}$, $2a = 16 \text{ \AA}$, $m \sim m_0$

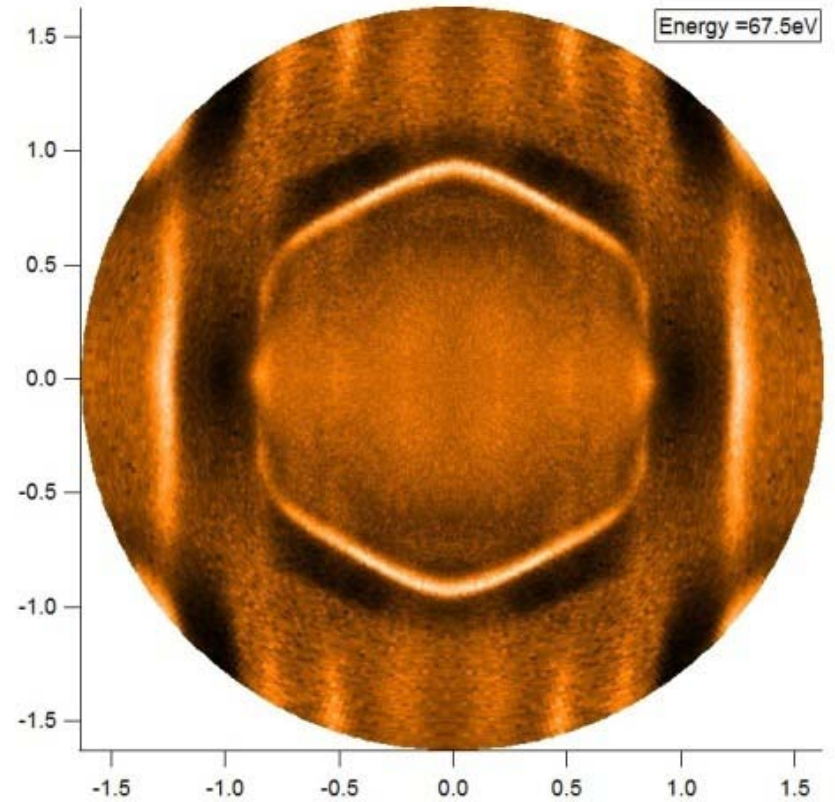
C. Léandri et al. Surface Sci. 574 (2005) L9



Constant energy slices

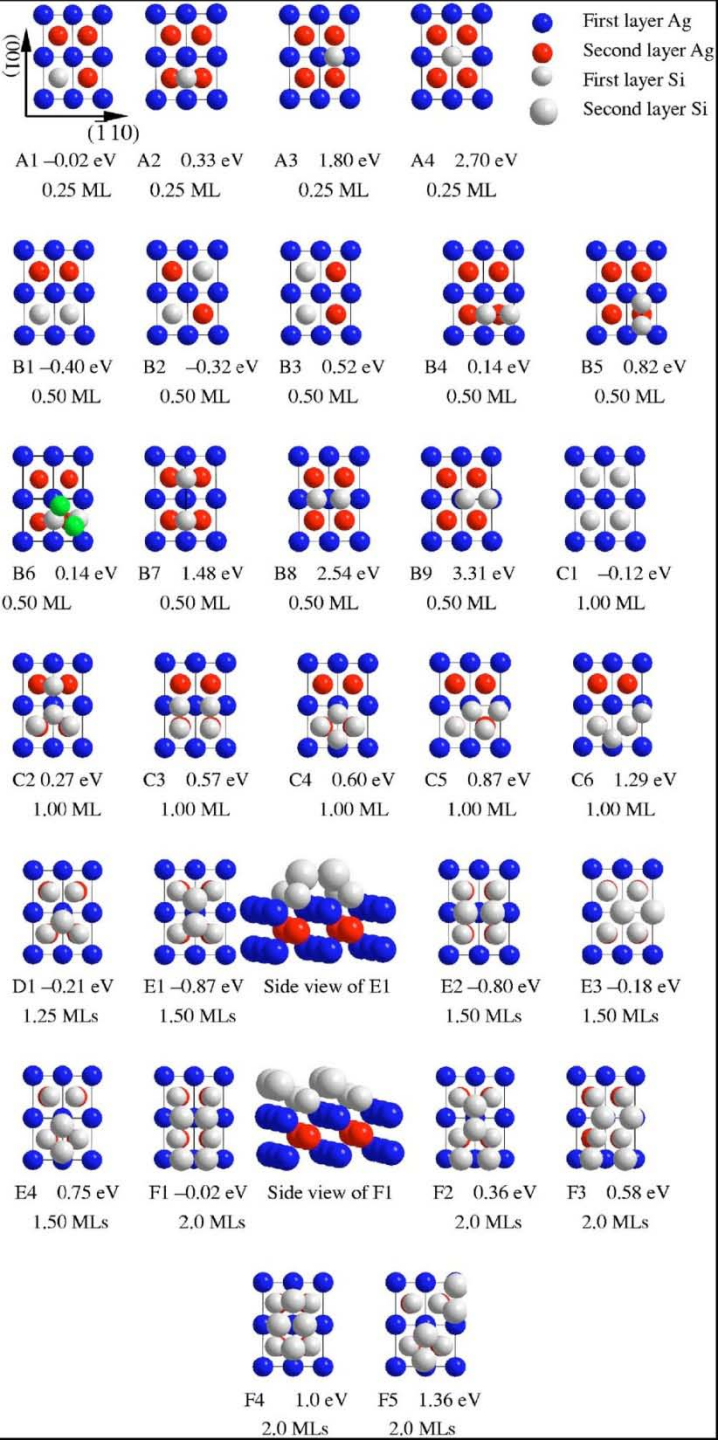


Bare Ag(110)

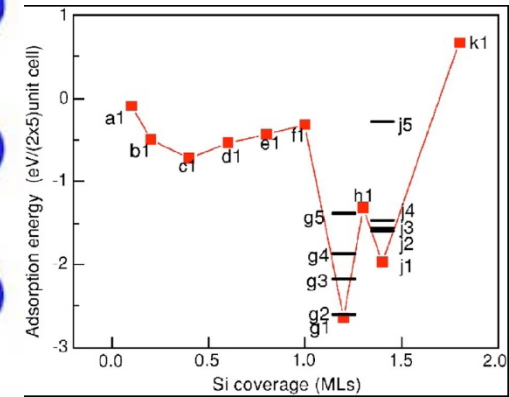
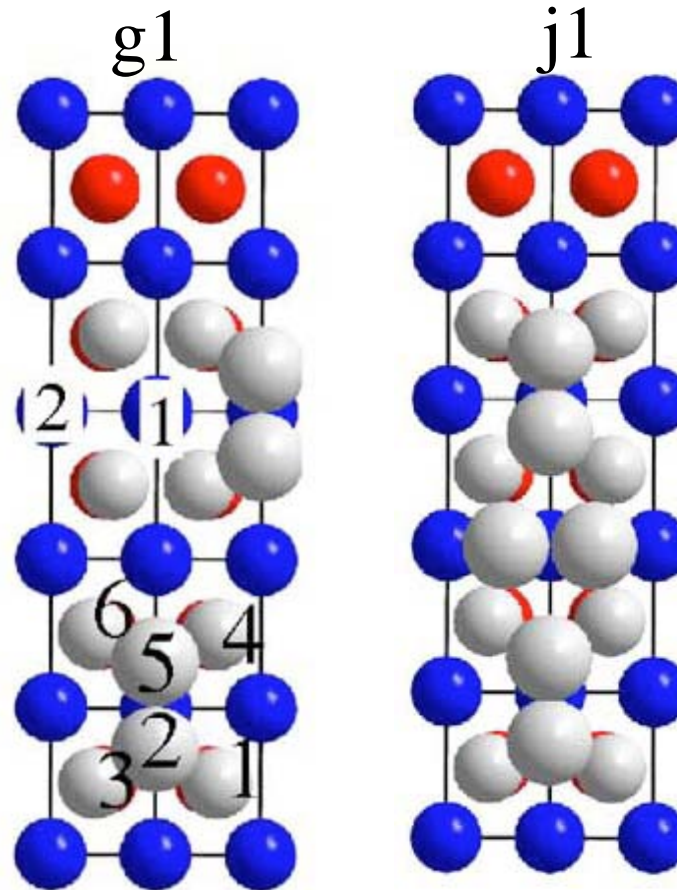


Si nano ribbons on Ag(110)

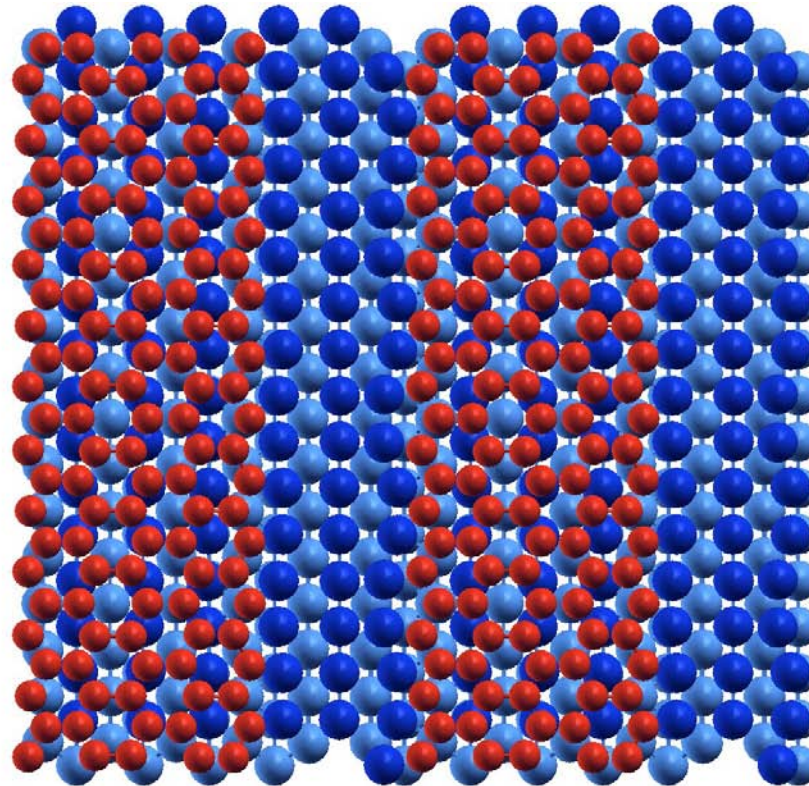
Atomic structure



Possible atomic geometries of Si adsorption on Ag(110) within the 2x5 unit cell for various Si coverages: DFT-LDA (SIESTA code)

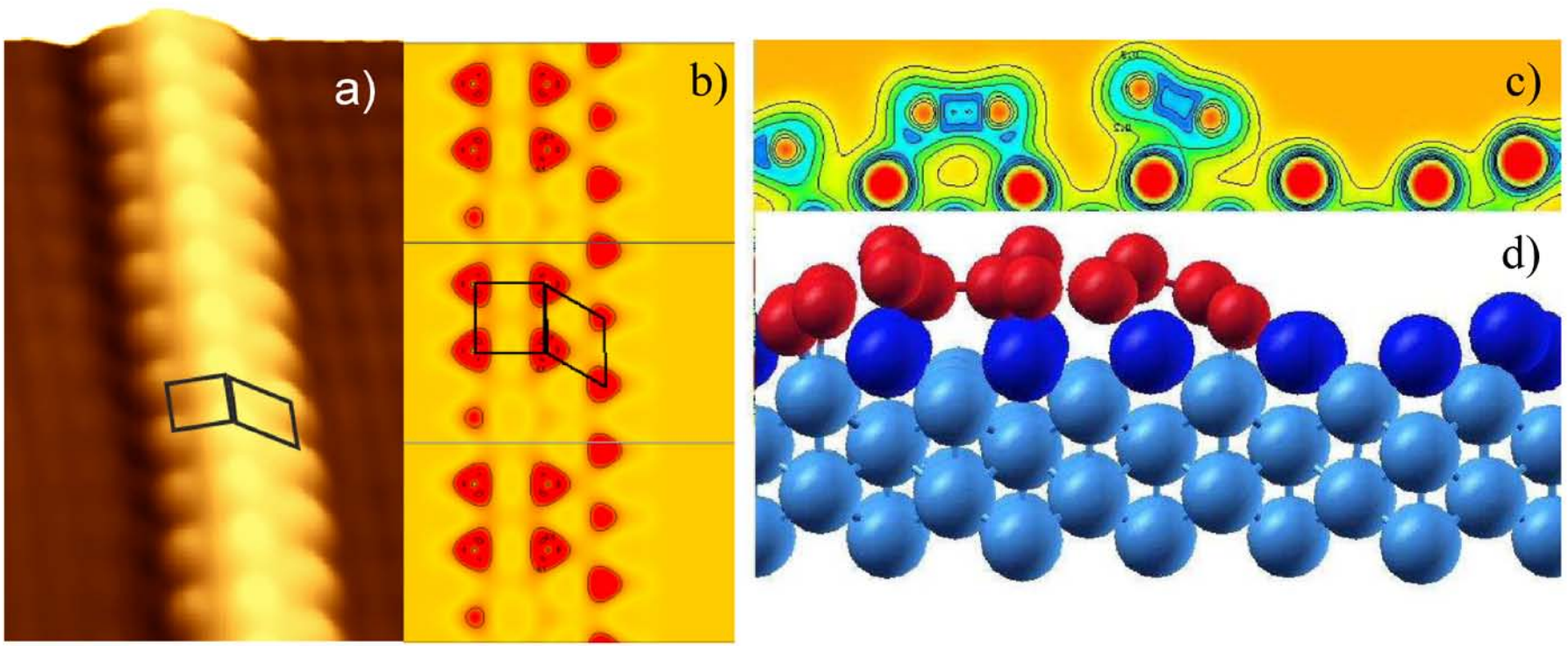


DFT-GGA (Vasp code) calculations

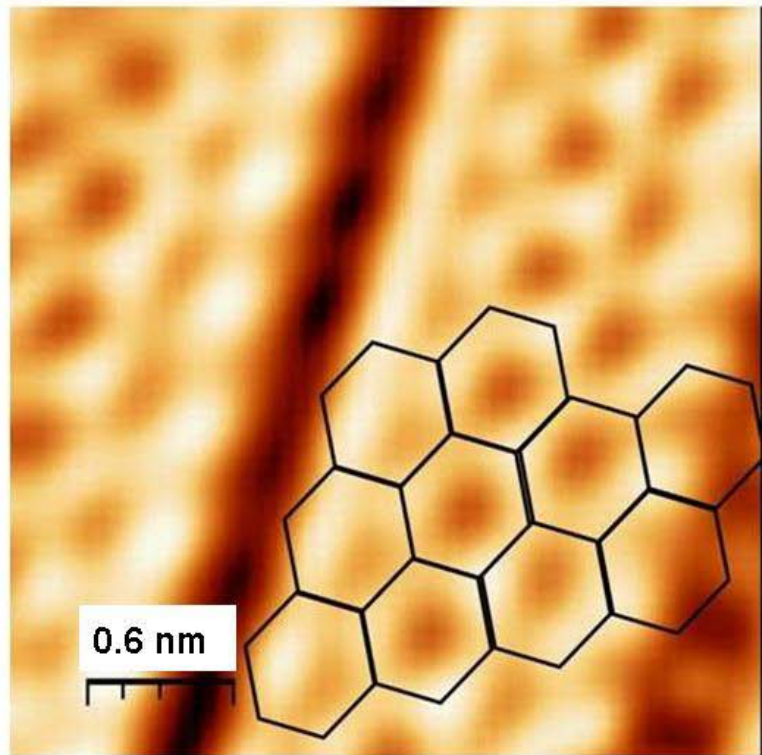


Top view of the configuration for the silicene **zig-zag** nano-ribbons with **4 Si hexagons**

- a) Geometrical aspect of the *silicene stripes*, a square joined to a parallelogram, drawn on the STM image.
- b) Charge density in a horizontal plane containing the topmost Si atoms.
- c) Charge density in a vertical plane containing some top most Si atoms.
- d) Side view showing the curved shape of the stripes (Si red balls).

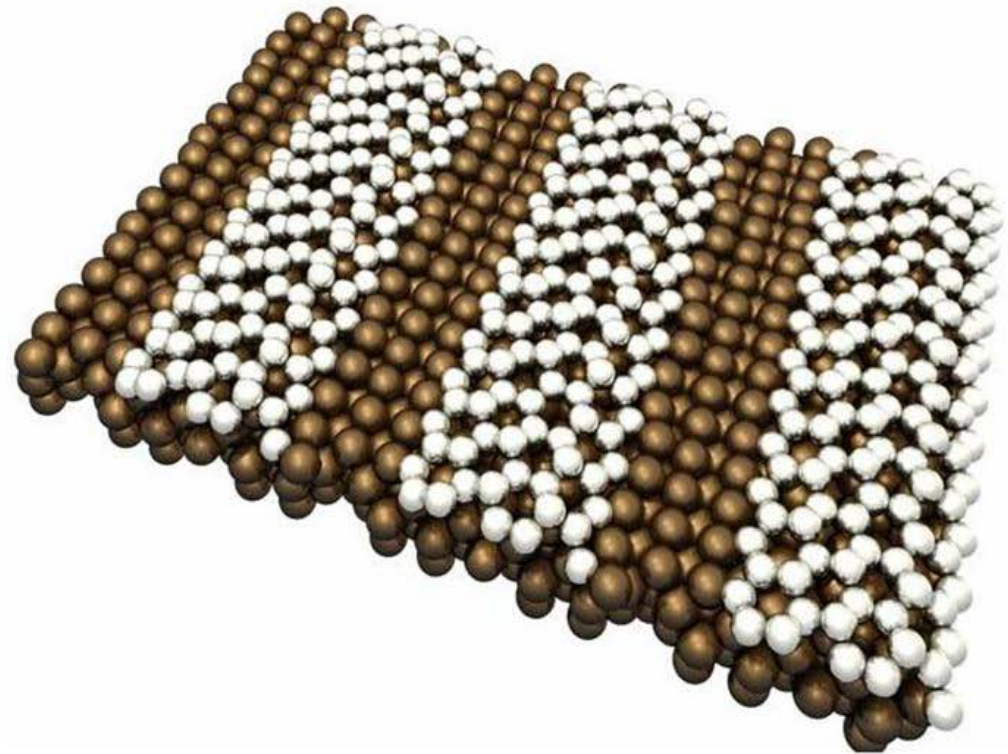


a) STM



b)

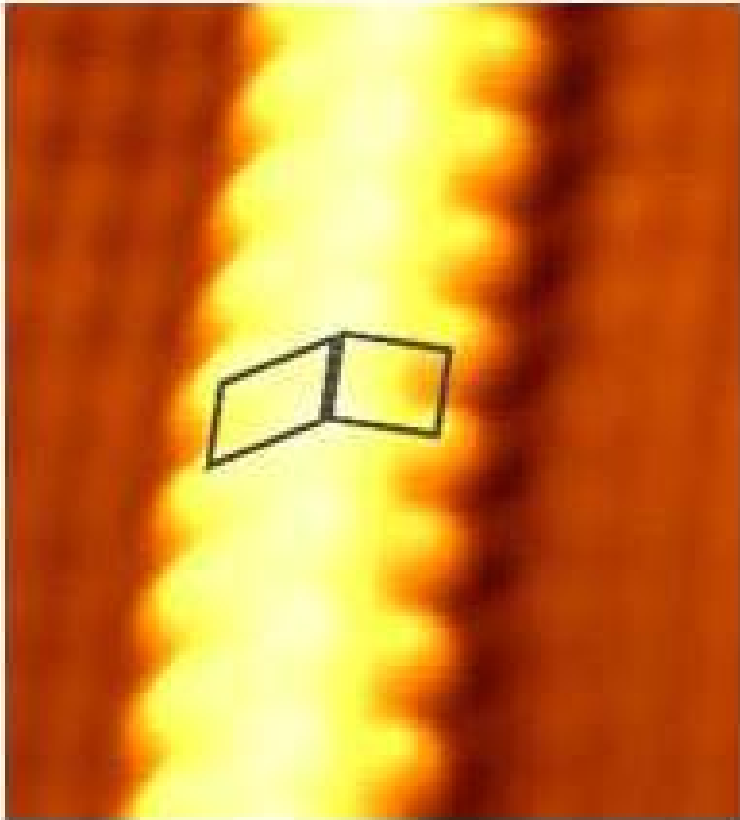
DFT calculations



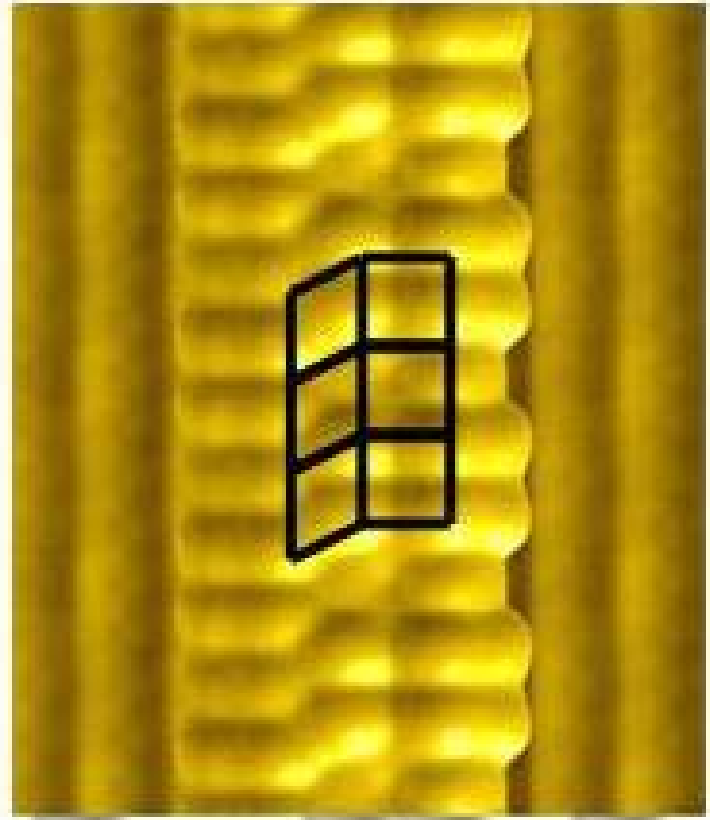
The honeycomb structure of the nanoribbons reveals that they are strips of graphene-like silicon sheets, i. e., true silicene stripes

Experimental & calculated STM images

a)

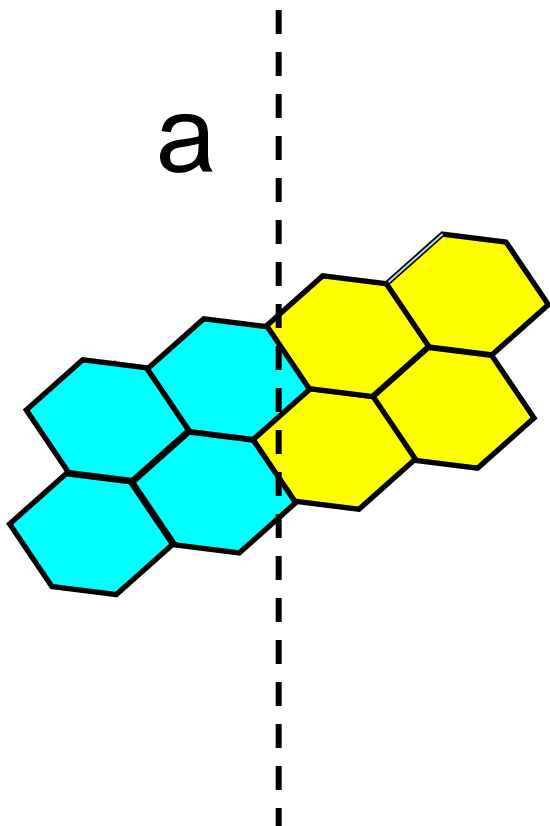


b)

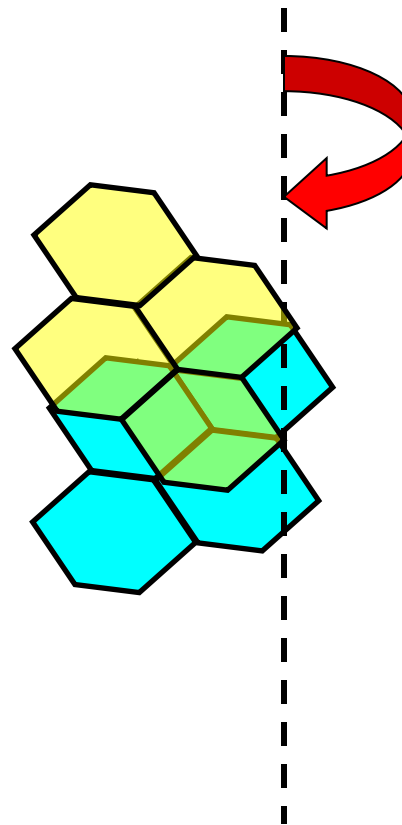


intrinsic chirality

a



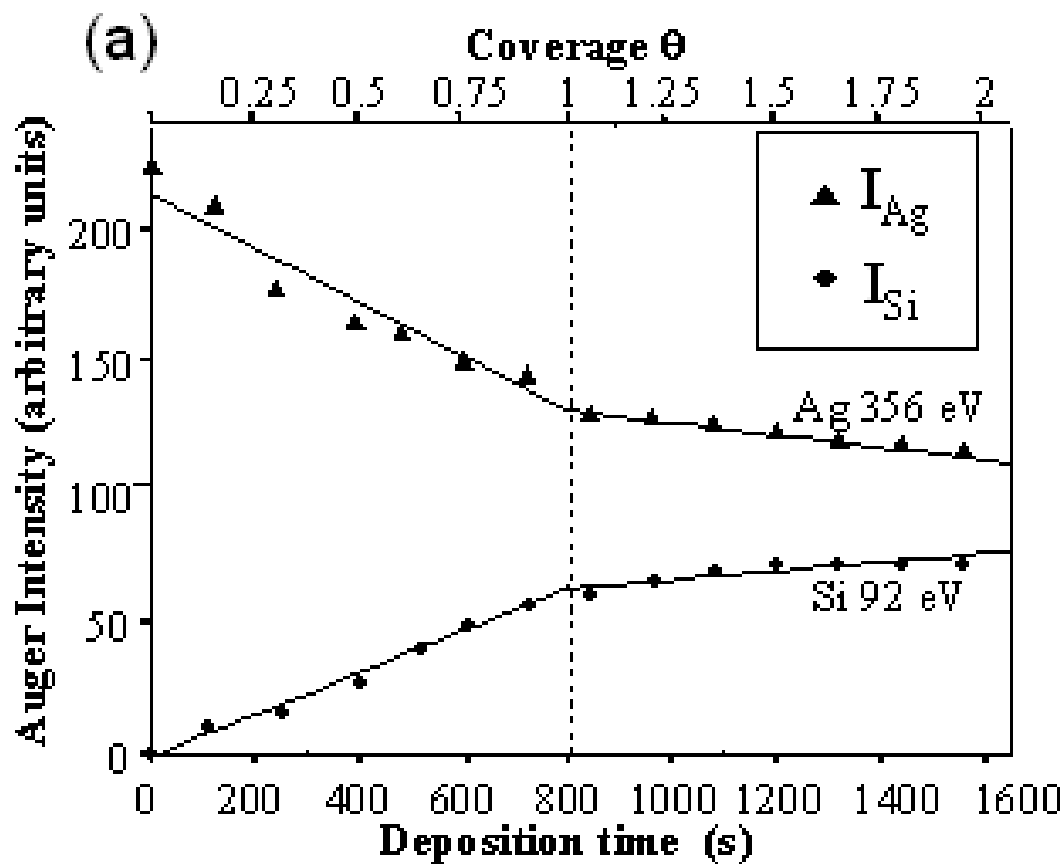
b



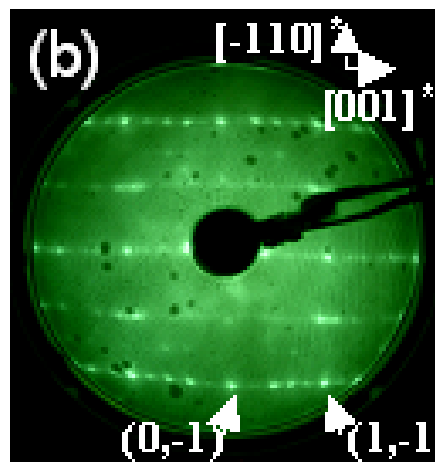
Mirror

Mirror

Formation of a grating
with a 2 nm pitch



**Growth by Si deposition
@ 200°C**

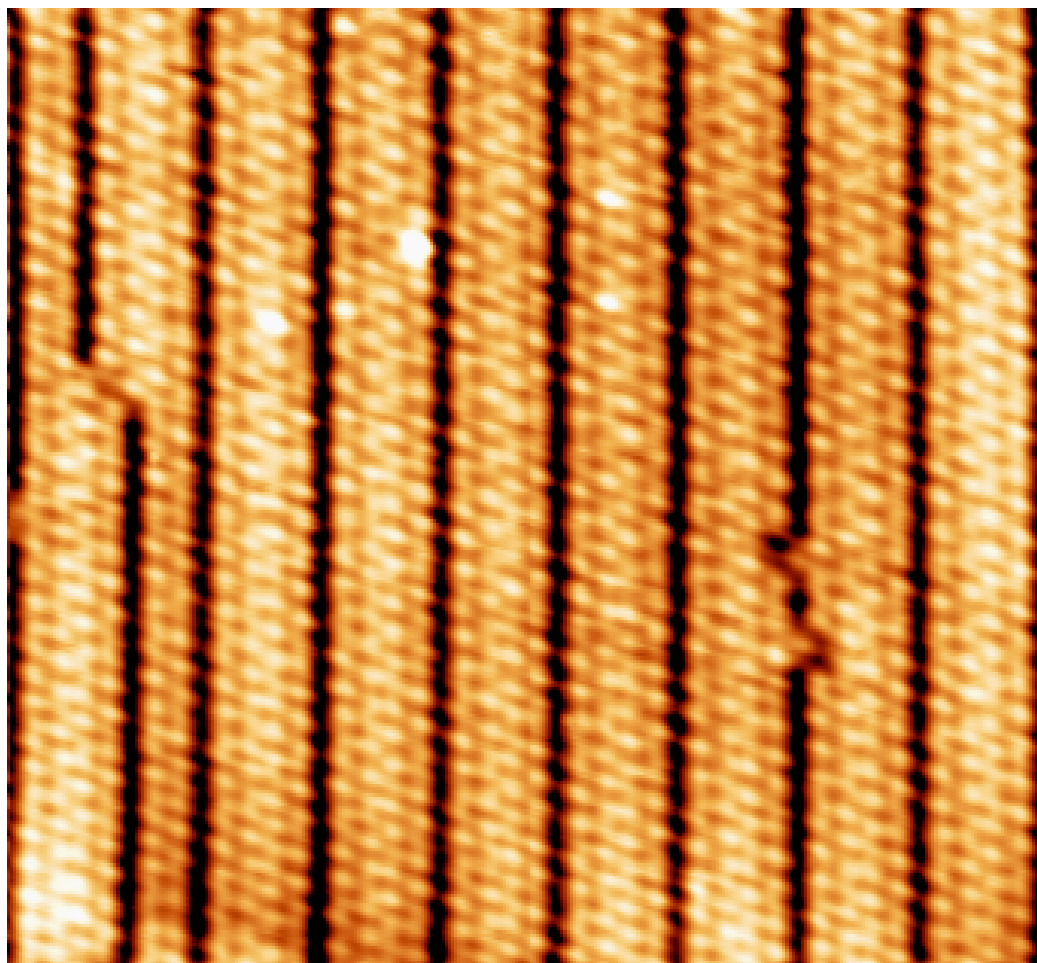
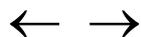


5x4 LEED pattern @ 43 eV

A grating with a pitch at the molecular scale: ~ 2 nm

Periodic self-organization of Si nano-ribbons in a lateral superlattice

~ 2 nm



22 x 20 nm²

190 pA ; - 3.3 V

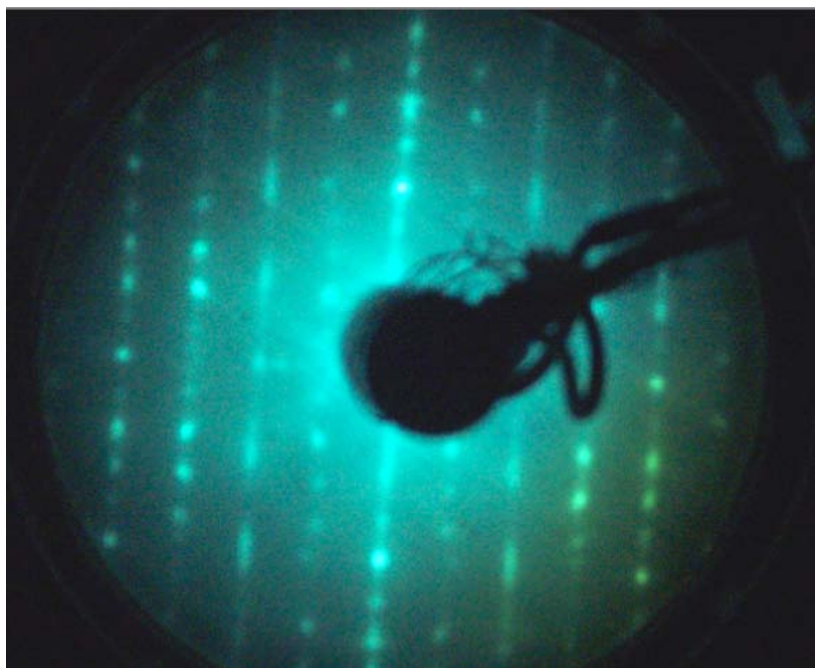
Upon growth at 200°C, these Si stripes self-assemble by lateral compaction to form at macroscopic scale a 1D grating with a pitch at the molecular scale

5x4 Si/Ag(110)

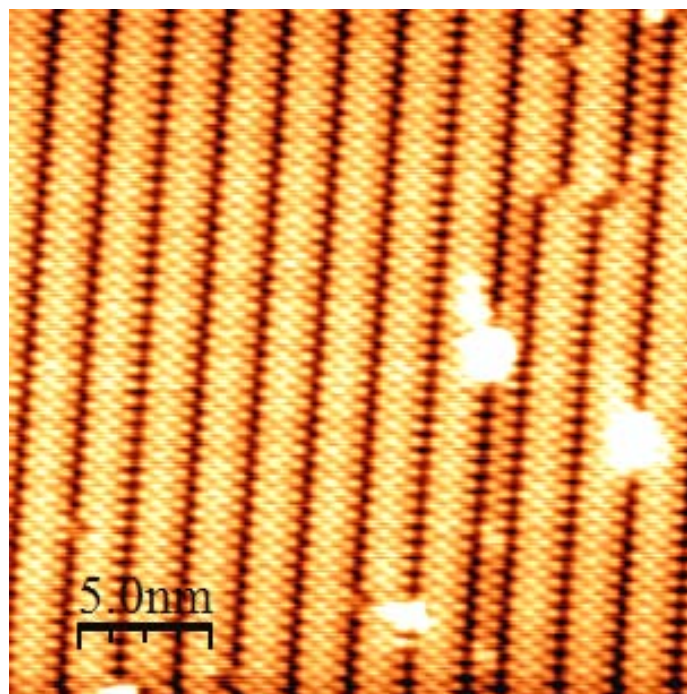
T = 4.48 K

↑ [100]

LEED



STM Filled-states



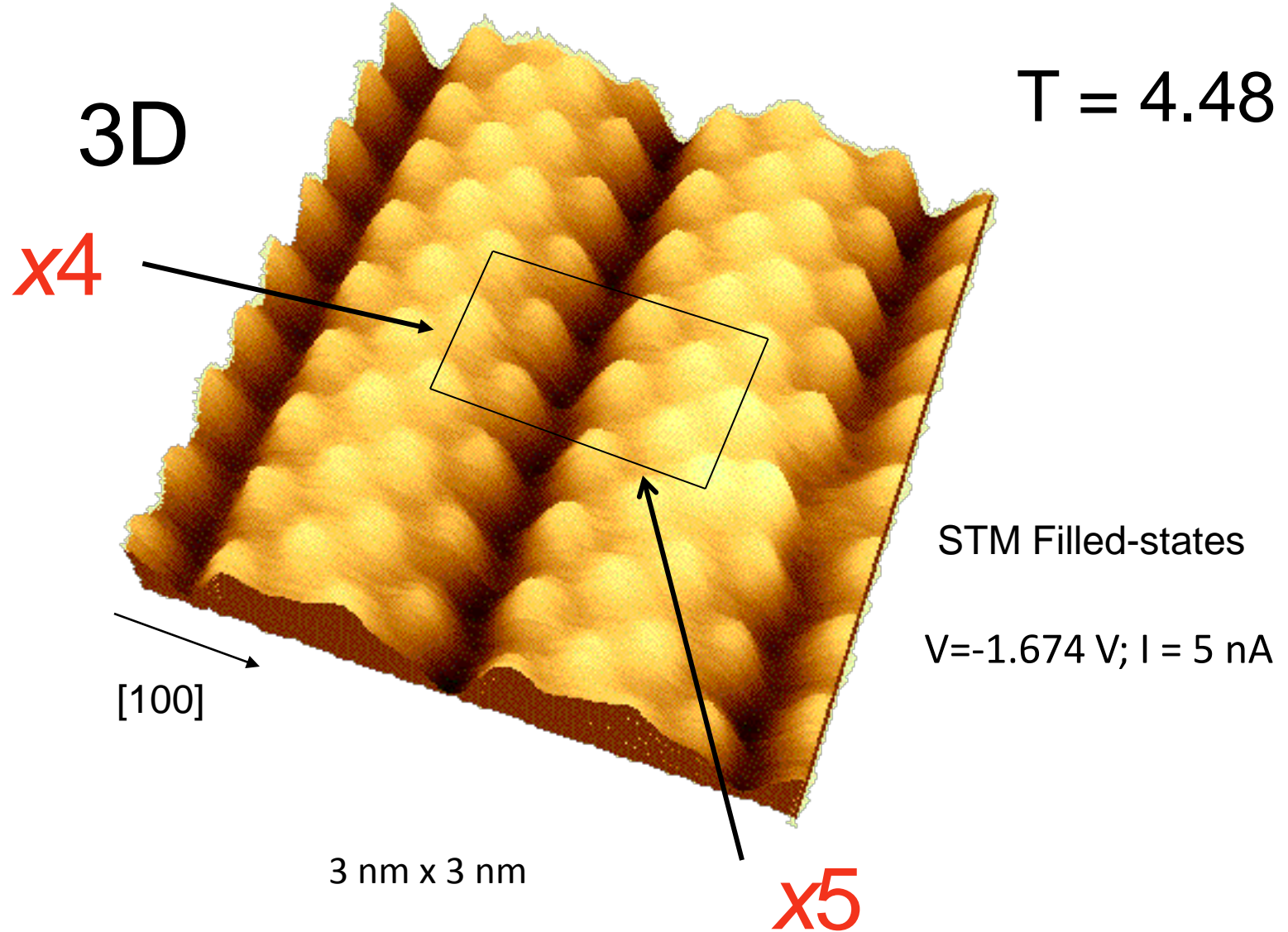
→ [100]

25 nm x 25 nm

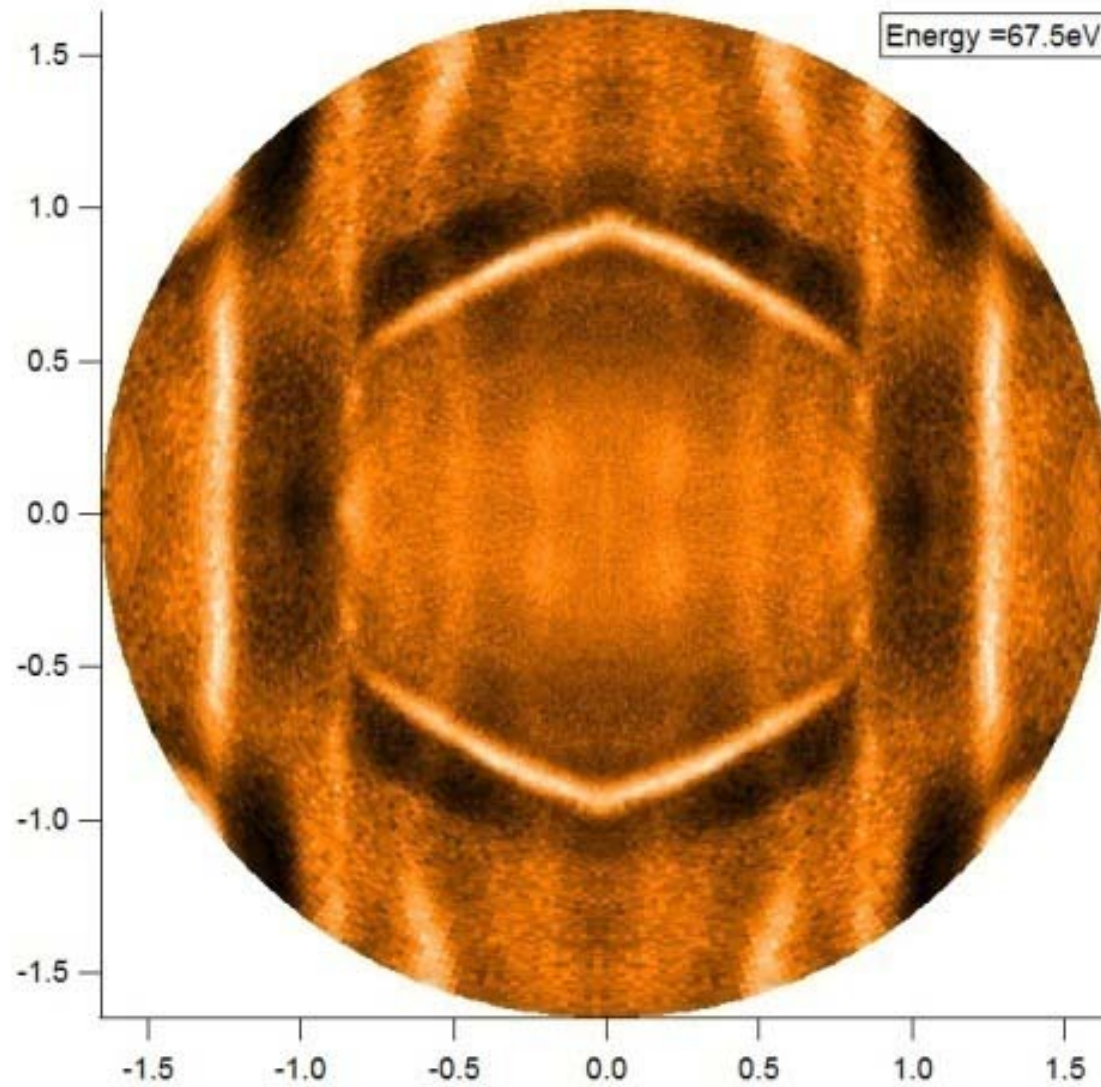
V=-1.674 V; I=5 nA

5x4 Si/Ag(110)

T = 4.48 K

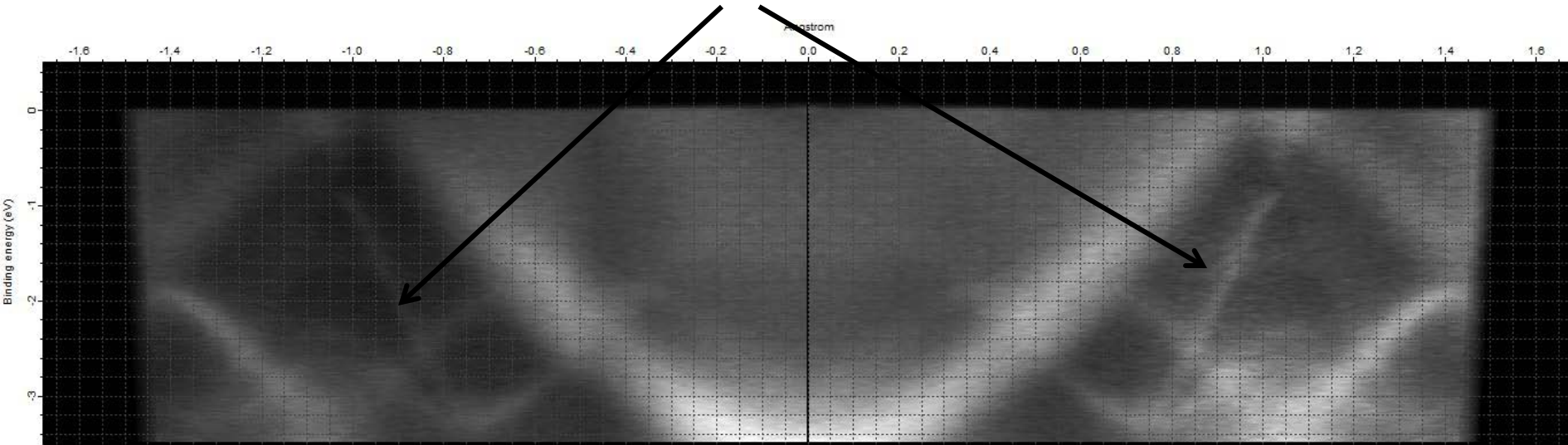


Constant energy slice

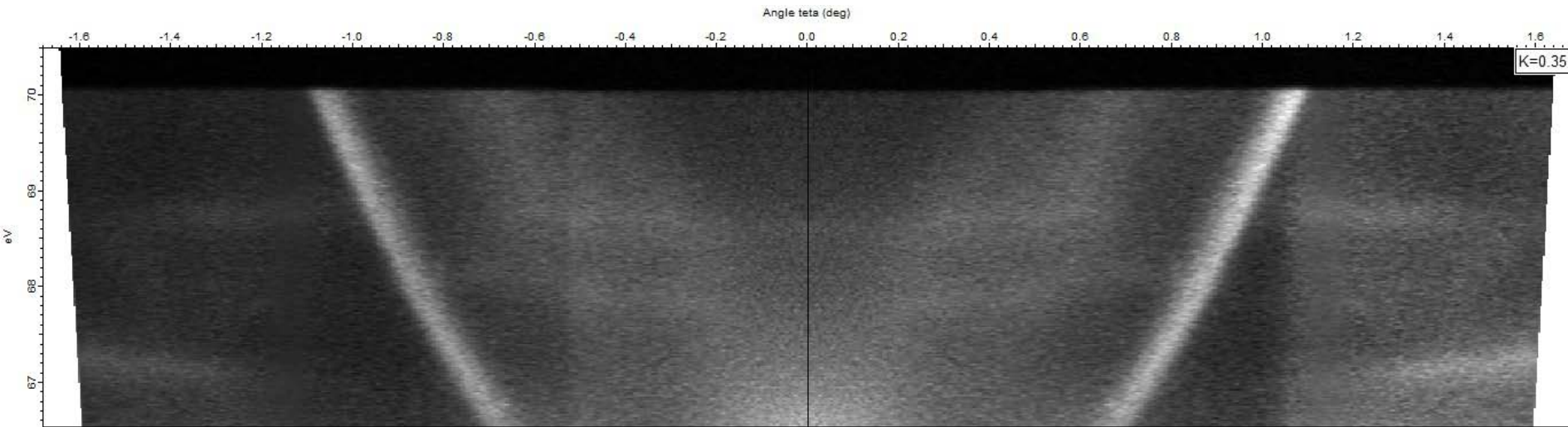


5x4 lateral superlattice

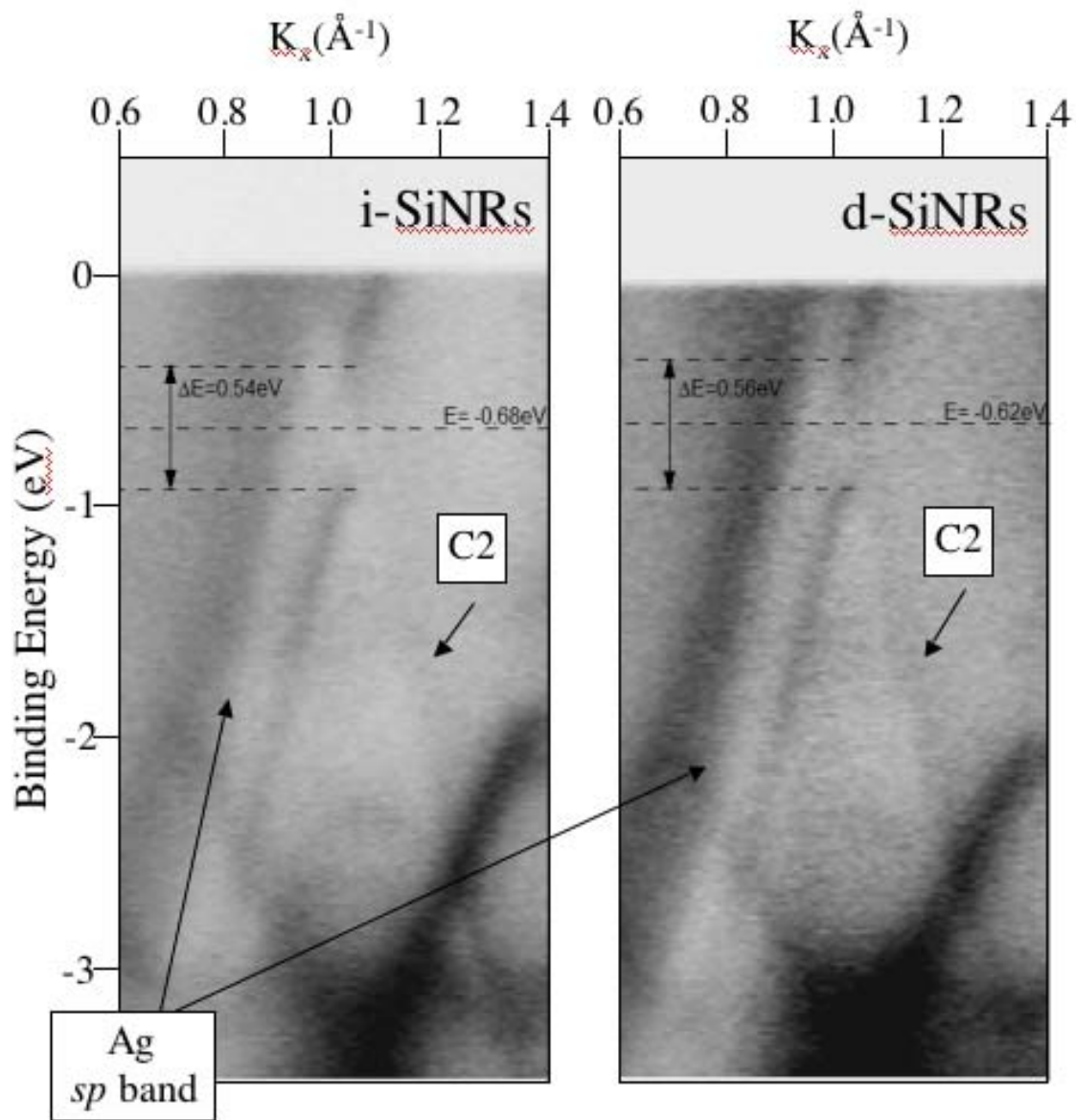
Dispersion along the stripes: linear portions point to **massless Dirac fermions**



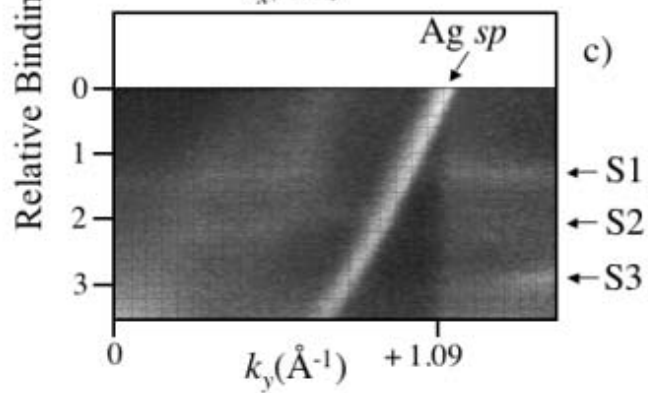
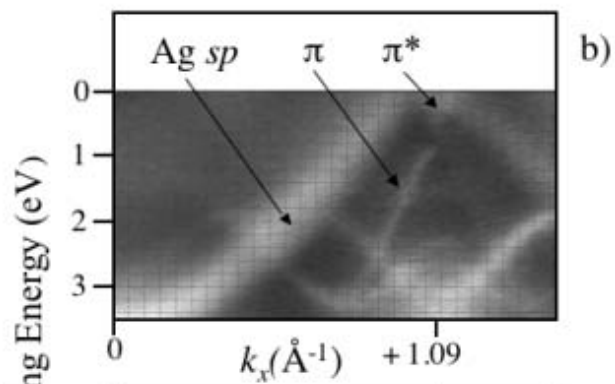
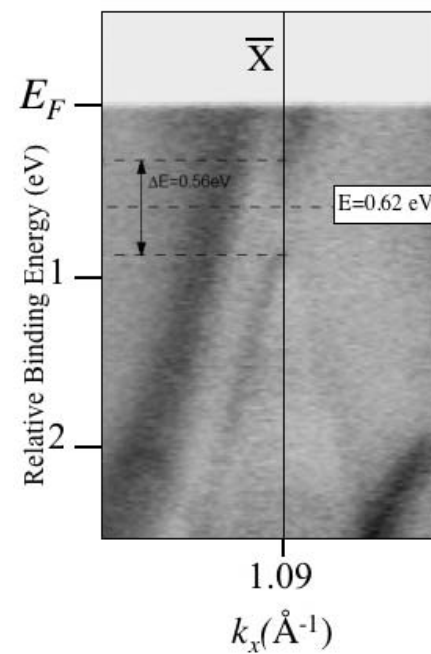
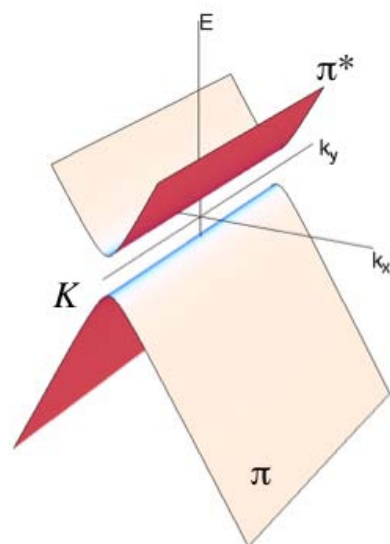
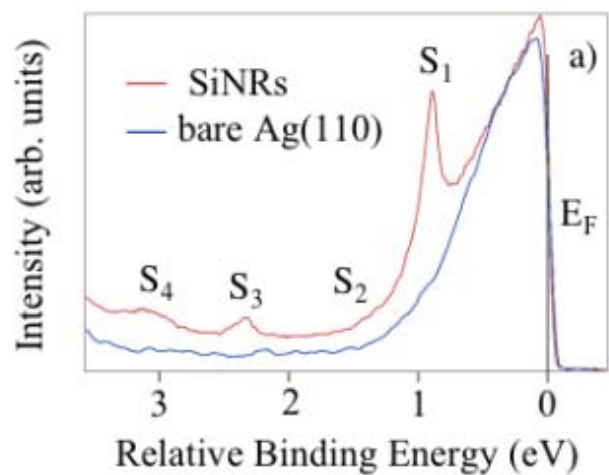
Dispersion along the stripes



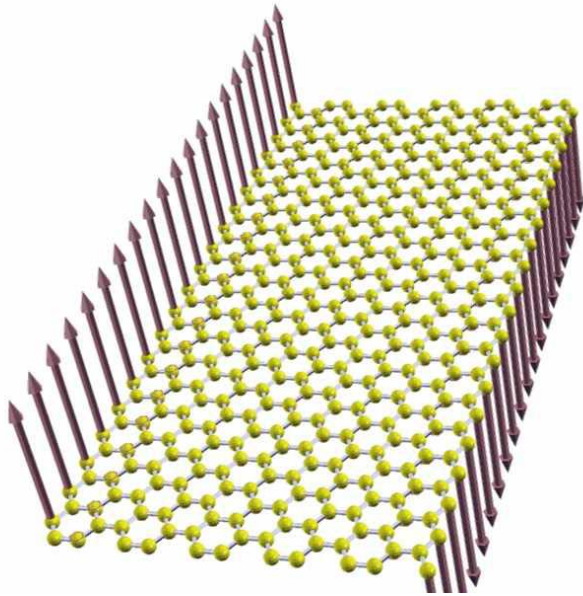
Only very weak dispersion perpendicular to the stripes



Horizontal slices $I(E, k_x)$ integrated on k_y from 0.55 to 0.7 \AA^{-1} for
 (left) isolated SiNRs and (right) 5×4 dense array $K \Leftrightarrow 1.06 \text{ \AA}^{-1}$

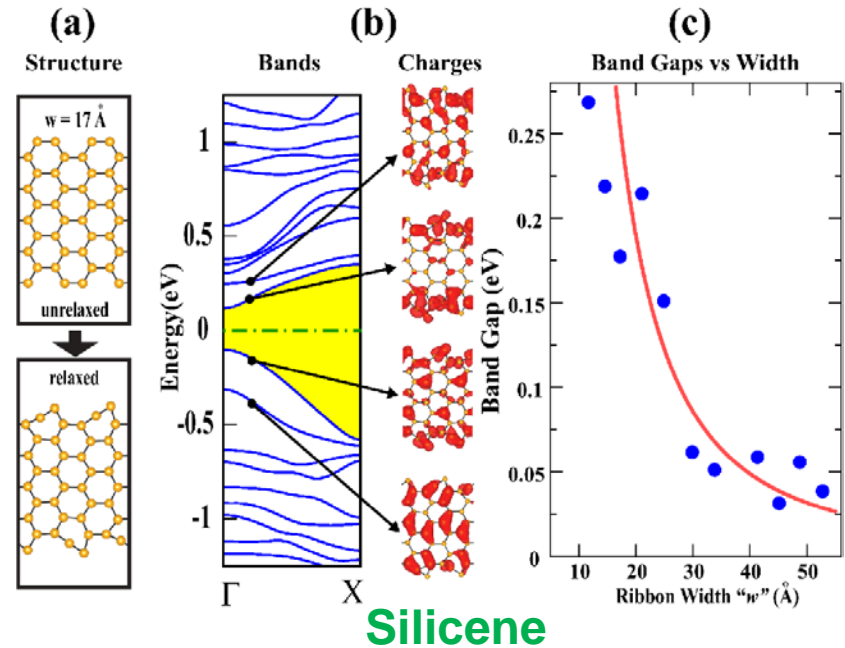


Silicene versus graphene nano ribbons

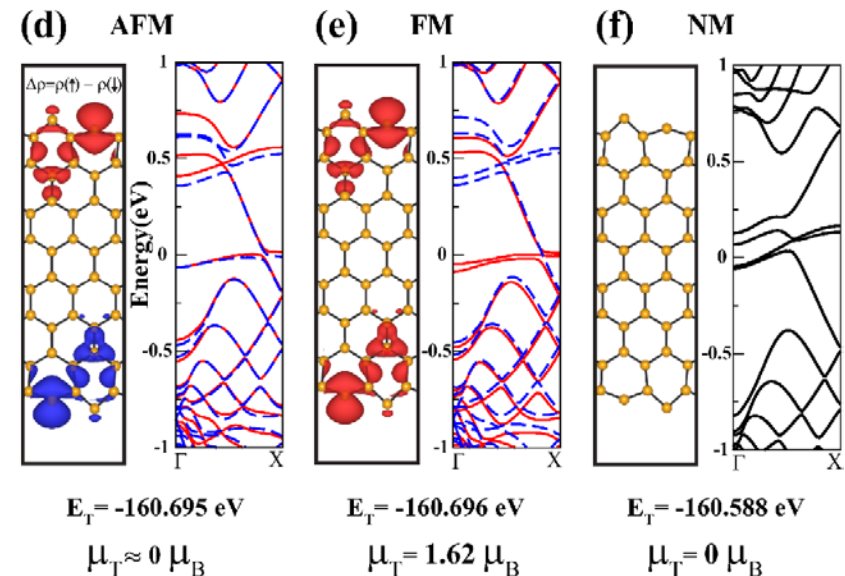


Graphene nanoribbon showing spin-polarized edge states

Armchair Ribbons



Zigzag Ribbons

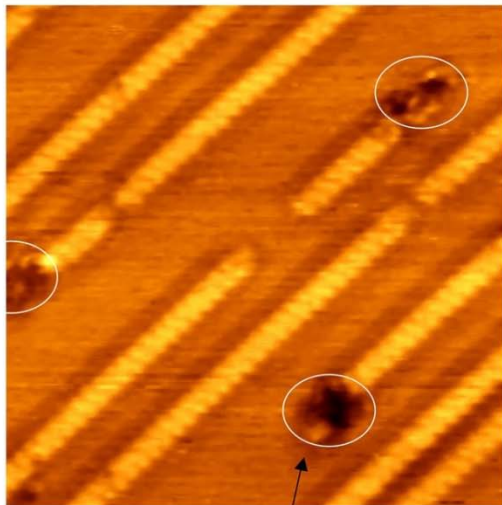


- a)** Ideal and relaxed atomic structure of **silicene nanoribbons**
b) electronic energy bands and isosurface charge density of selected states,
c) variation of band gap, E_g with the width of Si armchair nanoribbons,
 Isovalue surfaces of spin density difference $[\uparrow - \downarrow]$ for spin-up (red/light) and spin-down (blue/dark) states of zigzag silicon nanoribbons in different magnetic states together with spin-up (solid red/light) and spin-down (dashed-blue/dark) bands.
d) antiferromagnetic (AFM), **e)** Ferromagnetic (FM) and **f)** nonmagnetic (NM) states together with their calculated total energies and magnetic moments. Zero of the energy is set to E_F .
 S. Cahangirov et al., PRL (2009)

Chemical properties

15 L

(a)



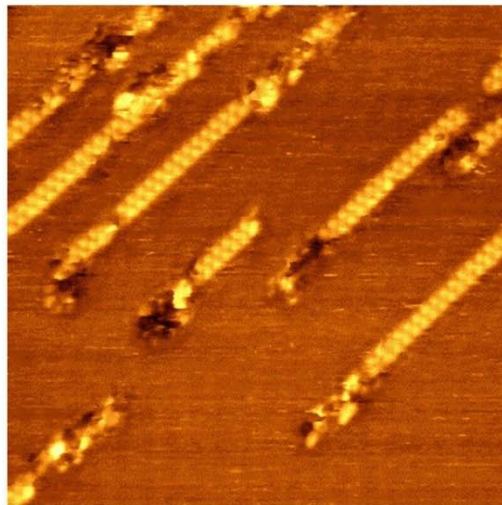
22 nm x 22 nm

Hollow

[-110]

30 L

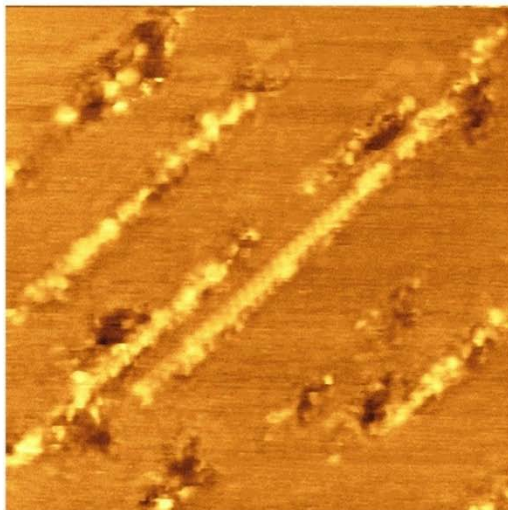
(b)



27.3 nm x 27.3 nm

60 L

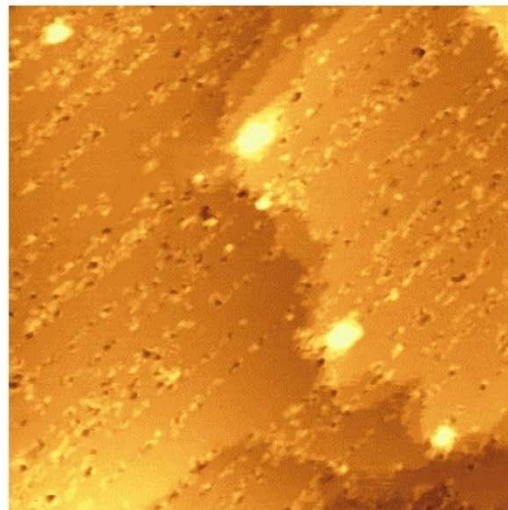
(c)



30 nm x 30 nm

300 L

(d)



100 nm x 100 nm

Oxidation of the Si stripes

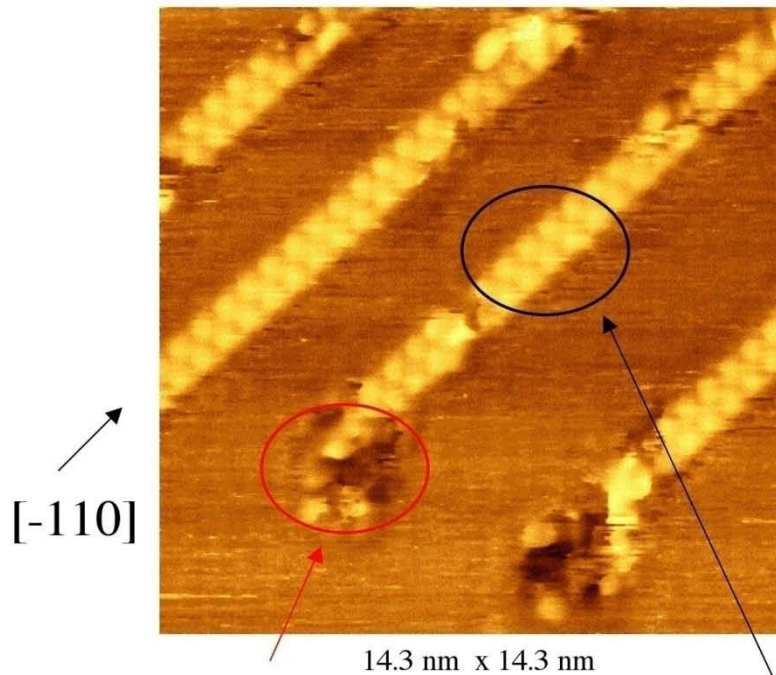
It starts at their extremities!

Burning-match process!

Filled-states STM images of Si NWs on Ag(110) at different oxygen doses at RT

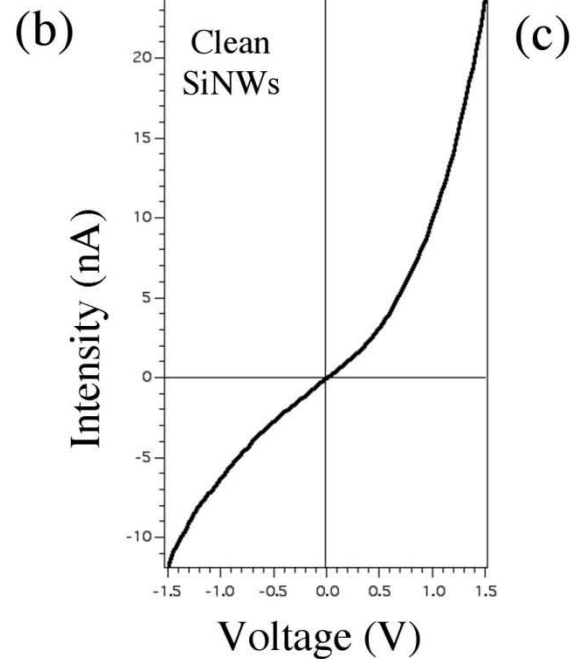
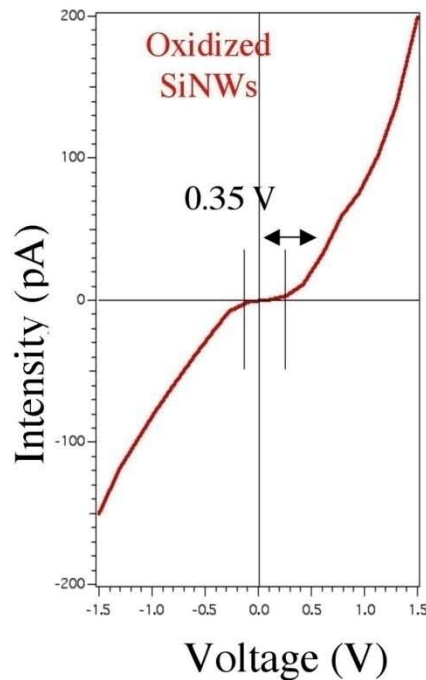
**De Padova et al.,
Nano Letters, 8 (2008) 2299**

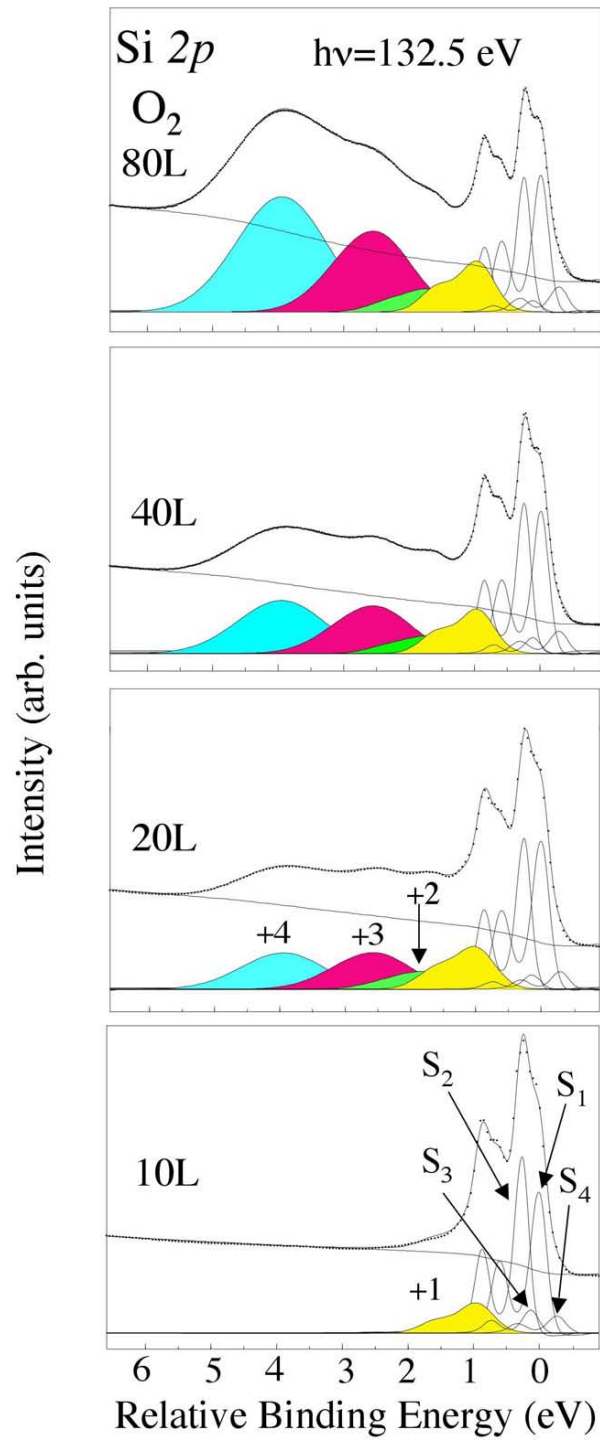
30 L



(a) **Formation of an internal nano-junction**

14.3 x 14.3 nm² filled-states STM images at 30 L of oxygen exposure; (b). I-V characteristic of oxidized SiNWs; (c). I-V on bare SiNWs. Selected areas on the STM image indicate where the I(V) curves have been recorded.



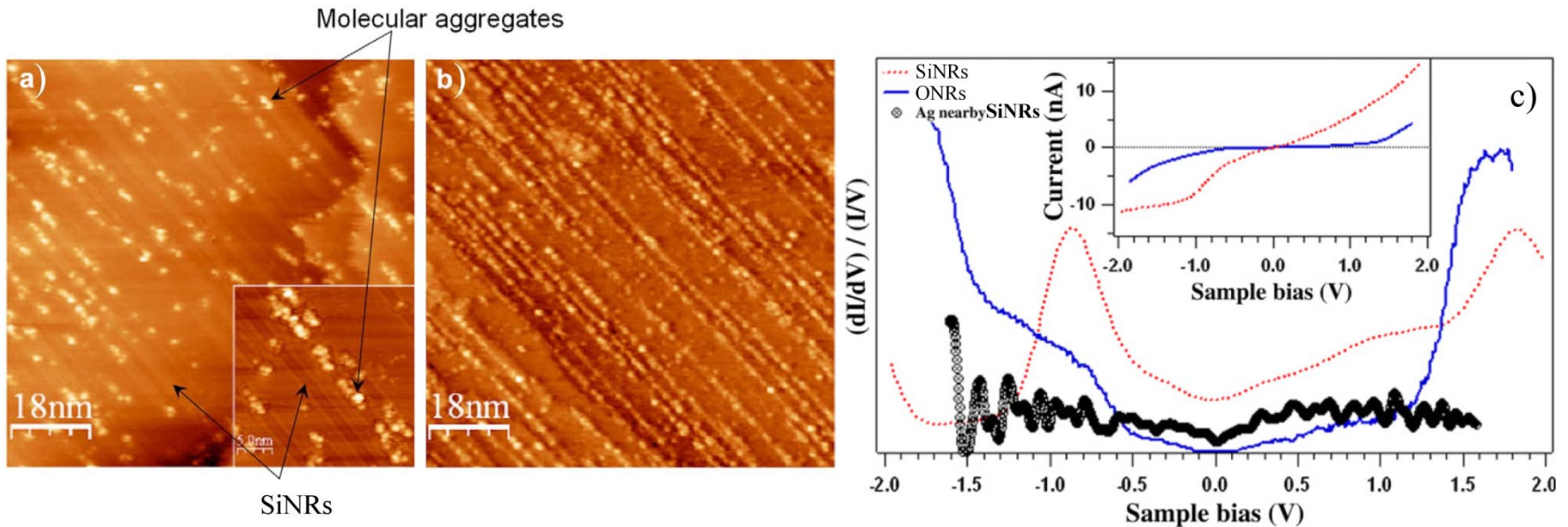


Si 2p core-level spectroscopy @ Elettra

Convolutated Si 2p core levels of the SiNWs grown on the Ag(110) surface at increasing oxygen exposures @ RT. The colored components (S 1+, S 2+, S 3+ and S 4+) related to the different oxidation states (+1 to +4) grow at the expense of the 4 initial components (S1, S2, S3, S4) of the virgin SiNWs.

The 4 oxidation states resemble those found upon oxidation of the **Si(111) surface** (Himpsel et al. PRB 38, 6084 (1988))

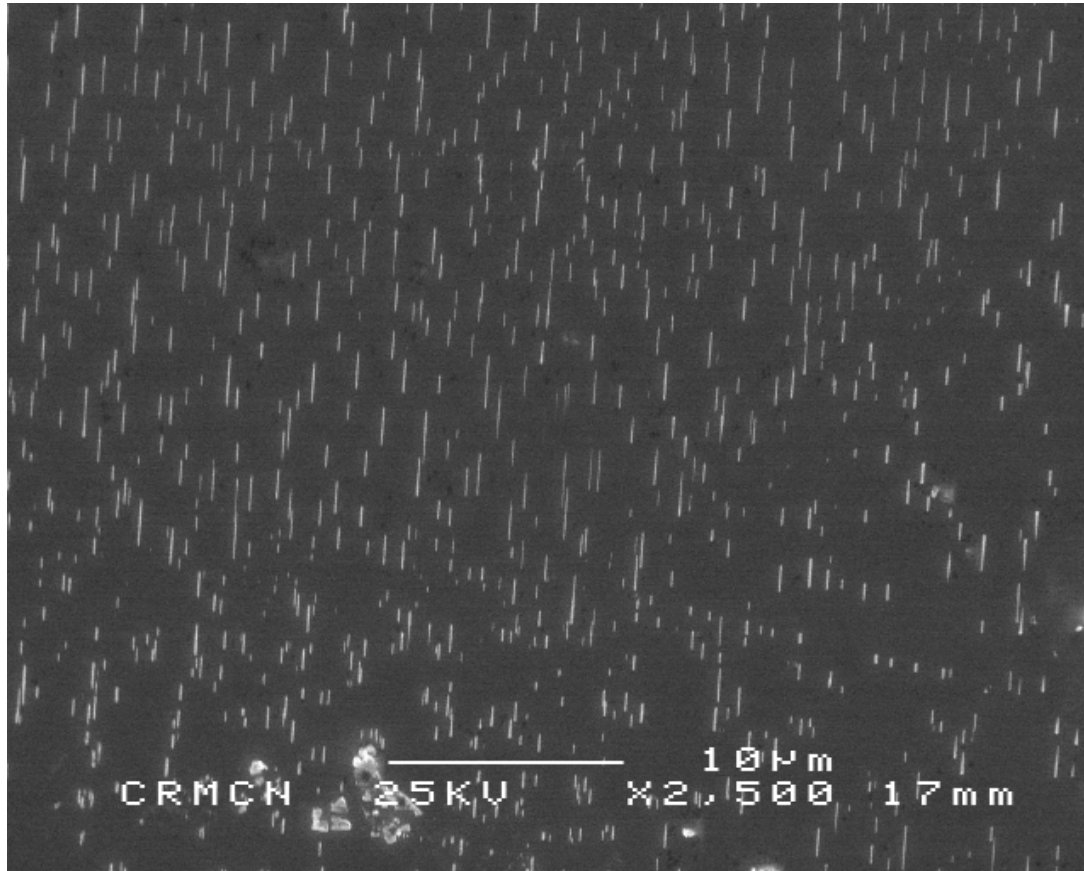
Selective interaction with organics

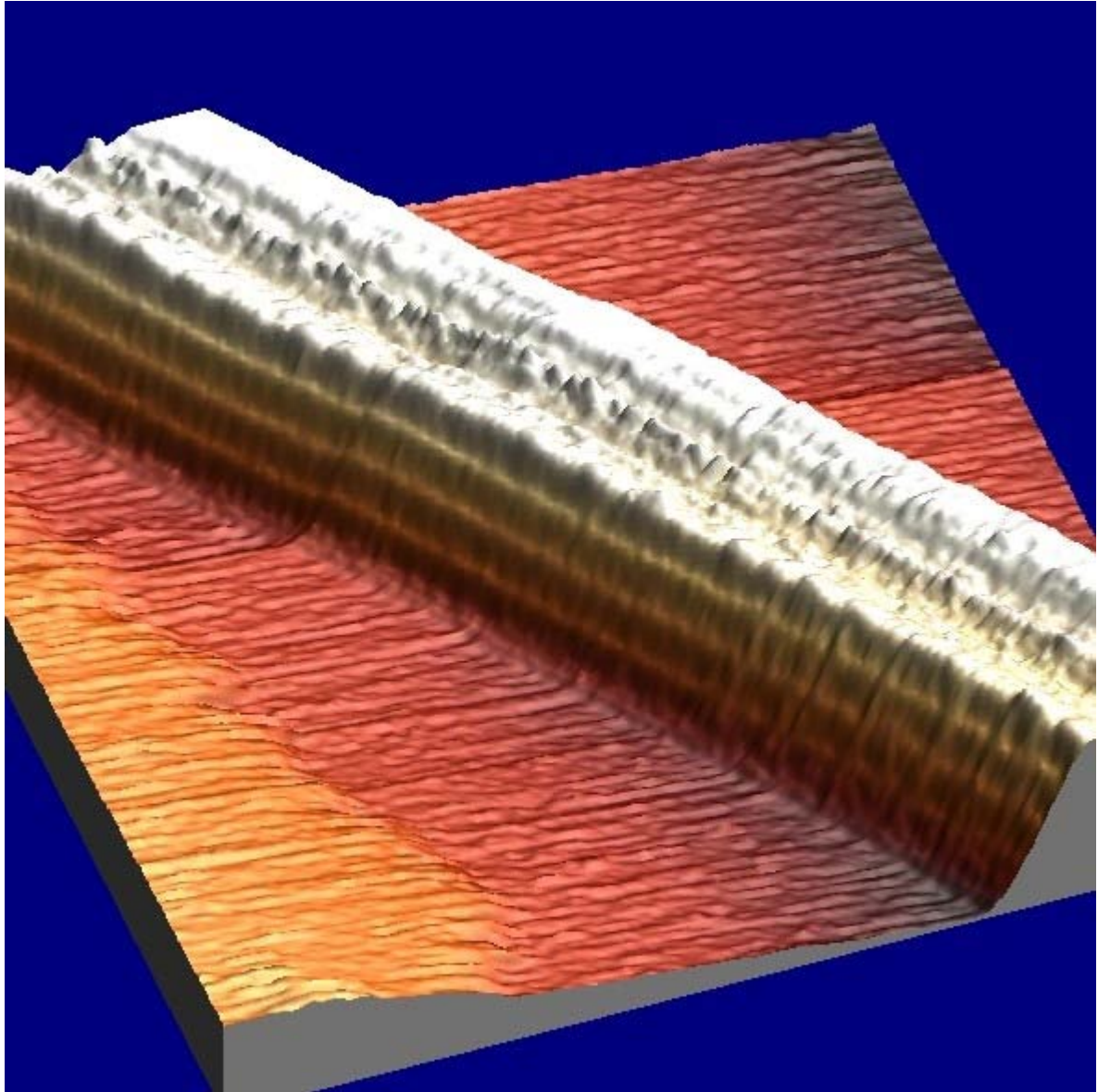


- a)** STM filled state images of the SiNRs/Ag(110) surface exposed to 1 L of PQ (9,10-phenanthrenequinone) ($I_t = 0.33$ nA, $V_s = 1.10$ V). The inset corresponds to a zoom-in of 25×25 nm².
- b)** STM filled state images of the SiNRs/Ag(110) surface exposed to 4 L of PQ ($I_t = 0.2$ nA, $V_s = 1.50$ V).
- c)** Average STS spectra representing the normalized differential conductivity of both the SiNRs (dotted line) and the organic NRs (solid line) obtained upon the adsorption of 4 L of PQ. The inset shows the corresponding $I(V)$ curves.

E. Salomon and A. Kahn, *Surface Sci.* 602 (2008) L79

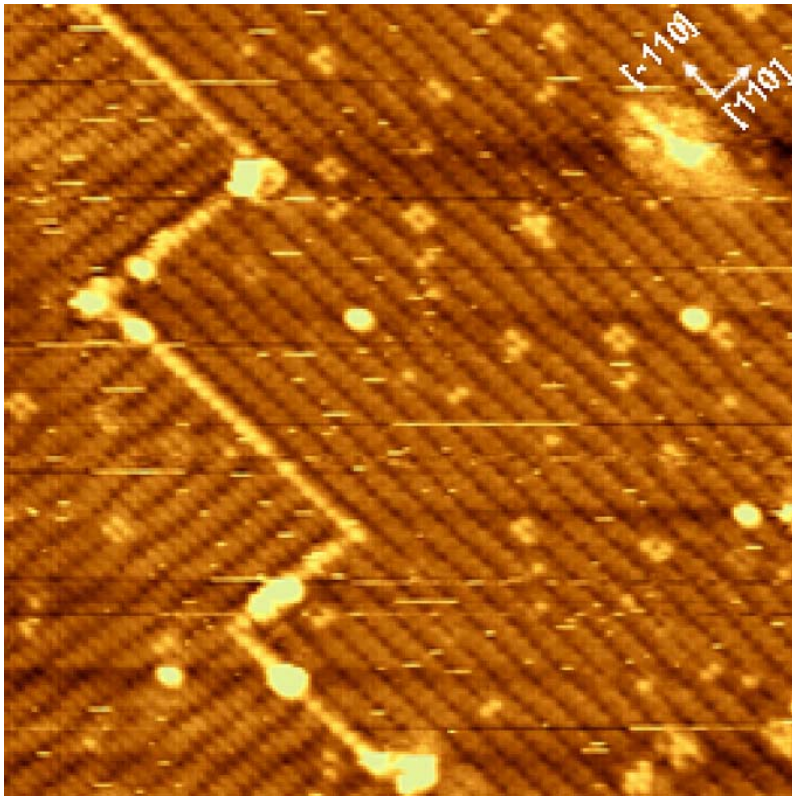
SEM image of *in situ* H exposed Si NWs after transport through air



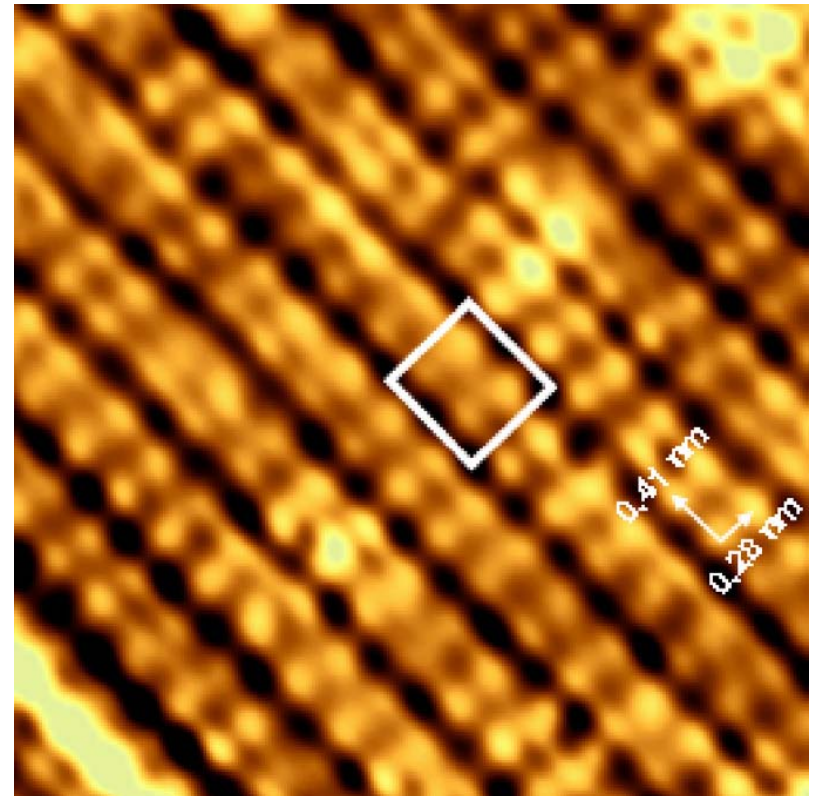


Si on Ag(100)

First adsorbed monolayer of silicon on the silver (100) surface 3x3 superstructure



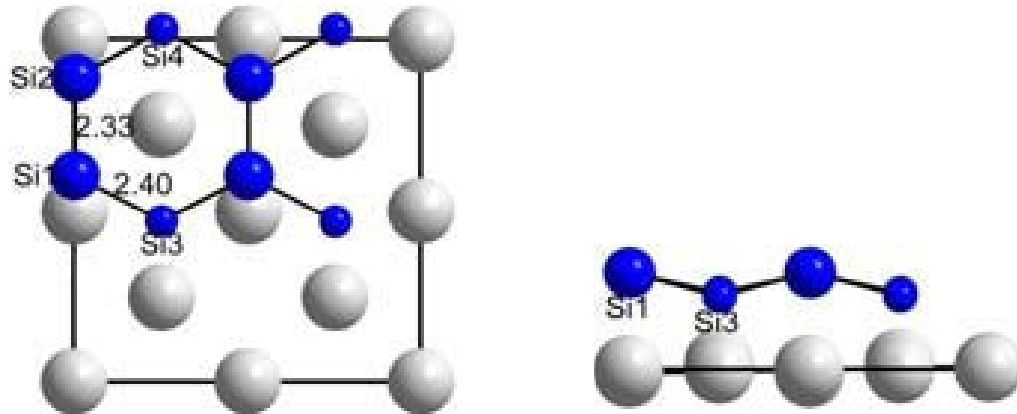
a)



b)

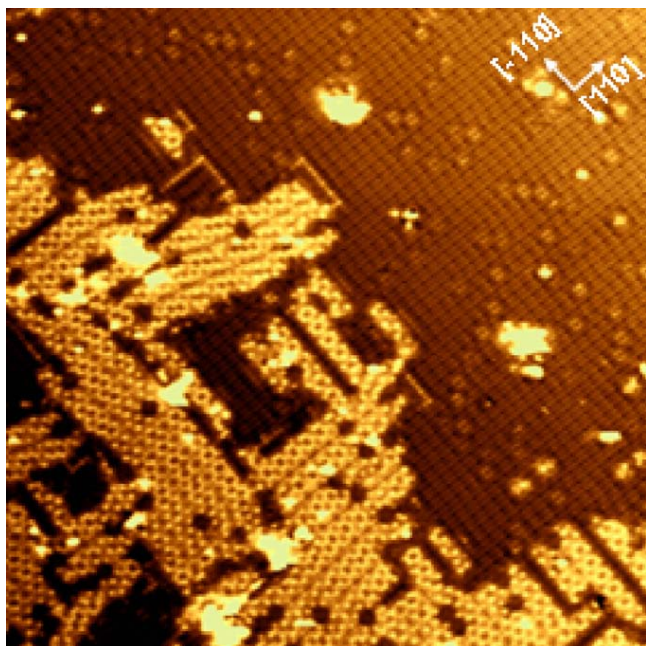
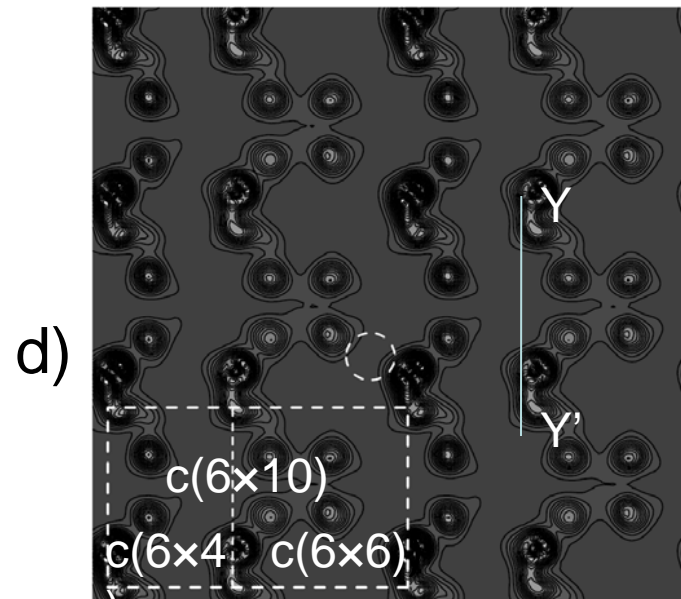
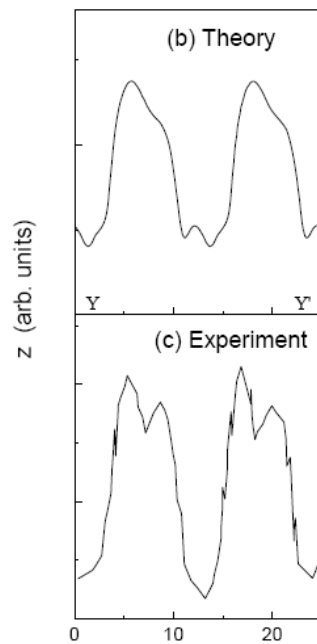
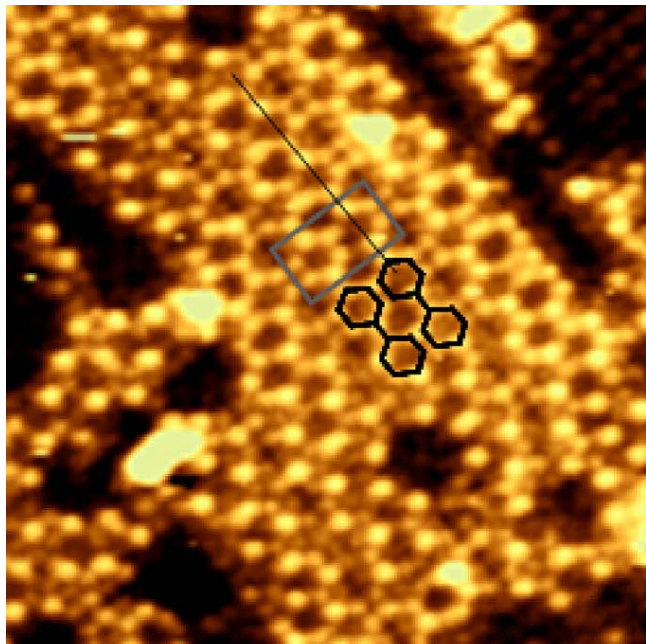
- a) filled-state STM image after the deposition of ~ 0.8 Si ML on Ag(001) revealing two orthogonal domains of the 3x3 superstructure ($23.4 \times 23.4 \text{ nm}^2$, $V = -1.02 \text{ V}$, $I = 1.14 \text{ nA}$),
b) a zoom at this superstructure ($6.4 \times 6.1 \text{ nm}^2$); the 3x3 unit cell is indicated.

Atomic model of the 3x3 structure derived from DFT-LDA calculations by **Guo-min He**



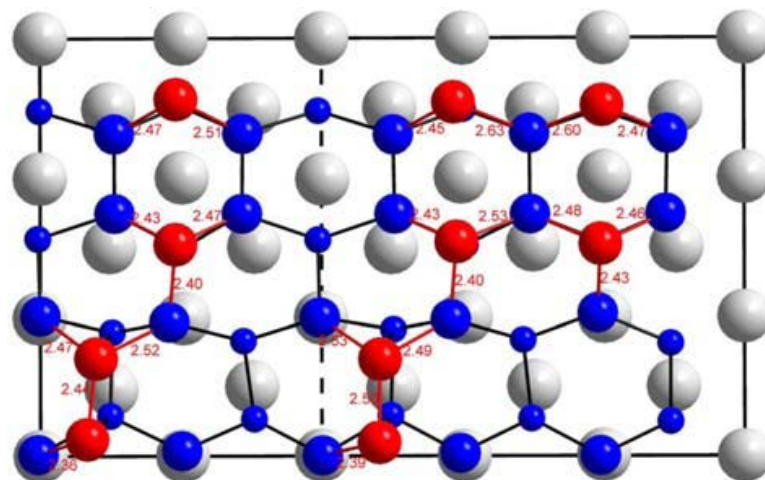
Top and side views of the 3x3 structure of Si (blue balls) on Ag(100) (white balls) at 1ML derived from DFT-LDA (SIESTA code) calculations: **a precursor of silicene**
Atomic distances between differently labeled Si atoms are indicated.

3x3 + « complex » superstructures: ~ 1.6 Si ML on Ag(100) deposited at ~ 230° C



Filled states
 STM image
 22.3 x 22.3
 nm² and
 zoom-in
 6.4 x 6.4 nm²
 C. Léandri et
 al., *Surface
 Sci.*, 601
 (2007) 262

e)



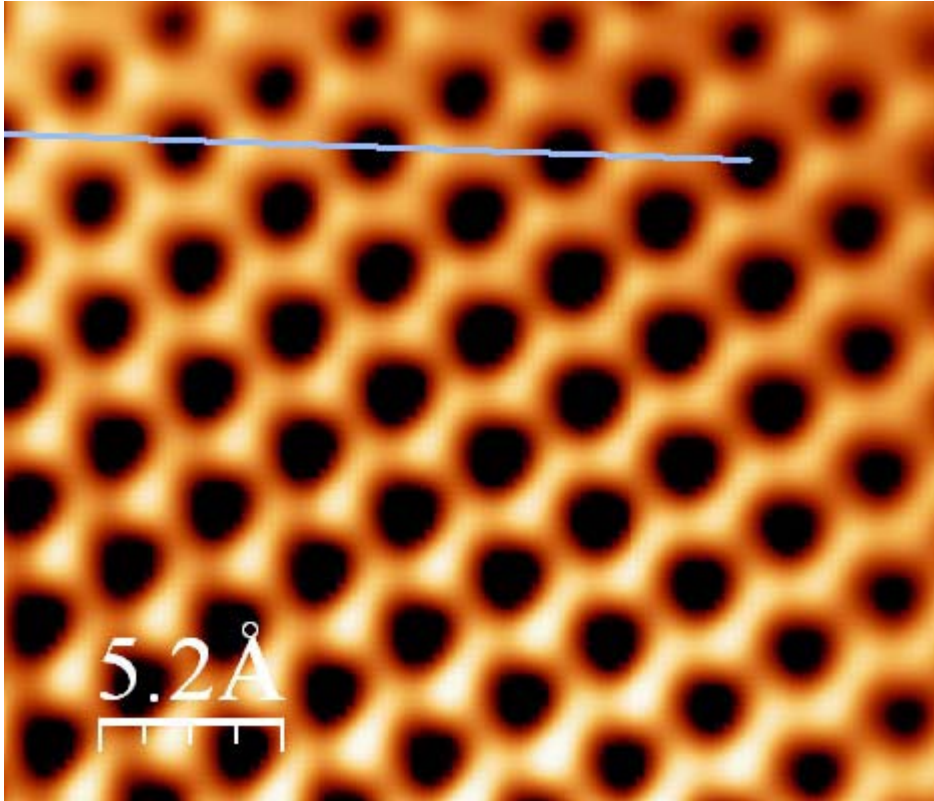
Atomic model, STM image simulation
 and comparison of theoretical and
 experimental profiles.

Guo-min He, *Surf. Sci.*, (2009)

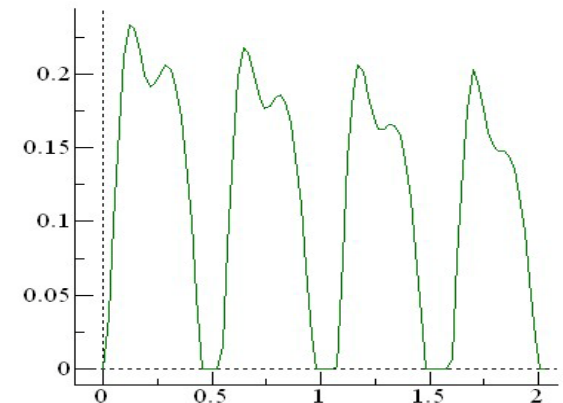
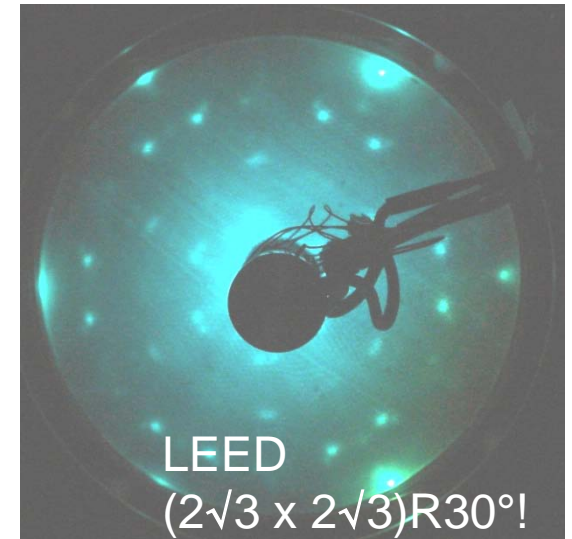
Si on Ag(111)

1 Si ML

2D silicene sheet on Ag(111)



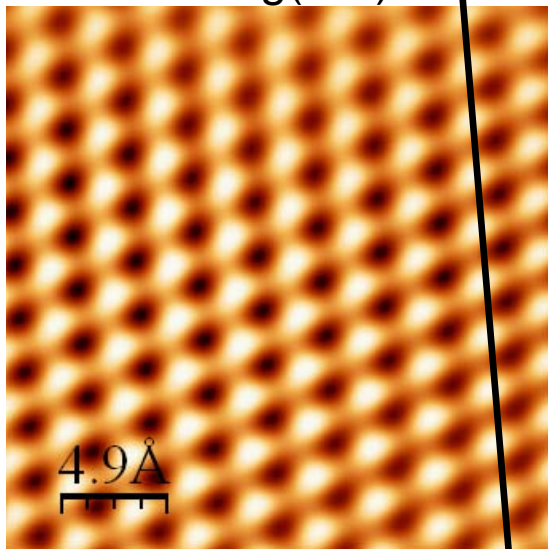
perfect silicon monolayer in a honeycomb lattice which covers the whole scanned area.



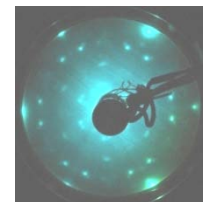
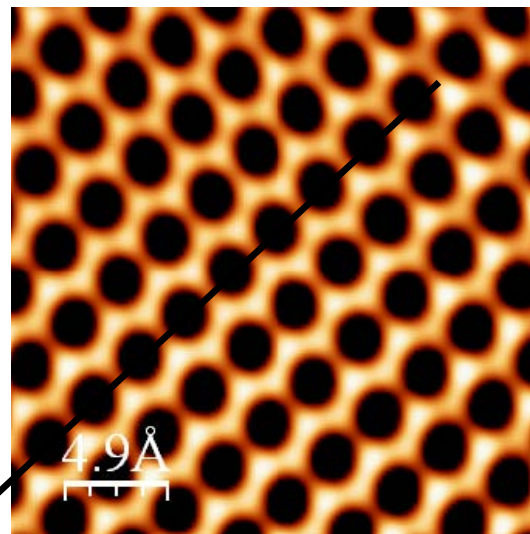
Si-Si $\sim 2.1 \text{ \AA}$

Buckling $\sim 0.02 \text{ \AA}$

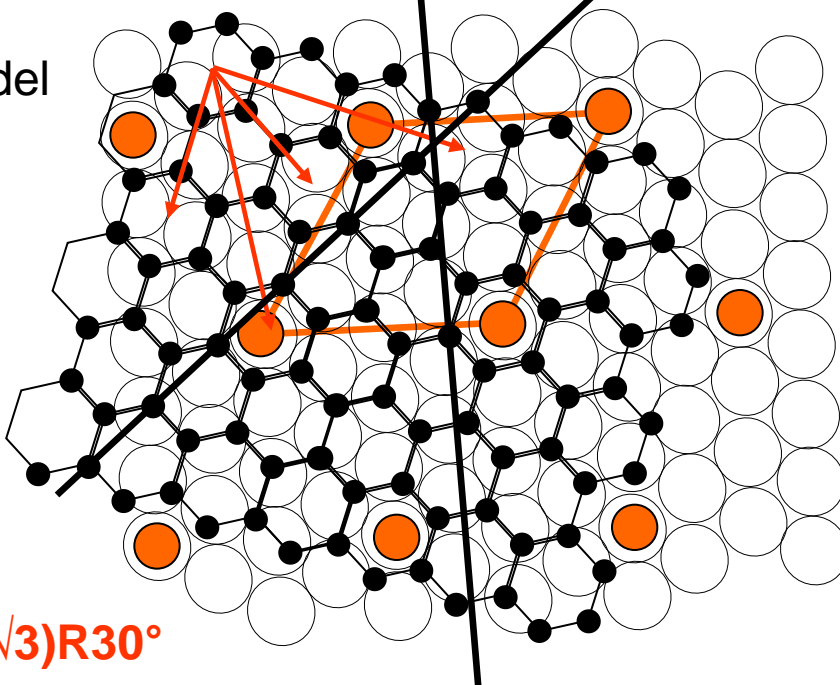
Bare Ag(111)



1 Si ML on Ag(111)



Balls model



$(2\sqrt{3} \times 2\sqrt{3})R30^\circ$

From LEED and ball model

$$d_{\text{Si-Si}} = 2.11 \text{ \AA}$$

Si bulk

$$d_{\text{Si-Si}} = 2.35 \text{ \AA}$$

Silicene

~10% shorter !!

(submitted)

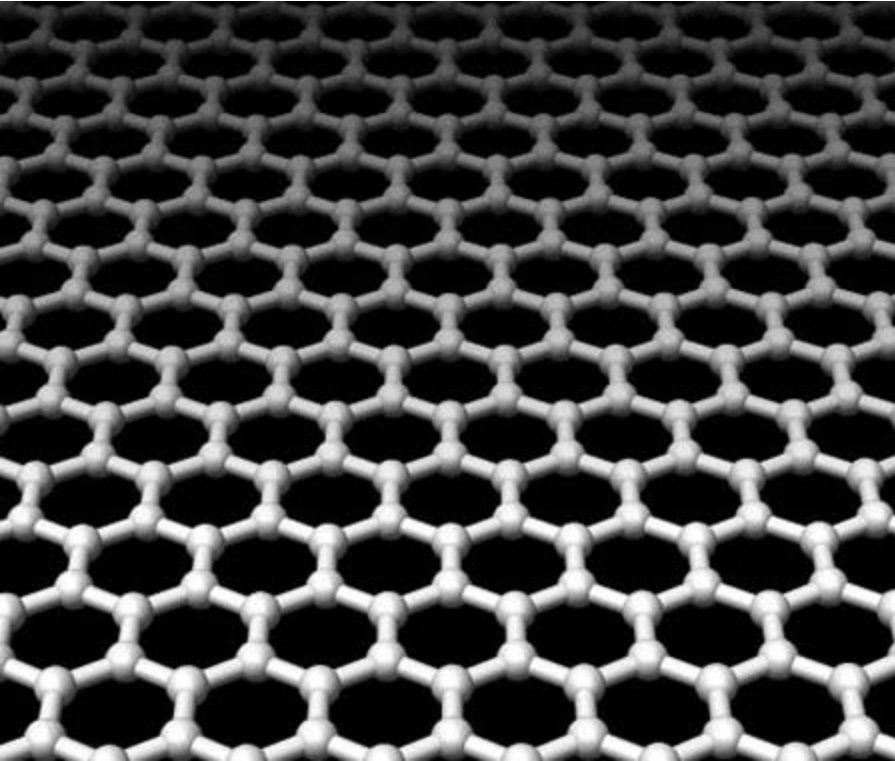
Potentialities

- Capping, e.g., with SiO
- n/p-type doping using e.g., phosphene and diborane
- Fabrication by CVD of ultimate membranes of, typically
 - SiC
 - Si_xGe_{1-x}
 - Si₄N₃

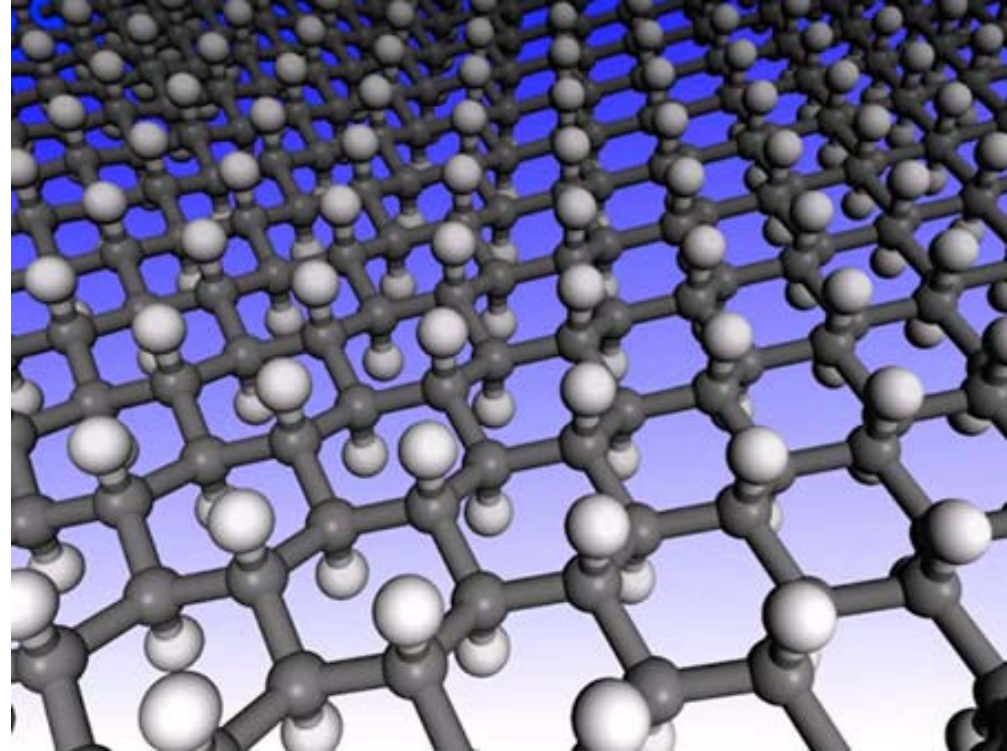
Perspective: CVD growth using disililane; core/shell architecture for **planar** p-i-n silicon nanowire structures for solar cells and nanoelectronic power sources

(Cf B. Tian et al., Nature 449 (2007) 885; B.M. Kayes et al., J. Appl. Phys. 97 (2005) 114302)

Perspectives for hydrogen storage!



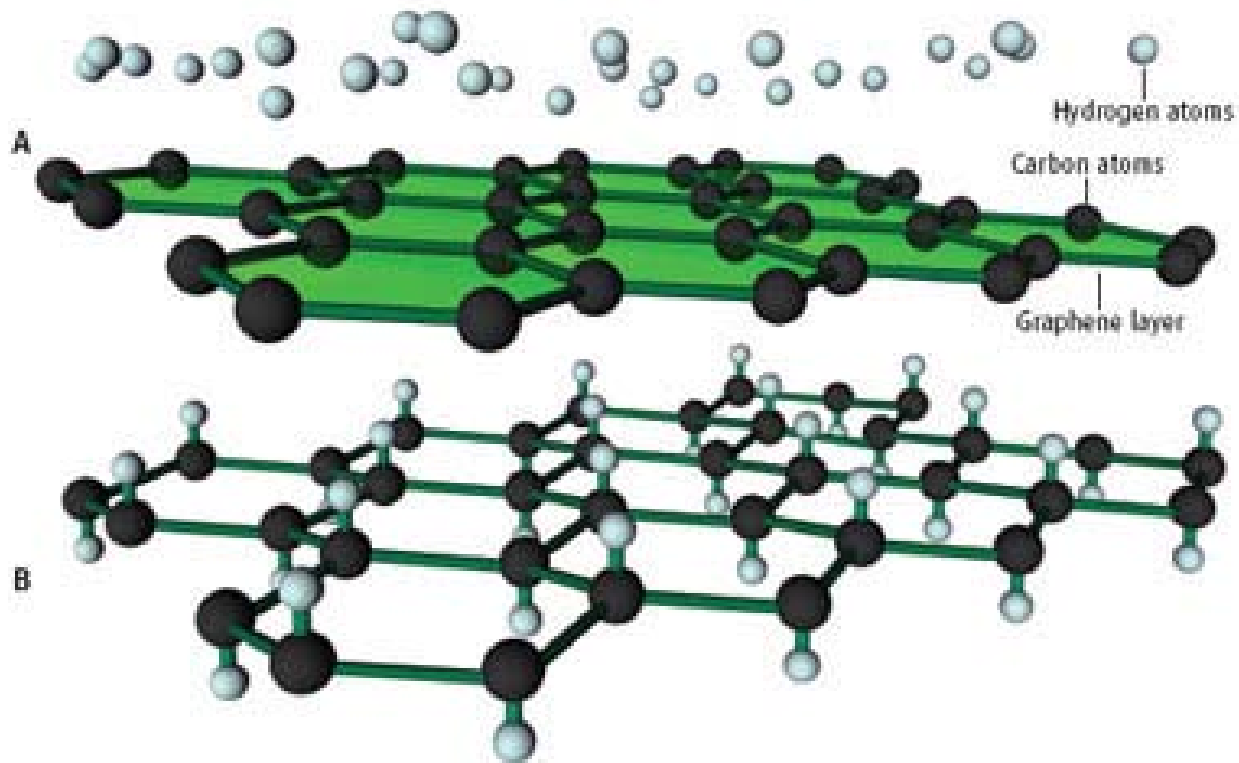
Graphene



Graphane

Structure of graphane in the chair conformation (carbon atoms are in dark, hydrogen atoms in white). The figure shows the hexagonal network with carbon in the sp^3 hybridization.

Adding hydrogen converts graphene (A) into graphane (B)

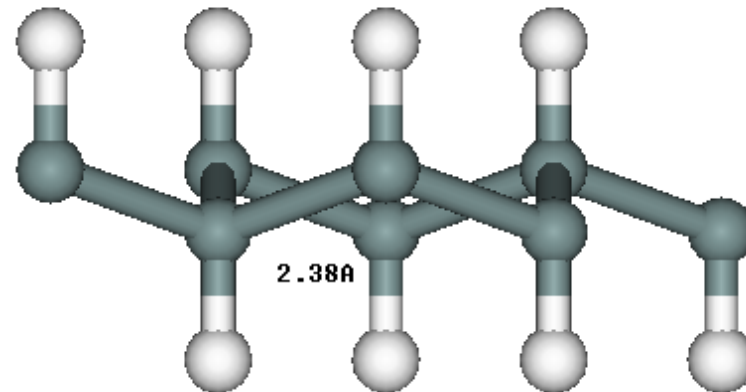
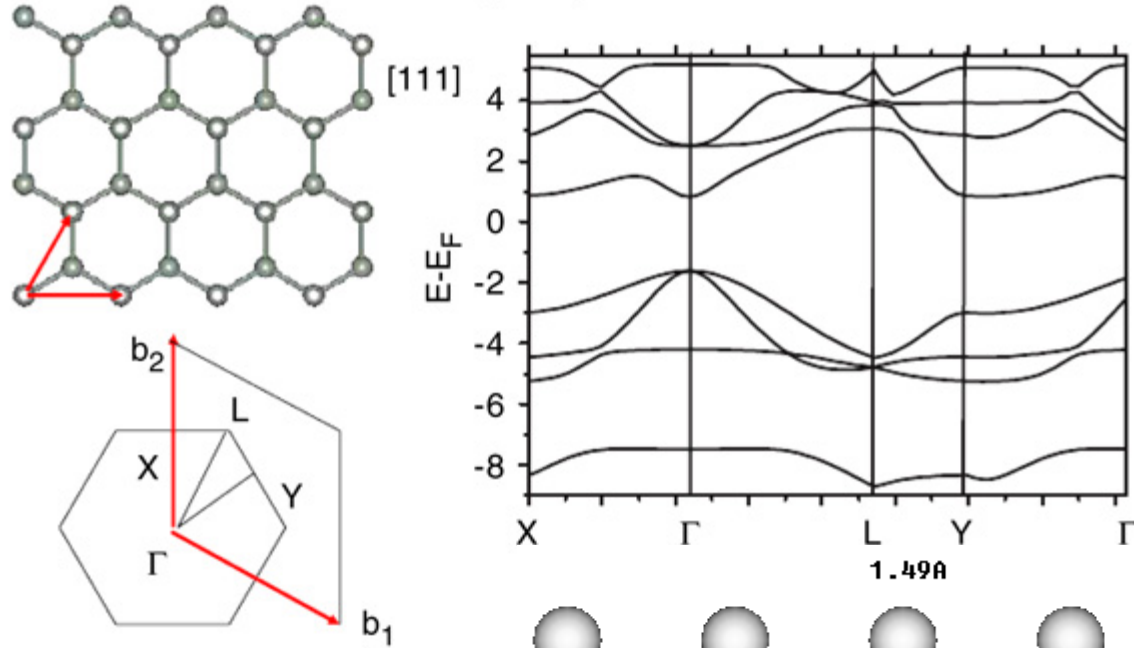


D.C. Elias et al., *Science* 323 (2009) 610

Fig. from A. Savchenko, *Science* 323 (2009) 589

“Silicane?”

Si(111) sheet



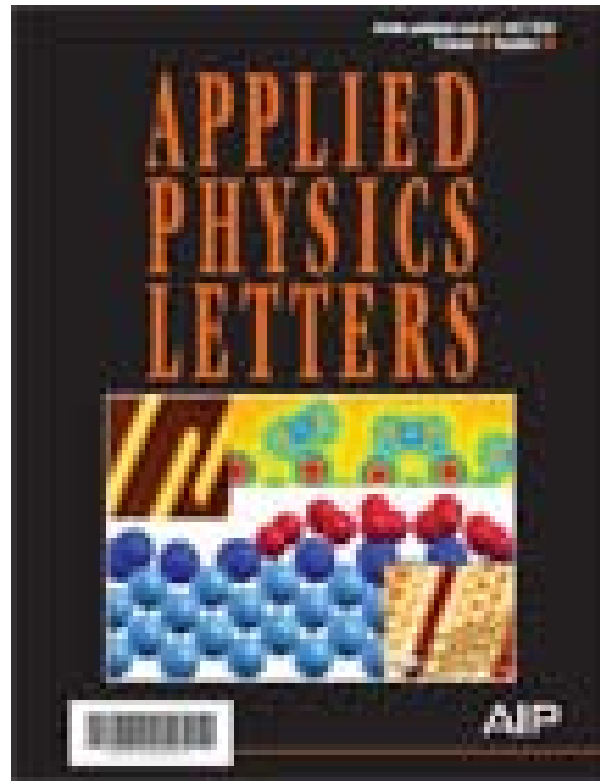
Atomic structure and energy band structure of (111) single-layered silicon sheets. The red arrows show the primary vectors in the configuration and the diagram of reciprocal space is provided below the corresponding atomic structure.

Summary and perspectives

- Formation at RT of massively parallel, straight, quantized Si nanoribbons on Ag(110) with a « magic » width of just ~1.6 nm. Surf. Sci. 574 (2005) L9
- These nanoribbons are atomically precise, metallic, novel silicon nano-objects
- These Si stripes present a strong transverse symmetry breaking. They exist in two left and right handed chiral species that self-organize in large magnetic-like domains Nano Letters 8 (2008) 271
- This asymmetry results from their unique atomic structure: graphene-like, silicon nanoribbons, i.e. **silicene stripes**. J. Supercond. Nov. Magn. 22 (2009) 259
They display a 1D electronic structure and reveal linear dispersions along their lengths, a characteristics of **relativistic massless Dirac Fermions**
- These silicene stripes self-organize to form a grating with a pitch of just 2 nm Appl. Phys. Lett., 90 (2007) 263110
- They are usable as a new template for the growth and ordering of 1D nanostructures, e.g., **organics nanowires**, magnetic dots
- These silicene stripes oxidize in a match-burning process; the propagating front creates a moving internal nano-junction. Nano Letters 8 (2008) 2299
- Mild hydrogenation preserves the massively parallel array of Si NWs; they are stabilized after air exposure, which is encouraging for solar cells and nanoelectronic power sources
- **Silicene stripes are also grown on Ag(100)**. C. Léandri et al., Surface Sci. 601 (2007) 262
- **2D silicene sheets can be grown on Ag(111)**; after hydrogenation they might form « **silicane** », a **direct gap semiconductor** with potential applications in the energy domain, typically, for photovoltaics and hydrogen storage

Graphene nanomaterials are not compatible easily with the Si-based electronics industry. Hence, “graphenium” microprocessors are unlikely to appear in the near future as it is hard to see chip makers re-tooling to use carbon instead of Si.

Indeed, there is an immediate possibility of application of silicene based nano-materials in existing Si-microelectronics



Graphene-like silicon nanoribbons on Ag(110): A possible formation of silicene

B. Aufray, A. Kara, S. Vizzini, H. Oughaddou, C. Léandri, B. Ealet and G. Le Lay

Appl. Phys. Lett. **96**, 183102 (2010)

Collaborators

**B. Aufray, B. Lalmi, C. Léandri, H. Sahaf, S. Vizzini, L. Masson,
B. Ealet, H. Oughaddou**
Marseille, France

**P. De Padova, C. Ottaviani, F. Ronci, C. Quaresima, B. Olivieri,
P. Moras, C. Carbone & P. Perfetti**
Rome, Italy

A. Kara
University of Central Florida, Orlando ,USA

M.E. Davila
Madrid, Spain

THANK YOU!